# The role of Arctic shelves in the global carbon cycling assessed using stable isotope geochemistry of Arctic and sub-Arctic pore waters.

**By**

**Malin Lunde**


**Master thesis in Geology**

**Department of earth science**

**University of Bergen**

**June 2021**

## Abstract

Shelf regions play a critical role in marine carbon (re)cycling, influencing both the distribution of carbon in the water column and its sequestration into marine sediments. Arctic shelf regions contain a disproportionately large amount of the global shelf area relative to the basin size, yet little is known about carbon recycling in these areas. Initial pore water stable carbon isotope results from the Nansen Legacy project cruise in 2018 suggest higher rates of carbon turnover in Arctic sediments than are observed in other oceanic settings and may indicate that these regions play a unique role in the global carbon cycle.

In order to establish under what conditions such high sedimentary carbon turnover rates occur, and delineate the processes sustaining them, we present a new database of pore water carbon isotopes spanning a range of sub-Arctic sedimentary regimes. The new pore water $\delta^{13}C_{DIC}$ data were acquired on a research cruise circumnavigating the Nordic seas in late summer/early fall in 2020 onboard the RV Celtic Explorer. Pore waters were recovered from multi, box, and gravity cores, using rhizons and analyzed immediately using a Delta Ray mobile isotope instrument onboard. Additional bottom water and water column isotope data was acquired from Nansen bottle, water column, samples.

The carbon isotope results show strong depletions in the shallow sediments relating to the addition of respired organic carbon to the dissolved inorganic carbon (DIC) pool. The strongest gradients (highest respiration) occur in the eastern Nordic Seas and sites west of Svalbard and in shallower sites most likely due to higher productivity and organic matter input at these locations. Pore water $\delta^{13}C_{DIC}$ decreased by 3.5 to 4.5‰ in the upper 10cm at the shallow stations but only by 0.5 to 2‰ at deeper stations. Stoichiometric estimates suggest that aerobic respiration dominates in the upper portion of the cores at most sites, but cannot explain all of the changes downcore, including in the upper centimeters at some sites. We conclude that other electron acceptors must be playing an important role in sub-Arctic and Arctic settings supporting carbon turnover in excess to that explained by oxygen. In addition, our results suggest that carbon isotope-based approaches to reconstructing past bottom water oxygen levels may be strongly impacted in some environments by other factors sustaining higher rates of carbon respiration than is explained simply by oxygen concentrations.

# Acknowledgements

A sincere thank-you to my main supervisor Ulysses Ninnemann and co-supervisors Pål Tore Mjørkved and Allyson Tessin, for help and guidance throughout this process. Thank you for letting me be a part of the Nansen Lagacy project, for all the zoom meetings, for all the feedback and all the new knowledge. I would also like to express my appreciation towards Audrey Morley for the organization of a very successful marine cruise even though it met a lot of challenges due to Covid-19.

I am very grateful for being given the opportunity to join the CIAAN cruise 2020. These 2 weeks on the sea nourished so many great memories both scientifically and socially. Thank you to all the scientist and crew for sharing their experience and knowledge with me. Thank you for all the laughter, for introducing me to all the new music and for good times in the lounge. I am forever grateful.

Last but not least, I want to thank my family and friends for all the support and for cheering me on during this process. A special thank you to Morten for being extremely patient and understanding during these two years, for letting me stay at his place and for all the extra support because of a really challenging year of 2020. It would not have been the same without you.

We made it!

Egersund, May 2021

Malin Lunde

# Contents

# 1. Introduction

## 1.1 Project:

This thesis is part of CIAAN (Constraining the impact of Arctic amplification in the Nordic Sea) project and builds on results from the Nansen Legacy project. These projects are mainly focusing on the magnitude of future climate changes in the Arctic and to integrate scientific knowledge required for future sustainable management of the environment and marine resource of the Barents Sea and adjacent Arctic Basin.

The CIAAN project is an international collaboration between 3 institutions: the National University of Ireland Galway, the Bjerknes Centre for climate research at the University of Bergen and the University of Southampton. The project is funded by the Marine Institute of Ireland. The key objectives for the CIAAN project are to collect an extensive hydrographic dataset for surface- and deep-water including temperature, salinity, nutrients, dissolved inorganic carbon (DIC), total alkalinity, and climate relevant dissolved gases. One other objective is to map the distribution and concentration of Color Dissolved Organic Matter (CDOM), nitrate, nitrite, silicate, phosphate, Oxygen, dissolved DMS (dimethyl sulfide) and the $O_2$/Ar ratio in the upper water column. These data are retrieved by using stratified plankton nets and multicore tops to collect living and recently dead planktonic foraminifera and to collect gravity cores, CTD (conductivity, temperature and depth), together with water column and pore water samples (Anon., 2020).

This master thesis is a presentation of newly retrieved and processed data during the CIAAN cruise, which may throw light upon the research regarding carbon turnover in glaciated regions. This master thesis contributes to the Nansen goal in understanding carbon cycling in the Arctic and Sub-Arctic regions and how it can change with a changing climate. In addition, it expands the dataset for the Barents Sea, and it places the Barents Sea results from the Nansen Legacy cruise in 2018 into context with other sedimentological, productivity and geochemical settings. This master will provide an initial overview of how pore water carbon turnover occurs and varies in different settings. The results will provide a baseline to guide further targeted and multi-parameter studies in the region.

## 1.2 Aim of this study:

The main purpose of this study is to investigate glaciated regions and its effect on the global carbon cycle. Newly retrieved pore water samples are analyzed for their carbon isotope values

(of DIC) using a Delta Ray in order to quantify the sources and amount of carbon respiration occurring in different sedimentary environments. The majority of organic matter (OM) respiration is thought to be accomplished aerobically in deep and open ocean settings, particularly in the upper portion of the sediments where $O_2$ is available (Hoogakker, et al., 2015). The balance between the renewal rate of bottom water oxygen levels and organic matter flux to sediments is thought to be a major determining factor setting the rate at which carbon is sequestered into sediments and removed from the ocean-atmosphere system. However, recent results from the Barents Sea suggest that more respiration occurs than can be (stoichiometrically) supported by available $O_2$; suggesting that other electron acceptors could be playing a more important role than previously appreciated (The Nansen Legacy, 2018). To the extent that shallow pore water carbon and carbon isotope gradients are influenced by factors other than the concentration of bottom water oxygen [$O_2$]. This would affect the interpretation of pore water isotope gradients and their utility as a proxy for past bottom water $O_2$, a proxy widely used within the geoscience community, e.g., (Hoogakker, et al., 2015) and (Hoogakker, et al., 2018). The hypothesis for this master thesis is that bottom water $O_2$ is a poor predictor of the rate and amount of carbon turnover in shallow sediments which complicates the use of pore water isotope gradients as a proxy for bottom water $O_2$.

The main objectives of this study are to test this hypothesis and:

1) To analyze carbon isotopes ($\delta^{13}C_{DIC}$) to quantify the amount and source(s) of carbon added to pore water just below the sediment water interface in different sedimentary environments.
2) Investigate if oxygen is the only electron acceptor responsible for the carbon respiration, or to what extent and under what conditions other acceptors are important.
3) Compare the $\delta^{13}C_{DIC}$ data collected on the CIAAN cruise with the Nansen Lagacy cruise in 2018 to evaluate which parameters are critical for anaerobic respiration.
4) To evaluate the simple assumptions used in the literature (refs) that the $\delta^{13}C$ gradient between the bottom water and $O_2$ minimum in pore waters is a proxy for bottom water oxygen concentrations.
5) To better understand what controls carbon transfer from ocean to the geologic reservoir (sediments) and how this might be climatically sensitive.

# 2. Background

The sequestration of organic carbon from the ocean-atmosphere system into marine sediments represents a crucial step in the long-term (geological) carbon cycle. While most marine organic carbon is efficiently remineralized into inorganic forms within the ocean a small percentage is transferred to the sediments, where, if it survives it can be stored long term. Globally the sedimentary burial of organic carbon is on the order of $169*10^{12}$ gC $yr^{-1}$ (Smith, et al., 2015) and is thought to play a key role in modulating atmospheric $O_2$ and $CO_2$ through the Earth's history (Berner, 1982). Despite this, the processes governing burial (versus respiration) remain somewhat unclear (Hedges & Keil, 1995) although bottom water oxicity and $O_2$ exposure times are considered crucial factors. Since carbon burial rates are much higher on continental margins and shelf areas the Northern Hemisphere represents an area of major importance for the modern carbon cycle. The Northern Hemisphere has kept pace in absorbing increasing amounts of carbon dioxide in the atmosphere over the last 60 years, partially offsetting the effects of global warming. The ocean has absorbed 22% of the global $CO_2$ from human activities (Simpkins, 2019). This section aims to provide a brief introduction to the phenomena and drivers of the carbon cycle in the Nordic seas.

## 2.1 The carbon turnover:

There are two types of carbon systems that control the distribution of carbon on Earth, the organic carbon system and the inorganic carbon system. These systems involve different reactions and quite different isotopic fractionation effects making stable isotopes a useful tool in tracing the movement of carbon through both systems.

Stable carbon isotopes are reported with the notation of $\delta^{13}C$ which relates the measured ratio of the heavy ($^{13}C$) to the light ($^{12}C$) stable isotopes of carbon in a sample relative to a given standard. The $\delta^{13}C$ notation is presented in equation 1.

$$\delta^{13}C = \left( \frac{\frac{C^{13}}{C^{12}} sample}{\frac{C^{13}}{c^{12}} standard} - 1 \right) * 1000$$

*Equation 1: The $\delta^{13}C$ is a ratio of the heavy $^{13}C$ and the light $^{12}C$ from a sample compared to the ratio in a standard ( (Debajyoti & Grzegorz, 2006)*

The organic carbon system is controlled by photosynthesis. Biological carbon fixation is controlled by two steps, (1) uptake and intracellular diffusion of $CO_2$ and (2) the biosynthesis of cellular components. The two-step model is presented as:

$$CO_{2(external)} \leftrightarrow CO_{2\,(internal)} \rightarrow organic\ molecule$$

*Equation 2: The organic carbon system is the transformation of CO2 in the atmosphere to organic molecules (Hoefs, 2015, p. 67).*

The isotopic fractionation is dependent on the partial pressure of $CO_2$ of the system. In a system with unlimited access to $CO_2$ the fractionation is dependent on the enzymatic fractionation, and this may vary from -17 to -40 ‰. While the range is large, most organic matter has quite similar values clustering around the values of the $C_3$ and $C_4$ plants, which represents the two main photosynthetic pathways. The two pathways result in a $^{13}C$ depletions of -18‰ for $C_3$ plant and a -4‰ for the $C_4$ plants. The carbon isotope fractionation in aquatic plants, such as phytoplankton, is even more complex. The fractionation is controlled by temperature, availability of $CO_2$, light intensity, nutrient availability, pH and physiological factors (Hoefs, 2015, p. 67).

The inorganic system is controlled by the reaction where atmospheric $CO_2$ dissolve into bicarbonate and mineralizes to solid carbonate (Hoefs, 2015, p. 66). This system is comprised of multiple chemical species linked by a series of equilibria *(see equation 3).* Each of these equilibria is associated with an isotope fractionation.

$$CO_{2\,(aq)} + H_2O \leftrightarrow H_2CO_3$$
$$H_2CO_3 \leftrightarrow H^+ + {HCO_3}^-$$
$${HCO_3}^- \leftrightarrow H^+ + {CO_3}^{-2}$$
$$Ca^{2+} + {CO_3}^- = CaCO_3$$

*Equation 3: The inorganic carbon system is the processes where atmospheric $CO_2$ transform into solid carbonate (Hoefs, 2015, p. 66).*

The carbon isotopic composition of the ocean differs between surface waters and deep waters. This difference is primarily the result of the organic carbon cycle and the biological pump. Marine phytoplankton photosynthesizes in the surface water. They preferentially incorporate the light carbon isotope, leaving the surface waters depleted in $^{12}C$ and enriched in $^{13}C$. When the phytoplankton dies it sinks to the bottom and remineralizes. This releases $^{12}C$ to the bottom water making the DIC pool isotopically lighter, thus setting up a surface to deep ocean

gradient. These gradients are then modified by circulation in the ocean. Well ventilated waters have higher $\delta^{13}C$ than less ventilated waters due to lower content of remineralized carbon. Thermodynamic fractionation, exchange of $CO_2$ between the surface ocean and the atmosphere, also influences the $\delta^{13}C$. Although this surface equilibrium takes time, the process tends to drive colder waters have higher $\delta^{13}C$ than warmer waters (Eide, et al., 2017).

The major carbon reservoir in the ocean is in the dissolved inorganic carbon (DIC). DIC is the total of aqueous $CO_2$, bicarbonate ($HCO_3$) and carbonate ($CO_3$) (Cole, 2013). The Bjerrum diagram in Figure 1 show the relationship between the pH and the concentration of $CO_2$, $CO_3$ and $HCO_3$ (Aarnes, 2020) and how the speciation is pH dependent. The pH in seawater is approximately 8 and therefore $HCO_3^-$ (and secondarily $CO_3^{2-}$) is most dominant. When the concentration of $CO_2$ increases the pH drops. When the concentration of $CO_3^{2-}$ increase the pH increases (Aarnes, 2020).

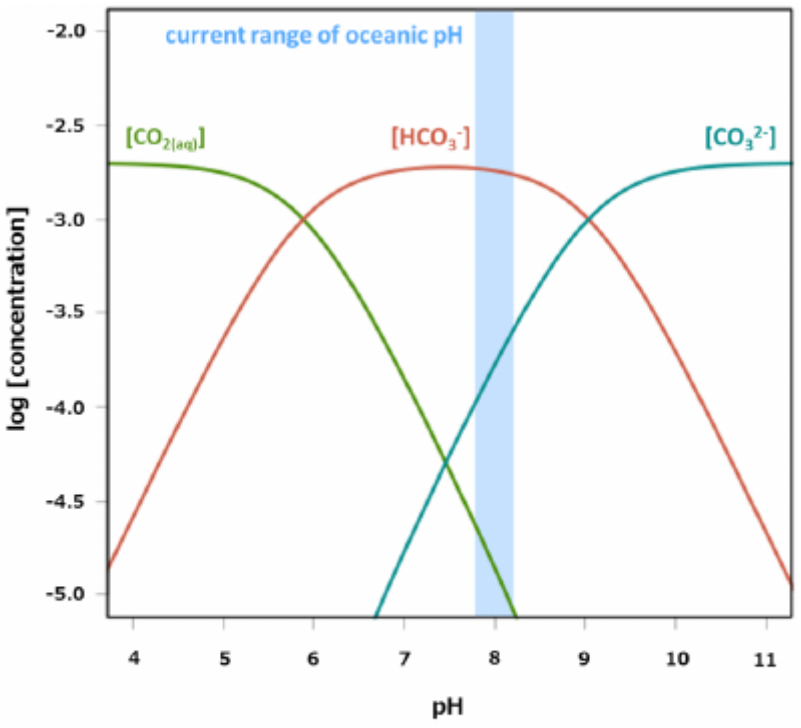


$$CO_2 + H_2O \leftrightarrow H^+ + HCO_3^- \leftrightarrow 2H^+ + CO_3^{2-} \quad (1)$$

$$CO_2 + H_2O + CO_3^{2-} \leftrightarrow 2HCO_3^- \quad (2)$$

$$Ca^{2+} + 2HCO_3^- \leftrightarrow CaCO_3 + CO_2 + H_2O \quad (3)$$

*Figure 1: The relationship between $CO_2$, $CO_3$ and $HCO_3$ and how this relationship effects the pH (Heinze, et al., 2015)*

The concentration and isotopic composition of DIC of the deep-sea sediments of the world's oceans is primarily controlled by organic matter decomposition and the dissolution of calcium

carbonate. The net results of these processes make the pore water in sediments isotopically lighter than the overlying bottom water (Hoefs, 2015, p. 69). In regions where methane is produced/oxidized, this process causes strong isotopic fractionation and can have a clear (enriching/depleting, respectively) influence on the carbon isotopic value of pore water DIC.

## 2.2 Sedimentary environment and biogeochemical reactions

The deep-sea environments represent highly dynamic geo-biospheres (Jørgensen & Boetius, 2007). The seafloor around Greenland and Norway representing sedimentary environments from the sub-Arctic to the high-Arctic, from coastal to deep water and from rocky to soft seafloor (Greenland climate research centre, n.d.). This section will introduce the microorganisms living in the Norwegian and Greenland Sea and the biogeochemical reactions happening due these microorganisms.

### 2.2.1 Microorganisms, biogeochemical zones and electron acceptors:

Surface sediments serves as a habitat for organisms and controls the burial and recycling of material (Middelburg, 2018). The Norwegian and Greenland Sea are dominated by different microorganisms, varying with different water depths but the same species is observed even though the physical-environmental parameters are different. Between 600 and 1200m water depths the upper sediments are dominated by *Melonis barleeanum, Pullenia bulloides and Islandiella norcrossi.* From 950 to 1500m it is dominated by *Passidulina teretis*, and from 1250 to 3200m *Cibicides wuellerstrofi* dominates the sediments (Belanger & Streeter, 1979).

The sediments represent an active biogeochemical reactor where microbial, oxidation, reduction, precipitation, and dissolution processes occur (Luff & Moll, 2004). The chemical composition of the sediments is controlled by the flux of organic material and calcite onto the bottom and the diffusive exchange of metabolites between pore water and bottom water (Luff & Moll, 2004). Marine microorganisms gain energy from oxidation of organic matter with an external oxidant. The sediments are divided into biogeochemical zones with different mineralization processes based on the electron acceptor used by the microorganisms (Jørgensen & Kasten, 2006). The first zone is the oxic zone because oxygen is the most favorable electron acceptor thermodynamically. This zone increases with increasing water depth and decreasing with increased organic influx from the continental slope into the deep sea (Schulz & Zabel, 2006, p. 193). The zone can be from a few mm to a meter deep. Beyond the sediment oxygen penetration depth, where oxygen has been consumed, is the suboxic zone

where respiration is anaerobic. In this zone other terminal electron acceptors are being utilized by the microorganisms. The mineralization process following oxygen respiration is listed in order of decreasing energy gain and is called nitrate reduction/denitrification, manganese reduction and iron reduction *(see Figure 2 and 3)* (Jørgensen & Kasten, 2006). During these processes, nitrogen, manganese (2+) and iron (2+) are being added to the pore water. Below the suboxic zone is the anoxic zone with sulfate reduction as the organic carbon oxidation. Even deeper methane tends to accumulate, a process called methanogenesis. This zone is called the methanic zone. Methane slowly diffuses up towards from this zone to the sulfate zone where it oxidizes to $CO_2$ (Jørgensen & Kasten, 2006). The importance of the different oxidants for mineralization of organic carbon has been studied intensely and it is generally found that oxygen and sulfate play the major role in the sediments. Up to 25-50% of the organic carbon is mineralized by sulfate reducing bacteria. With increasing depth and decreasing organic influx the oxygen increases its importance and sulfate reduction loses its significance (Schulz & Zabel, 2006, p. 193).

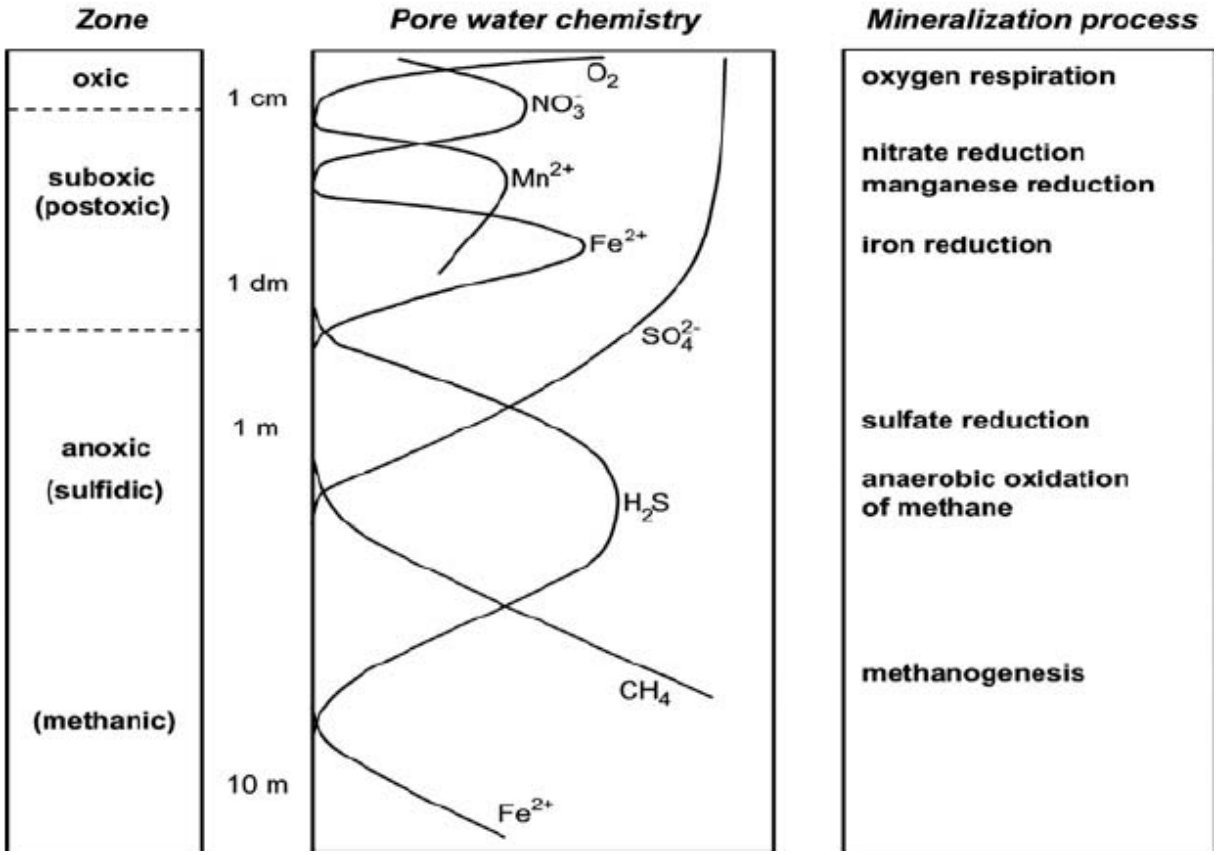


*Figure 2: Biogeochemical zones, mineralization processes and the abundance of different ions down in the sediments is presented in this figure (Jørgensen & Kasten, 2006).*

| Pathway and stoichiometry of reaction | $\Delta G^0$ (kJ mol$^{-1}$) |
|---|---|
| ***Oxic respiration:*** | |
| $[CH_2O] + O_2 \rightarrow CO_2 + H_2O$ | -479 |
| ***Denitrification:*** | |
| $5[CH_2O] + 4NO_3^- \rightarrow 2N_2 + 4HCO_3^- + CO_2 + 3H_2O$ | -453 |
| ***Mn(IV) reduction:*** | |
| $[CH_2O] + 3CO_2 + H_2O + 2MnO_2 \rightarrow 2Mn^{2+} + 4HCO_3^-$ | -349 |
| ***Fe(III) reduction:*** | |
| $[CH_2O] + 7CO_2 + 4Fe(OH)_3 \rightarrow 4Fe^{2+} + 8HCO_3^- + 3H_2O$ | -114 |
| ***Sulfate reduction:*** | |
| $2[CH_2O] + SO_4^{2-} \rightarrow H_2S + 2HCO_3^-$ | -77 |
| $4H_2 + SO_4^{2-} + H^+ \rightarrow HS^- + 4H_2O$ | -152 |
| $CH_3COO^- + SO_4^{2-} + 2H^+ \rightarrow 2CO_2 + HS^- + 2H_2O$ | -41 |
| ***Methane production:*** | |
| $4H_2 + HCO_3^- + H^+ \rightarrow CH_4 + 3H_2O$ | -136 |
| $CH_3COO^- + H^+ \rightarrow CH_4 + CO_2$ | -28 |
| ***Acetogenesis:*** | |
| $4H_2 + 2CO_3^- + H^+ \rightarrow CH_3COO^- + 4H_2O$ | -105 |
| ***Fermentation:*** | |
| $CH_3CH_2OH + H_2O \rightarrow CH_3COO^- + 2H_2 + H^+$ | 10 |
| $CH_3CH_2COO^- + 3H_2O \rightarrow CH_3COO^- + HCO_3^- + 3H_2 + H^+$ | 77 |

*Figure 3: Shows the gradual decrease in redox potential of the oxidant and the decrease in free energy available by respiration with the different electron acceptors (Schulz & Zabel, 2006, p. 181)*

## 2.3 The $\delta^{13}C$ as an $O_2$ proxy

Reconstruction of paleo bottom water oxygen concentration is increasingly being used to understand biogeochemical cycling and constrain the behavior of the carbon cycle in the past. One increasingly applied technique is to use gradient in $\delta^{13}C$ of DIC between bottom water and pore water values at the oxygen penetration depth (essentially where oxygen is consumed). As mentioned in the section above oxic respiration of organic carbon is the dominating process happening in the upper part of the sediments and the consumption of oxygen would be accompanied by the addition of isotopically light carbon into the pore water DIC pool. To the extent that carbon turnover is entirely aerobic in upper zone of the sediments where oxygen is still present, then the total change in the $\delta^{13}C$ of pore water DIC

should reflect the total amount of $O_2$ consumed by respiration, which in turn is set by the original $O_2$ concentration of the bottom water (McCorkle & Emerson, 1988). A number of recent high-profile studies have used the isotopic gradient between benthic foraminifera calcifying their shells in bottom water and near the oxygen penetration depth, as a proxy for the pore water gradient between these two sites—and thus for bottom water $O_2$ in the past (Hoogakker, et al., 2015) (Hoogakker, et al., 2018). However, the validity of this approach requires that bottom water $O_2$ is the primary influence on the respiration of organic matter in the upper sediments and that the gradient reflects a simple/stable stoichiometric consumption of $O_2$ and release of isotopically light carbon.

Ideally, in order to make this calculation, one needs to know, or assume/estimate, the original DIC concentration in bottom water and the isotopic composition of bottom water and the organic matter being remineralized (added to the DIC pool). However, one or more of these values are often not known. Therefore, here I use basic stoichiometry together with global ocean relationships derived empirically to estimate oxygen concentrations from the $\delta^{13}C$.

Equation 4 presented by Eide et al (2017) shows the relationship between $\delta^{13}C$ and $PO_4$ in the global ocean related to the production and oxidation of organic matter. It is assumed a carbon isotope fractionation in marine photosynthesis of -19‰, a mean ocean DIC of 2200 µmol/kg, a carbon to phosphate ratio of 128, a mean ocean $\delta^{13}C$ of 0.5‰ and a mean ocean $PO_4$ of 2.2µmol/kg (Eide, et al., 2017). The $\delta^{13}C$ in photosynthesis in colder waters is found to be close to -30‰ which results in a $\delta^{13}C$ versus $PO_4$ slope of -1.7‰ *(see Equation 4b)* (Eide, et al., 2017). The Redfield ratio in the ocean, 1:16:106, represents the average ratio of C:N:P in phytoplankton biomass and in the dissolved nutrient pool of the ocean due to photosynthesis and respiration. During aerobic respiration of organic matter, the ratio of $O_2$:C is 138:106. Organic matter and the oxygen required to respire it has the values P: N:C:-$O_2$ of 1:16:106:138 (Lenton & Watson, 2000). By using this relationship together with Equation 4, the change in oxygen concentration can be calculated from the variation in $\delta^{13}C$ due to organic matter production and aerobic respiration. This carbon-based approach will be tested on the CIAAN data in section 6.4.

$$a)\ \delta^{13}C_{BIO} = 2.8 - 1.1 * PO_4$$

$$b)\ \delta^{13}C_{BIO} = 2.8 - 1.7 * PO_4$$

*Equation 4: The relationship between oceanic δ13C and PO4 are presented (Eide, et al., 2017) and represents the global oceanic relationship for how DIC changes its $\delta^{13}C$ value as organic matter is produced and respired in a) warm waters and c) cold waters.*

# 3. Study area

In this section the geographical-, oceanographic- and climatic settings and additionally the productivity, sediment flux and terrestrial influences for the core sites collected in this master thesis are presented.

## 3.1 Geographical and bathymetric setting

The sediment cores used in this study were collected from the GIN sea (Greenland-, Island- and Norwegian- seas) (*see Figure 5)* during the CIAAN cruise onboard RV Celtic Explorer in August and September 2020. The core sites are located along the coast of Norway, Svalbard, Greenland and Iceland *(see Figure 4).* These sites provide a range of sedimentary conditions spanning from glaciated and non-glaciated margins, from shallow/shelf to deep abyssal settings, and span a range of different biological productivity and carbon export regimes.

The core sites along Norway and Svalbard are influenced by the Norwegian current which is a part of the North Atlantic Current. The core sites along the Greenland coast are situated along the east Greenland Current and is influenced by freshwater flux from the Greenland Icesheet (Hunter, et al., 2007). In general, the bathymetry of an area constitutes a crucial factor in the water mass circulation. The topography of the seafloor may exhibit limitations to the circulations and effect the mixing of water masses (Hopkins, 1990). The area of interest in this study is the Nordic Sea. The bathymetry of the Nordic Sea comprises two basins which is separated by the Mohns mid oceanic-ridge system, The Greenland Basin and the greater Norwegian basin *(see Figure 5).* The Greenland Basin is defined by the Fram strait in the north, The Greenland continental shelf to the west and Mohns ridge to the south and east (Hopkins, 1990). The greater Norwegian basin is comprised of the Norwegian Basin, the Lofoten Basin and the Iceland Plateau. The Norwegian Basin is a deep abyssal plain located between Jan Mayen and The Farao Islands. The Lofoten Basin is a slightly shallower abyssal plain located to the east of the Mohns Ridge with Jan Mayen fracture zone to the south (Hopkins, 1990).

Important water mass exchange to the Nordic seas occurs through 4 passageways. The Fram strait represents the connection between the GIN sea and the Arctic Ocean. The opening between Svalbard and the Norwegian coast is the connection between the GIN seas and the Barents Sea. Denmark Strait and the Faroese-Shetland channel represents the connection between the GIN seas and the Atlantic Ocean (Hopkins, 1990).

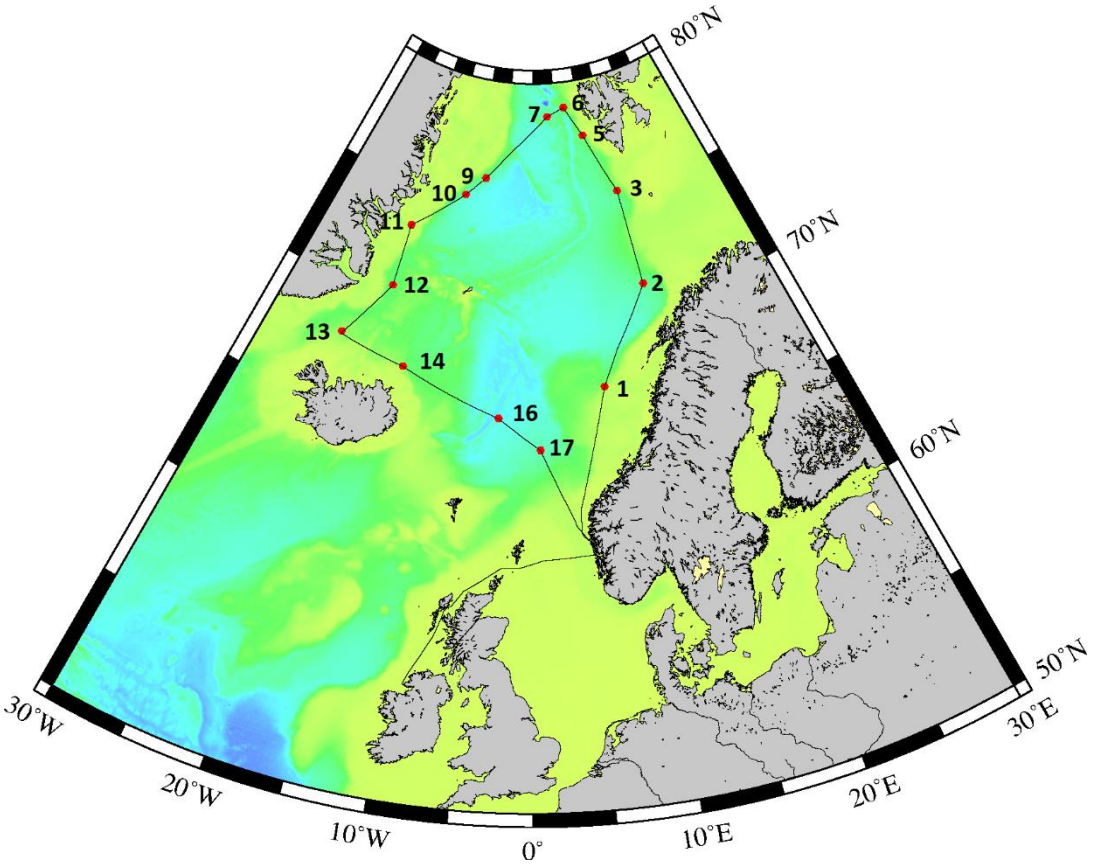


*Figure 4: CIAAN planned expedition station locations demarked by numbers 1-17 on the map. Note that stations 4 and 8 were dropped due to adjustments in the timetable prior to departure. In addition, no pore water data exist for stations 6, 13, 14, and 17 due to limited time or inclement weather conditions forcing reduced activity for those locations.*

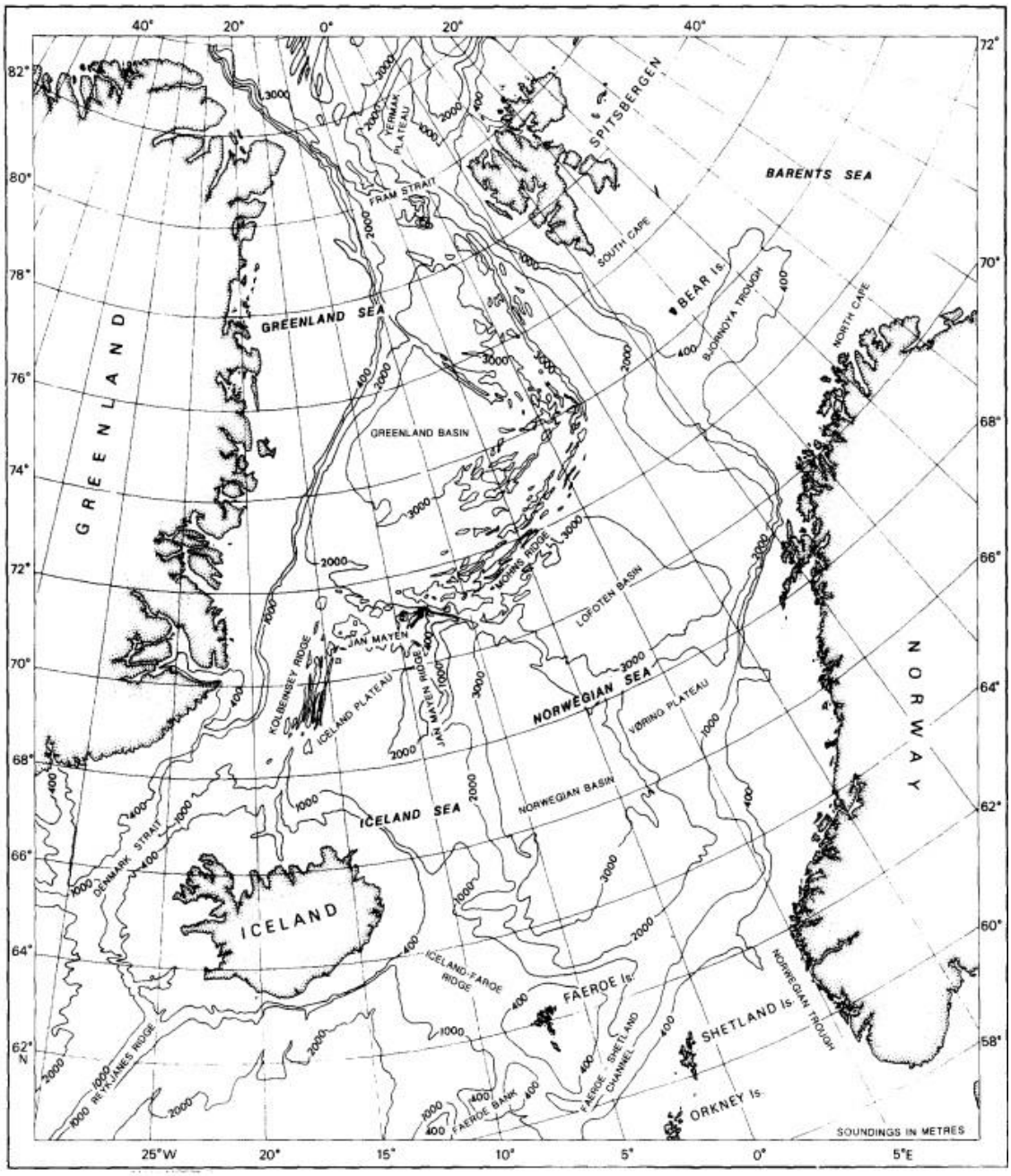


*Figure 5: This map shows the basins and seas located in the Nordic Sea (Hopkins, 1990).*

## 3.2 Oceanographic setting

The oceanic area of interest in this master thesis is the GIN seas. The water masses found here arise from two parent water masses, The Polar Water (PW) and the North Atlantic Water (NAW) *(see Figure 6).* The PW is cold and have low salinity whiles the NAW is warm and have high salinity. The division of the GIN seas occurs longitudinally in salinity and vertically

in temperature. The vertical differentiation of water masses is based on density, dividing surface water, intermediate water and deep water (Hopkins, 1990).

### 3.2.1 Surface waters

The Norwegian Atlantic water (NwAtW) is defined as surface water that enters from the Atlantic water through The Faroe Channel. This water is a part of the Norwegian Atlantic Current system and provides the Nordic Seas with warm and high salinity water. The average salinity is above 35 ppt. The water travels along the Norwegian coast influencing the areas of station 1,2,3,15 and 16. The water then enter the Barents Sea or travels along the southwest coast of Svalbard influencing station 5.6 and 7. On this path northward it loses heat and salt and becomes less dense. Polar water enters the GIN sea through the Fram Strait as the Greenland Polar Water (GPW). This is a surface water mass that flows southward along the continental margin of Greenland influencing station 9-14. It is cold with a temperature lower than 5 degrees average and low in salinity with an average of less than 34.4 ppt *(see Figure 10).* Underneath the GPW is a strong halocline originated from polar waters and maintained by the adding of freshwater due to melting of ice bergs (Hopkins, 1990).

The two previous surface water masses are the main surface waters, and they are constrained dynamically to the east and west sides of the basin. The large intervening region is occupied by the Arctic Surface Water (ArSW). This water arises within the GIN sea and is derived from mixture of the boundary waters. ArSW has a salinity from 34.4 to 35 ppt and a temperature range from -1.8 to 10 degrees. The ArSW are then divided into two surface waters. Surface waters in the Greenland Sea are called the Greenland Arctic Surface Water (GArSW). Surface waters in the Iceland Sea are called the Iceland Arctic Surface Water (IArSW) (Hopkins, 1990).

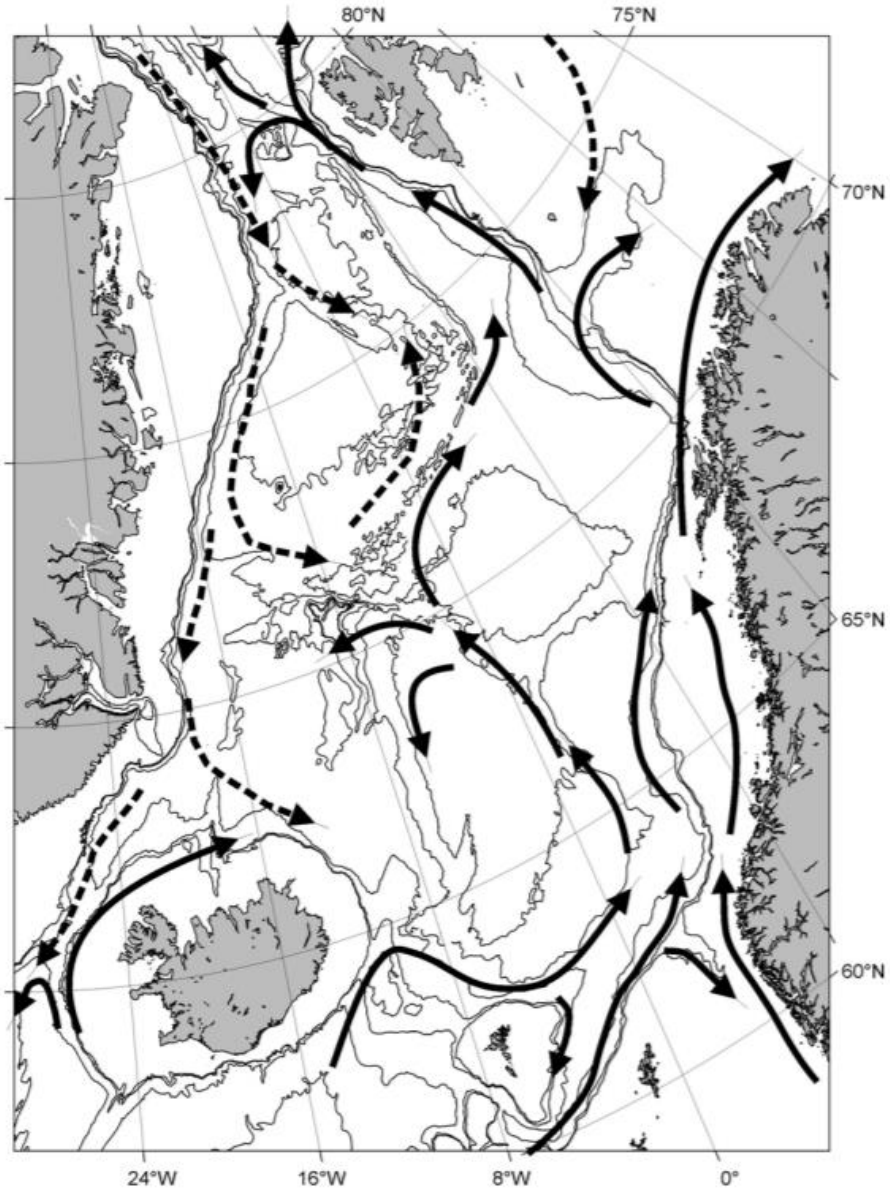


*Figure 6: Schematic of the surface circulation in the Nordic Sea. The black arrows indicate the warm saline waters from the south and the dashed arrows indicate cold and low saline waters from the north (Hopkins, 1990).*

### 3.2.2 Intermediate water

The intermediate waters in GIN sea are of two origins: those formed locally in the winter due to atmospheric buoyancy extraction processes (heat and water vapor losses to atmosphere, decreasing the temperature and increasing the salinity, with cooling being the dominant factor), and those formed elsewhere and are imported through advection (Hopkins, 1990).

Atlantic Intermediate waters (AtIW) are formed advectively from NwAtW when NwAtW submerges off Spitsbergen because of its high salinity it is denser than the fresher polar water

that it converges with, and it subducts to be overlayed by a mixture of polar waters from the Barents Sea through the East Spitsbergen Current. More specifically the AtIW is formed when NwAtW is divided into two branches, one portion going into the Polar Sea and the other portion recirculating to the west and becoming a part of the East Greenland Current (EGC) system as the AtIW. AtIW continues southward into the Iceland Sea.

There are a range of intermediate waters present in the Nordic Seas in addition to the ones mentioned above. The remaining is Arctic Intermediate Waters (ArIW), Jan Mayen Atlantic Intermediate water (JMAtIW), Greenland Arctic Intermediate Water (GArIW), Iceland Atlantic Intermediate Water (IAtIW), Iceland Arctic Intermediate Water (IArIW), Polar Intermediate Water (PIW), Icelandic Current Intermediate Water (ICIW) and Norwegian Arctic Intermediate Water (NwArIW). They generally relate to wintertime production of denser water or subduction of layers below fresher and lighter polar waters (Hopkins, 1990).

### 3.2.3 Deep water

The Greenland deep water (GDP) is different in the matter of being colder and fresher than other deep waters such as the Norwegian Sea Deep Water (NwDW). The formation process of deep water differs greatly, resulting in various water mass properties within deep waters. The Greenland deep water formation occurs, according to Carmack et al (1990), through subsurface cooling of GAtIW. GAtIW enters the Greenland Gyre Center and loses heat quicker than salt to the GArSW, through a double diffusion mechanism. The heat is then further transported through the surface layer to the atmosphere. The surface layer therefore receives heating from below and cooling at the surface. The buoyancy is altered and the GAtIW changes water properties to those of the GDW. The GDW flows The NwDW is formed when EADW flow through Mohns Ridge and mixes with GDW (Hopkins, 1990).

### 3.2.4 Currents

There are many currents influencing the GIN seas *(see Figure 7).* The most salient for this study are the Norwegian Atlantic Current (NwAtC) and the East Greenland Current which represent the dominant features of the eastern and western surface circulation systems in the Nordic Seas. Relatively warm and salty, the NwAtW transports water northward within the eastern Norwegian Sea from the Farao channel into the Greenland Sea. This current influence station 1-7, as well as stations 15 and 16. The flow from the Norwegian Sea to the Greenland Sea is essential to the thermohaline balance and circulation dynamics in the GIN sea. The northmost portion of the NwAtC is called the West Spitsbergen Current (WSC), it extends from the northern Lofoten Basin to Fram Strait. In addition, there is the East Greenland

Current (EGC) and the Jan Mayen Current (JMC). The EGC is a barotropic current that transports cold and fresh polar water southward from Fram Strait to Denmark Strait. This current influence station 9-14. The JMC is an eastward flow from the Greenland slope, it continues cyclonically on the Greenland side of the Mohns Ridge and joins the NwAtC and WSC on the eastern side. Between the EGC and the NwAtC there is a separation of around 1000km with a zonal flow called the Icelandic Current (IC). This current is a branch of the Irminger Current which imports Atlantic Water into the Iceland Sea through Denmark Strait. The current flows eastward along the northern continental slope of Iceland and its origin is Atlantic but it freshens by local runoff from Iceland *(see Figure 7)* (Hopkins, 1990).

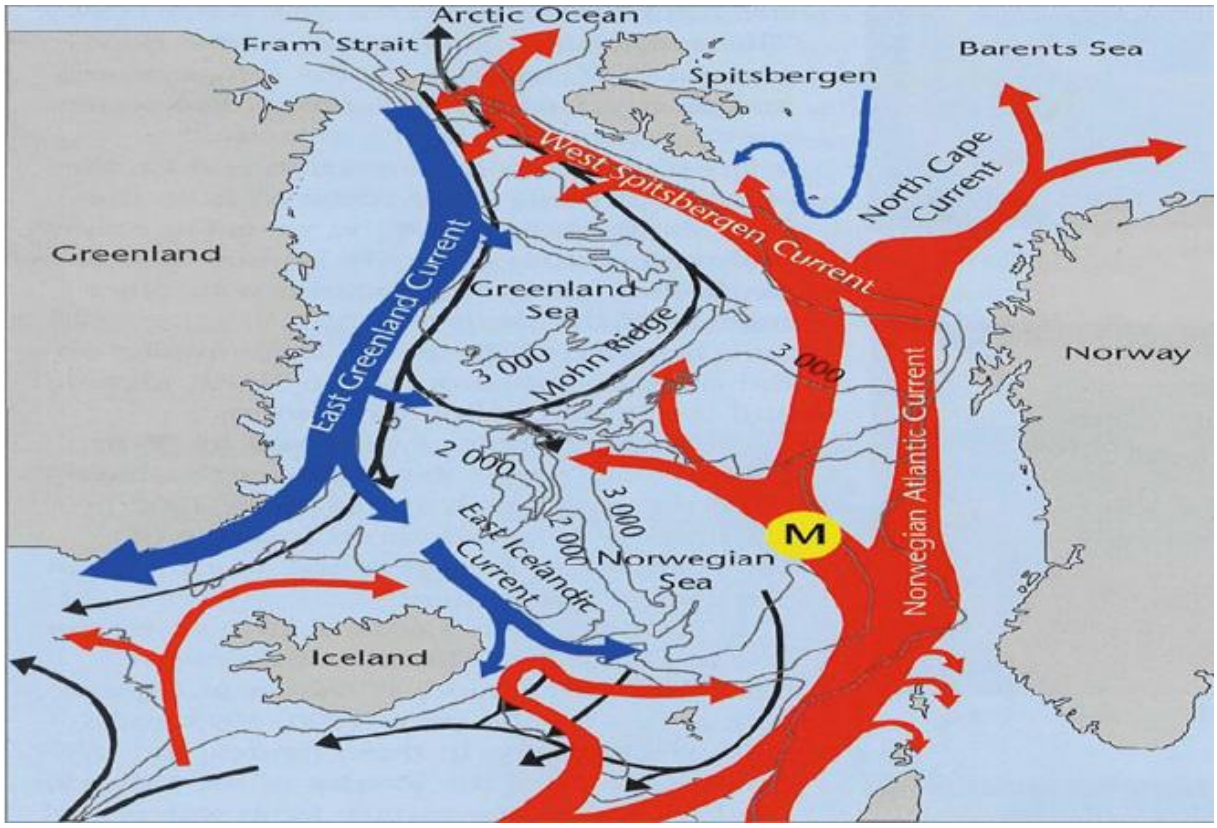


*Figure 7: Bathymetric map of the Nordic sea showing major surface currents. Red arrows represent warm and saline water from the Atlantic. Blue arrows represent cold and low saline polar water (Dylmer, et al., 2014).*

## 3.3 Meteorology and climatic setting

The climatic setting of a region is a result of atmospheric pressure, wind patterns and interactions between atmosphere and the surface ocean. The climatic region of the Nordic sea is divided from Iceland to Bear Island by the polar easterlies and the westerlies. This is the mean position of the Arctic Front and it separates the Norwegian Sea from the Greenland- and Iceland sea (Hopkins, 1990).

The atmospheric surface pressure field for the northernmost latitudes consist of 2 low pressure cells and 2 high pressure cells. The two low pressure cells are the Icelandic and the Aleutian which is located at 60$^{o}$N in the North Atlantic and the North Pacific. The two high pressure cells are the Siberian and McKenzie which is located at the latitude of 70$^{o}$N. The main influence in the GIN sea is the Icelandic low and secondarily influencer is the high pressures over the Polar Sea. The temperature gradient between north and south of Iceland contribute to the seasonal intensity of the Icelandic low. The Icelandic low is most intense during winter because at that time the temperature gradient is at its greatest. The low-pressure cell comprises all of the Barents Sea and much of the Eurasian Basin nearly to the North Pole. Cyclones are created from the Icelandic Low and traveling towards the Barents Sea. The Elongated portion of the low is called the trough. On the southeastern portion of the trough the winds are consistently from the southwest. To the north of the low is the easterlies, which is fairly steady. In March, the easterlies extend further southward, forming a line from Iceland to North Cape. During summer, the atmospheric pressure gradients are minimal, and the Icelandic low remains as a weak low (Hopkins, 1990). The different wind directions in the GIN seas throughout the year is presented in Figure 8.

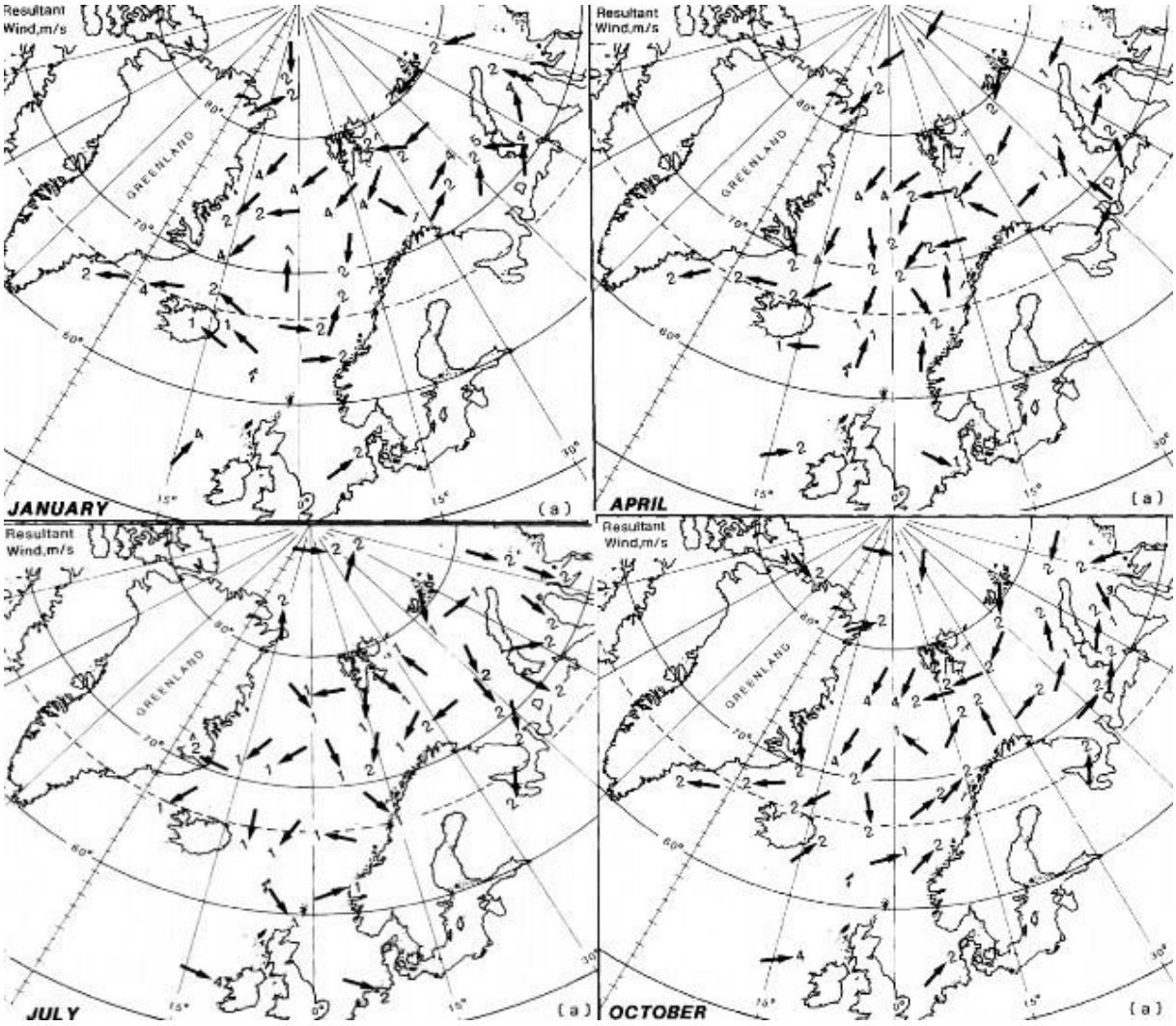


*Figure 8: The different wind directions from the months January, April, July and October are presented. The arrows indicate wind direction, and the numbers correspond to windspeed in m/s (Hopkins, 1990).*

In addition to wind patterns and atmospheric pressure the GIN sea is dependent on the heat and water exchange. The GIN Sea presents a large non uniformities for the ocean-atmosphere exchange. Some areas have high albedo due to ice coverage while some is ice-free. The area is divided into the Arctic ice-open water conditions and the Polar ice-covered conditions. Over ice-covered regions the reflection of incoming radiation is increased and due to the high latitude, the incoming radiation is decreased. In addition, the evaporation and heat losses from ocean to atmosphere is reduced due to the ice isolating the ocean from the atmosphere. While in areas with no ice the reflection of radiation is less and the evaporation and heat losses are greater (Hopkins, 1990).

The ice in the GIN sea occurs mostly as pack ice, icebergs, ice island, landfast ice and ice of the marginal ice zone. Pack ice is originated over the Siberian Continental shelf and drifted to the Polar Sea via the EGC. The thickness is normally 3-4m. Icebergs is originated from

glaciers and thus considered a source of runoff. Land fast sea ice grounded in shallow areas consistent over several years. Ice islands are large ice sheets which have broken off from the Polar Ice shelf. The thickness is often from 20-50m. Marginal ice zone is the boundary between the pack ice and the open waters. This zone is the main region for ice growth and decay and is therefore sensitive to variability in climate. Because of self-regulation within an annual cycle, there is a year-to-year variability in the sea ice. Station 9,10 and 11 lies within the area which can be covered by sea ice *(see Figure 9).* During cold winters, the production rate of sea ice increase but with a correspondingly rise in the amount of ice accessible for melting during the summer. In addition, the presence of sea ice cover inhibits heat loss and result in accumulation of heat underneath the ice. This can potentially influence the wind patterns and act as a feedback on sea ice distribution (Hopkins, 1990).

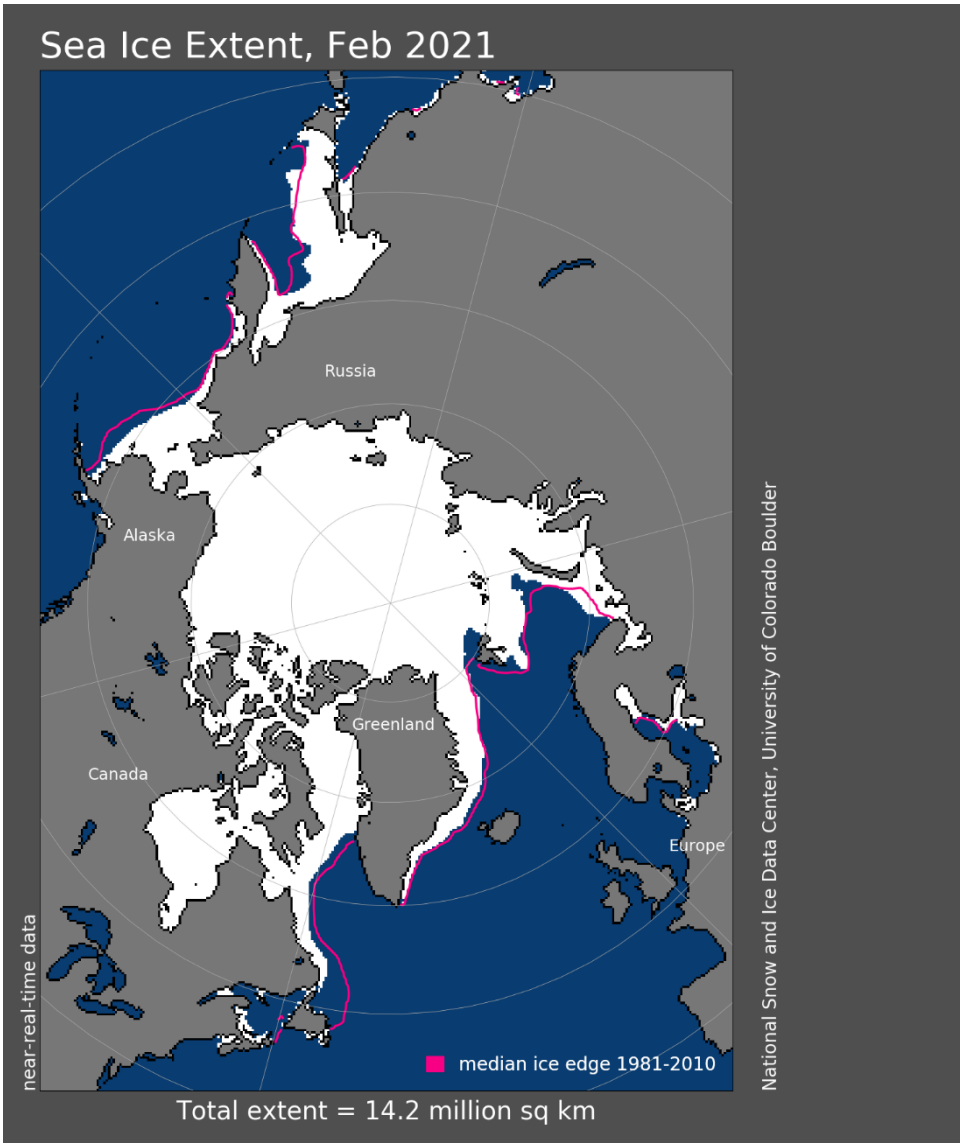


*Figure 9: Sea ice extent February 2021. (National snow and ice data center, 2021)*

## 3.4 Productivity, sediment flux and terrestrial influence

Phytoplankton represents the primary marine pelagic ecosystem and the main constituent of the biological pump responsible for vertical carbon flux to the sediments. Thus, the amount of phytoplankton in an area influences the amount of organic matter input in the sediments (Skogen, et al., 2007). Phytoplankton are subject to different physical forcing factor such as nutrient supply, temperature and light. The next subchapter investigates the nutrients, the organic matter input, the sediment flux, and the terrestrial influence in the Nordic Seas.

### 3.4.1 Physical-environmental parameters

Figure 10 shows a transect from station 1 to station 16 with the bathymetry data together with different physical-environmental parameters.

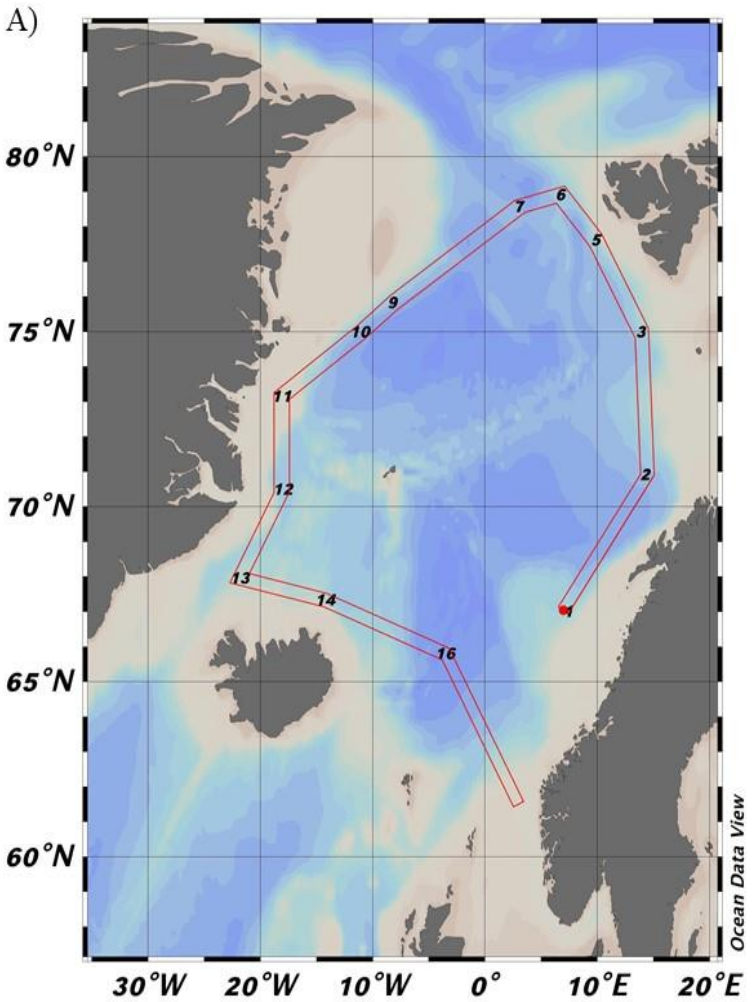

B)

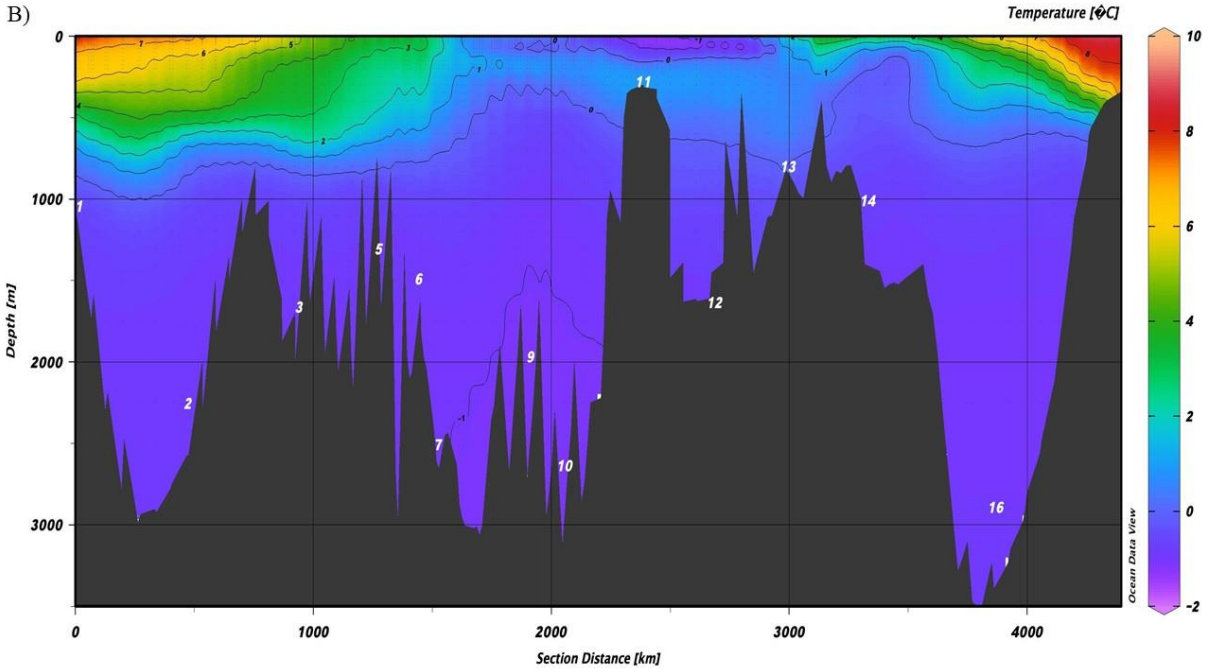
Temperature [°C]
Depth [m]
Section Distance [km]
Ocean Data View

C)

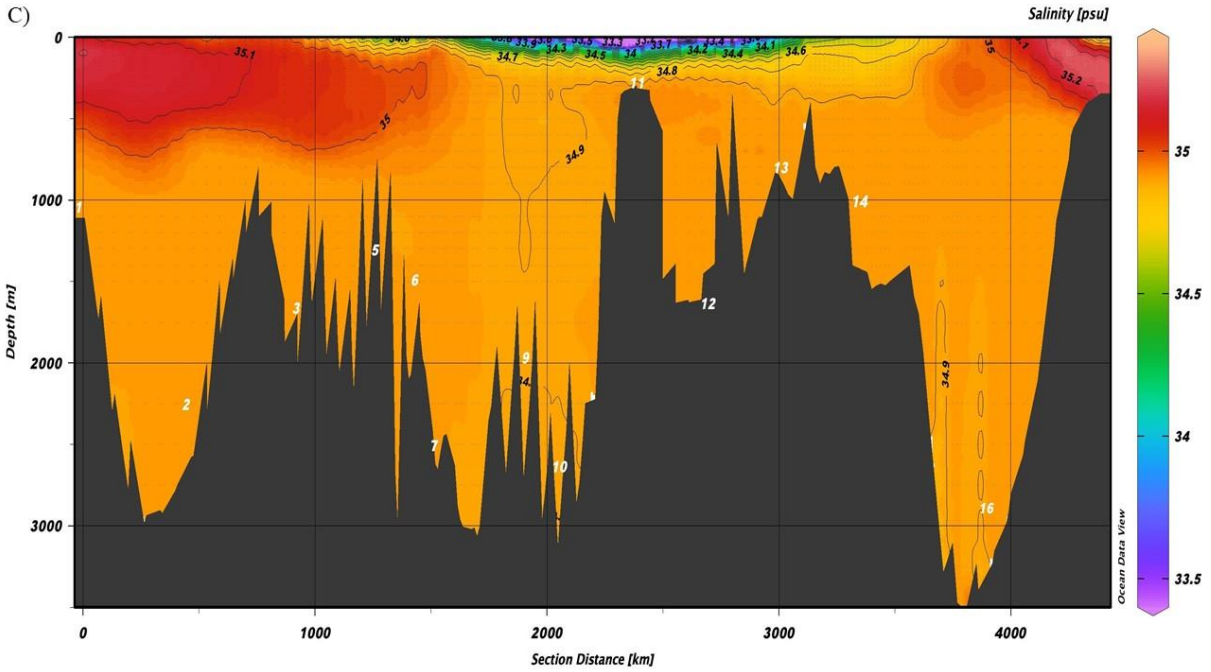
Salinity [psu]
Depth [m]
Section Distance [km]
Ocean Data View

D)

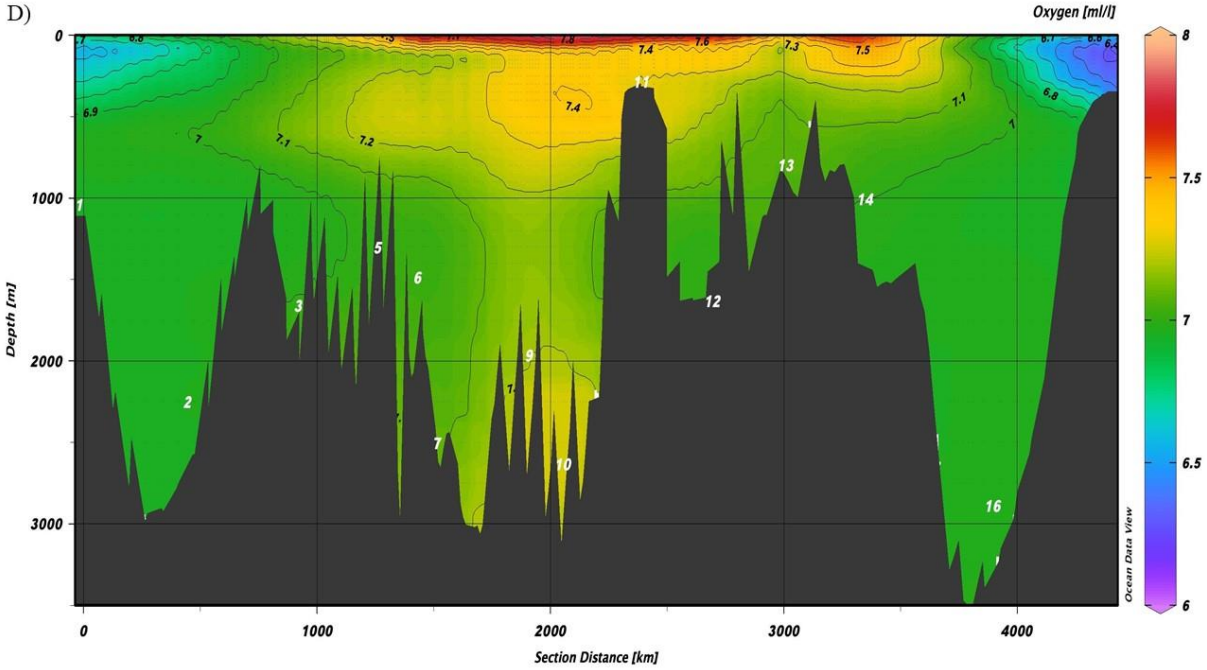
Oxygen [ml/l]
Depth [m]
Section Distance [km]
Ocean Data View

E)

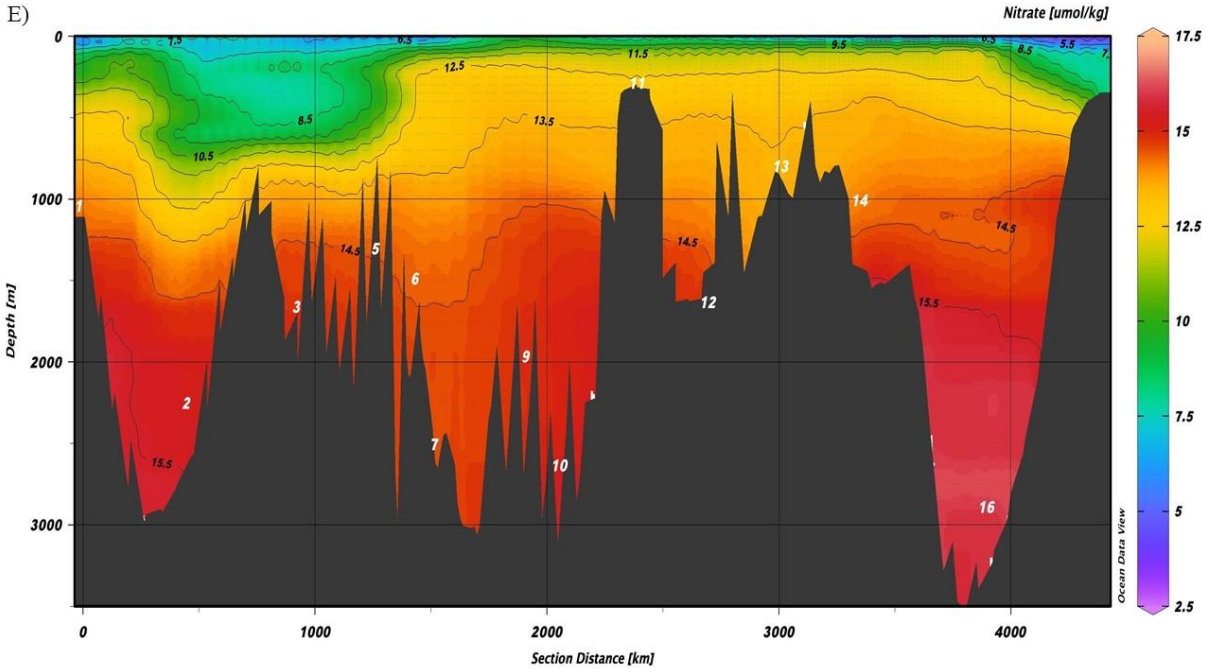
Nitrate [umol/kg]
Depth [m]
Section Distance [km]
Ocean Data View

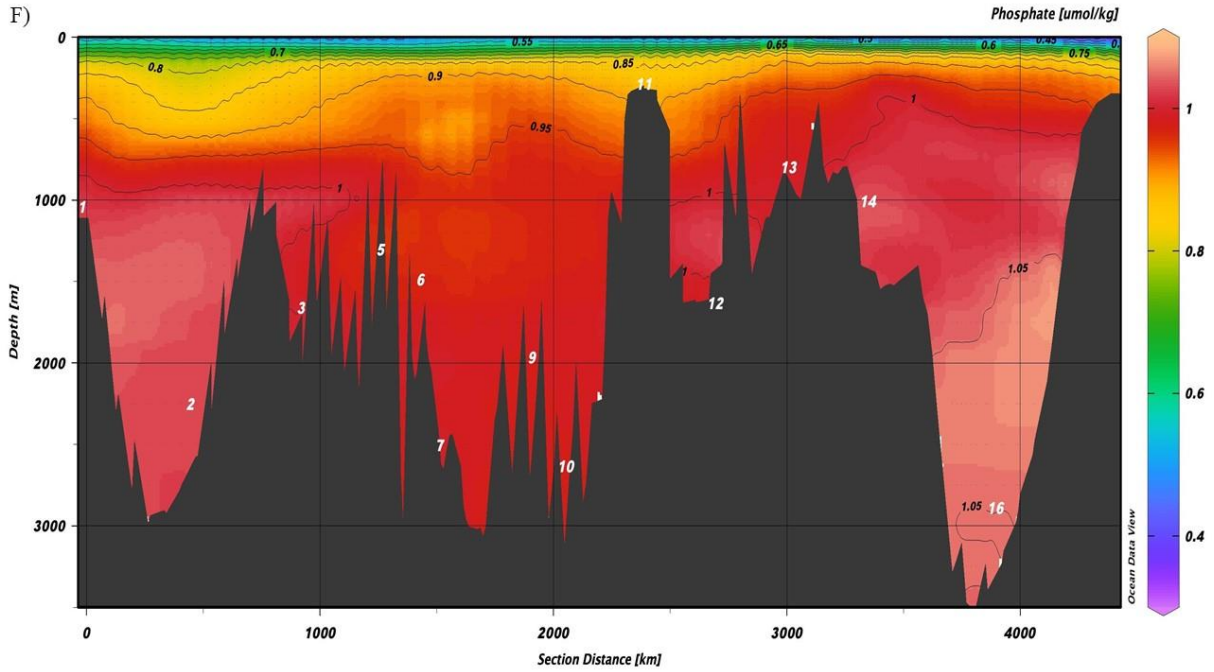


*Figure 10: A section from station 1 to station 16 is presented together with the bathymetry and different parameters. From B-F the different stations are indicated with white numbers. A) map over the cruise path included the stations and its location. B) temperature given in degree Celsius C) Salinity given in psu. D) Oxygen given in mg/L. E) Nitrate given in µmol/kg. F) Phosphate given in µmol/kg. Data Is collected from the gridded data se fog Gouretski and Koletermann 2004 gridded global hydrography. Plot made by Ulysses Ninnemann in Ocean Data Viewer version 5.4.0 (Mac OS X) copyright 2021 Reiner Schlitzer.*

The temperature in the bottom water along the section varies between +1 to -1 °C. The deeper the area the colder the bottom water. The salinity is approximately the same for the entire section, about 34.8 to 34.9psu. Oxygen concentration varies from station to station. Highest concentration is found along the east Greenland coast where station 9, 10 and 11 is situated. Similar to oxygen, the nitrate varies along the section. Highest values are found along the transect from Iceland to Norway and along the Norwegian coast. Lowest values are found in shallow areas, in the transect from Svalbard to Greenland and along the East Greenland coast. Phosphate varies from 0.85 to 1.05µmol/kg with similar trend as Nitrate with highest concentration found along the transect from Iceland to Norway and along the Norwegian coast and lowest concentration found from Svalbard towards Greenland and along the east Greenland coast.

### 3.4.2 Sediment transport in the Fram strait and on Svalbard continental margin (Station 5-7)

Station 6 and 7 lies within the Fram Strait. This area is influenced by the warm northward flowing West Spitsbergen Current on the eastern side and by the cold East Greenland Current on the western side. Sediments are added to the area by the current. The Atlantic water in the

WSC submerges beneath colder and fresher Polar water north of $80^0$N. Due to this interaction the extent of the sea ice cover is highly variable with permanent and seasonally ice cover as well as permanent ice-free areas. Ice-rafted material can be contributed to the area by the sea ice and investigations has confirmed that the central and eastern regions have a significantly high contribution of ice-rafted material (Hebbeln & Berner, 1993). Other processes contributing to sediment transported to the area are sediment gravity flow and wind transport. Near bottom transport is important across the continental slope of Svalbard while central Fram strait is unaffected by any significant supply of this material (Hebbeln & Berner, 1993). Station 5 lies on the south part of the continental margin of Svalbard and is therefore more affected by near bottom transport. The presence of terrigenous organic matter in near-bottom transport are indicated by light $\delta^{13}C$ values. Near-bottom transport of terrigenous material is present from land to the deep Fram Strait but with significantly more supply on the slope (Hebbeln & Berner, 1993). Low $\delta^{13}C_{DIC}$ values are expected for station 5 and 7 but lighter $\delta^{13}C_{DIC}$ values are expected for station 5 versus station 7.

### 3.4.3 Sediment transport in the Norwegian- and Greenland-sea (Station 1,2,9, 10 and 11)

The Norwegian coast is influenced by the warm and nutrients rich north Atlantic water which is favorable for phytoplankton (LaMourie, 2020). On the Norwegian continental margin, the fluxes of organic carbon to the sediments are estimated to 3.3-13.9mg C $m^{-2}d^{-1}$ (Sauter, et al., 2000). The organic carbon flux on the seasonally ice-covered east Greenland continental margin is lower, between 1.3 and 10.9mg C $m^{-2}d^{-1}$ To the extent that rates of organic matter input to the sediment influences the $\delta^{13}C$ values of the DIC in pore waters, station 1 and 2 from the Norwegian slope are expected to be lower than in station 9 and 10 from the east Greenland continental margin due to higher organic carbon flux in these areas. The organic carbon flux on the east Greenland shelf on the other hand is higher, between 9.1-22.5mg C $m^{-2}$ $d^{-1}$ being added and therefore the $\delta^{13}C_{DIC}$ values of station 11 are expected to be lighter than station 9 and 10 if the core sites are regionally representative (Sauter, et al., 2000).

### 3.4.4 Net productivity

The different fluxes in the Nordic Seas correspond to higher primary production in the eastern part of the Nordic Seas and is likely explained by the seasonally ice cover in the Greenland Sea and the different water masses dominating in the different regions *(see Figure 11)* (Sauter, et al., 2000). As the Atlantic water moves northward a downward (deep) mixing happens due to cooling at the surface and to wind driven turbulence. A deeper mixed layer is

formed during winter season. The turbulence mixes nutrients up into the euphotic zone and accumulate during the winter. In the spring the mixed layer becomes shallower, and the winter nutrients are available for the phytoplankton. A great explosion of phytoplankton happens, known as spring blooms. The high productivity along the Norwegian margin is due to this spring bloom (Ibrahim, et al., 2014)

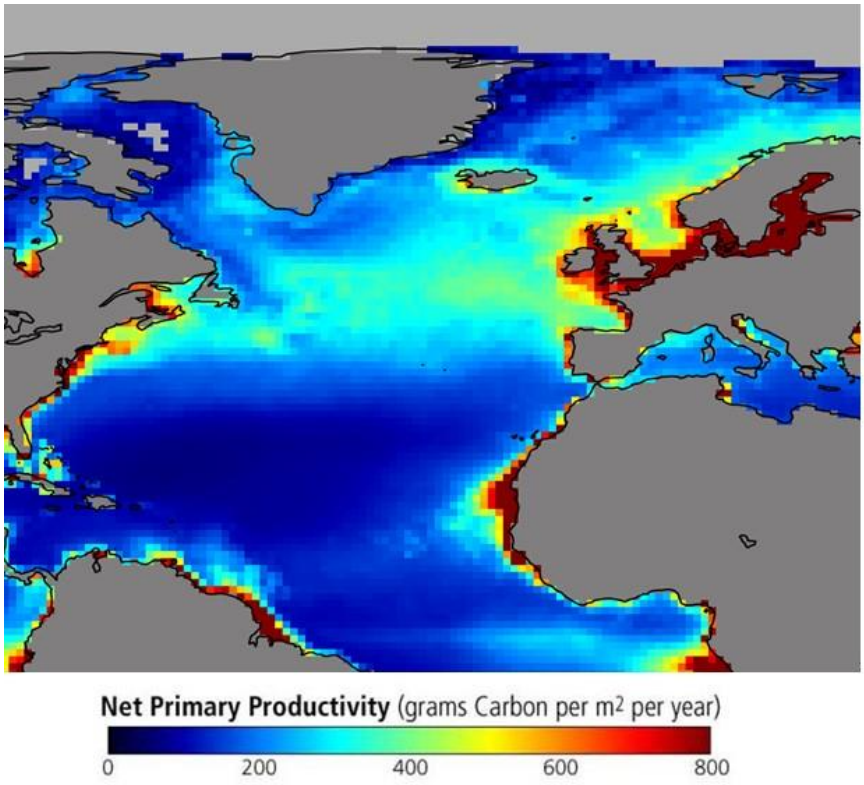


*Figure 11: A map with the net productivity of carbon in the surface water, indicated in grams carbon er $m^2$ per year. Red color being the highest productivity and blue color being the lowest (Gregg, 2003).*

# 4. Material and methods

This chapter provides an overview of the shipboard analyses and procedures on the CIAAN CE20009 cruise. In addition, information about the laboratory work following the cruise, the methods employed in this project and the errors connected to the methods are briefly presented.

## 4.1 Preparation before ship

Due to the difficulty of using microbalances onboard a moving vessel all standard materials had to be weighed in prior to the cruise. The preparation procedure used for standards was to fill 60ml exetainer with 200-400µg of different carbonate standards such as CM 12, NBS 18, NBS 19 and CO 8 (IAEA, n.d.). These were then capped with betyl rubber septa and stored for offshore analyzes. Further information about these standards is described in section 4.2.2.

## 4.2 Sampling, coring and shipboard analyses

Marine cores, including multicores, box cores and gravity cores, were recovered during the 2020 cruise of R/V Celtic Explorer in the Nordic seas, as part of the CIAAN project *(See Table 1)*. Additionally, CTD samples were collected. A map over the different station and the locations of the stations where samples were collected can be seen in Figure 4.

### 4.2.1 Sampling of pore water and bottom water

The same order of sampling was done in all stations. First the CTD was deployed and sampled for bottom water, then the gravity core and then the multicore/ box core. If the multicore/ box core was successfully then the sampling of pore water from this core was done before the sampling of pore water from the gravity core.

| Station number | Depth of the station (m) | Multicore (Name) | Gravity core (Name) | Box core (Name) | CTD (Name) |
|---|---|---|---|---|---|
| 1 | 1050 | X | GC-010301 | BC-010601<br>BC-010602 | X |
| 2 | 2170 | X | GC-020301 | X | CTD-0202-Bottle number |
| 3 | 1742 | X | GC-030301 | X | CTD-0302-Bottle number |
| 5 | 1296 | MC-050401A | GC-050301 | X | CTD-0502- Bottle number |
| 6 | 1490 | X | X | X | CTD-0602- Bottle number |
| 7 | 2520 | X | GC-070301 | X | CTD-0702- Bottle number |
| 9 | 1985 | X | GC-090301 | BC-090601A | CTD-0902- Bottle number |
| 10 | 2637 | MC-100401A | GC-100301 | X | CTD-1002- Bottle number |
| 11 | 287 | MC-110401A | X | X | CTD-1102- Bottle number |
| 12 | 1674 | MC-120401A | X | X | CTD-1202- Bottle number |
| 13 | 779 | X | X | X | CTD-1302- Bottle number |
| 14 | 1008 | X | X | X | CTD-1402- Bottle number |
| 16 | 2890 | MC-130401A | X | X | CTD-1602- Bottle number |
| 17 | 2647 | X | X | X | CTD-1702- Bottle number |

*Table 1: An overview of stations, depth, and the names of all the samples taken on the CIAAN cruise in September 2020.*

### *CTD:*

A CTD instrument measures the conductivity, temperature and depth in the ocean and in addition it measures the salinity, oxygen concentration, fluorescence and turbidity (Ocean exploration and research, n.d.). The CTD used on the cruise had 24 Niskin bottles for water sampling and was lowered until approximately 10-20m from the seafloor. Then the CTD was hoisted up toward the surface, stopping to sample at different depths on the way up where different Niskin bottles were triggered to close, trapping samples inside the bottle from the water masses present at each depth. Once the CTD was on board the sampling from the different Niskin bottles began. A valve on top of the bottle was opened and a gas tight silicone hose was attached to a tap on the bottom of the bottle. The water inside the bottle was sampled into a 60ml glass serum bottle with a betyl rubber septum. The bottle was rinsed two times with the seawater from each bottle and then sampled. Each glass sample bottle was labelled with a number corresponding to an identically labelled Niskin bottle. After sampling, each serum vial was capped with a stopper to reduce gas exchange and brought inside the wet lab for sub-further sampling (see section about pore water and bottom water extraction below).

### *Gravity core:*

The gravity core was lowered down the water column until 5-10 meter above the seafloor. It was then held there some minutes to stabilize in order to optimize the probability of perpendicular penetration of the sediments. Subsequently, the gravity core was lowered into the sediments trapping the sediments inside the core. Then the core device was hoisted up on deck. Immediately after recovery the core was cut into 1m long sections and sealed with caps and tape. The sections were then brought inside the wet lab. A drill was used to create small holes every centimeter in the upper part of the gravity core, multicore and box core. After approximately 10cm sample spacing increased to around 2-3 cm as the highest rates of change (geochemical gradient) were expected near the sediment water interface.

### *Multicore:*

Multicores were taken in addition to gravity cores. The multicore lander used on this cruise can sample in 4 tubes *(see Figure 12)* with a diameter of 100mm and a length of 600mm (KC Denmark AS, n.d.). The multicore device is used to recover the sediment-water interface undisturbed and cores of up to 40 cm sediment depth.  The devise was lowered down to the seafloor and when the instrument touched the sea floor a release mechanism allowed the weighted inner frame carrying the sampling tubes to descend slowly down into the sediment

column. After the tubes were filled with sediment a spring-loaded lid closed on top of each tube creating a vacuum that traps the sediments inside the tube. When the tubes emerged from the sediment a spring-loaded shovel was released under the tubes and covered the ends. The device was then brought up onto the deck. Another shovel with a handle was used to extract the tubes from the multicore and transport them safely to the wet lab where the tubes were capped, sealed and stored until analysis *(see Figure 13).* For pore water sampling some tubes were predrilled with holes every cm alternating sides of the core barrel so that the hole spacing was 2 cm on each side but 1cm sampling could be achieved. Holes were taped over prior to deployment *(see Figure 14).* Upon recovery, the tape was punctured at the locations where samples were taken from the pore water.


*Figure 12: The KC Denmark multicore used on the cruise (KC Denmark AS, n.d.).*

*Figure 13: The multicores were stored vertically in the wet lab until analyze. (Photo taken by Malin Lunde)*


*Figure 14: The first sampling of pore water was done with the core standing vertically, on later stations the core was sampled lying on the bench horizontal (Photo taken by Malin Lunde).*

*Box core:*

Because the multicore did not function perfectly under poor weather conditions, box core was taken as a backup alternative so that some information from the stations could be collected. The box corer used on this cruise was a Reineck box core (Flanders Marine Institute, n.d.). It was lowered down to the seafloor and when the machine hits the seafloor the box core was pushed down into the sediments. After the box core was filled with sediments a spade-closing lever arm traps the sediments inside the box. The box core was then brought up to the surface. Once the box core was secured on deck, the central box containing sediments was detached and transported into the lab. The sediment was subsampled using two plastic tubes *(see Figure 15).* These were pushed down in the sediments in the box and then capped in both ends. Holes were drilled in the same matter as with the multicore and then left taped over until pore water sampling.

*Figure 15: Holes were drilled in the box core and then the holes were taped until further analyzes. The cores were first sampled vertically then on later stations the cores were sampled horizontally.*

### 4.2.2 Carbon analyses using a Delta Ray.

A Delta Ray is an infrared laser-based spectrometer *(see Figure 17).* It measures $CO_2$ concentration, $\delta^{13}C$ and $\delta^{18}O$. The instrument has a universal reference inlet and an autosampler and was used here to measure $CO_2$ derived from dissolved inorganic carbon (DIC) in bottom water and pore water. The system is able to provide high precision measurements in the field and was used on this cruise for isotope results in near real time (Mørkved, n.d.). The results from the Delta Ray are reported as ‰ on a VPBD scale. The ‰ notation is representing parts per thousand. It presents parts per thousand difference between the carbon 13 to carbon 12 ratio in the sample relative to the ratio of the international VPDB standard as mentioned in part 2.1 *(see Equation 1).* In order to calibrate the instrument, different reference materials (standards) are analyzed simultaneous with the water samples. The international standards used in this thesis are CO8 (carbonatite with a $\delta^{13}C_{DIC}$ signature of -5.764‰ and a standard deviation of 0.032), NBS18 (carbonatite, -5.014‰, 0.035) and NBS19 (limestone, 1.95‰) ordered from The International Atomic Energy Agency (IAEA, n.d.). In addition, a house standard called CM12 with a $\delta^{13}C_{DIC}$ signature of 2.10‰ and a standard deviation of 0.03 is used. Two corrections are checked for in the $\delta^{13}C_{DIC}$ data, a size correction and a drift correction before its calibrated with the standards. The data was checked for linearity or the degree to which the same value of a standard is found when measuring the standard multiple times at different signal (or sample) sizes. If there is more or less of the standard then the values should remain the same but if there is a change in $\delta^{13}C_{DIC}$ with the amount of standard then this must be corrected for, which is the linearity correction. The standards were checked for linearity and no non-linearity was present in the data. If a sample changes value depending on its position in the run (e.g. different values if it is one of the first samples vs one of the last samples in one run) this is called drift and it requires a correction The same standard is run periodically throughout the run in order to assess within run drift. In some cases a small drift correction was applied and is relevant for the results from a number of stations (GC03, MC05, CTD05, BC09, GC09, CTD10, MC11, CTD11, MC12, CTD12 and MC16.). The reproducibility of standards through the run gives an indication of the precision of the analysis. Based on replicated analysis of CM12 the standard deviation for the Delta ray in this thesis is 0.145‰ or better depending on the run. Most runs, and standards, had a precision of 0.1‰ or better but a few runs were influenced by changing environmental conditions and machine stoppage.

*Preparing standards for carbon isotope analysis with a Delta Ray:*

The method involves 3 steps. First the preparation of standards as describes section 4.1 where 60ml exetainers were added 200-400 µg of different carbonates (CO8, NBS18, NBS19 and CM12). Then the exetainer were capped with betyl rubber septa. Prior to running onbard the ship, the exetainers were flushed with $CO_2$ free synthetic air (78% $N_2$, 21% $O_2$, 1% Ar, 5.0 quality) in the Delta Ray to remove any $CO_2$ in the exetainer headspace. (Debajyoti & Grzegorz, 2006). Next, 3 drops of phosphoric acid were added to the exetainers with a syringe to react with the carbonates. The dissolution of calcium carbonate proceeds as followed:

$$CaCO_3 + H_3PO_4 \rightarrow CaHPO_4 + H_2O + CO_2$$

*Equation 5:The dissolution of calcium carbonate by adding phosphoric acid in the sample (Debajyoti & Grzegorz, 2006)*

The exetainers were left in an oven at 60ºC for at least 4-12 hours to react. All the carbon present in the carbonate is stoichiometrically converted into $CO_2$ gas *(see Equation 5).* The standards are used to calibrate the machine and to monitor and evaluate the quality of the data.

*Preparing glasses for samples:*

A very similar process was used for the preparation of exetainer for the analyses of pore water and bottom water. First, 4 drops of phosphoric acid were added to exetainers and then exetainers were capped with septa and flushed in the Delta Ray with synthetic air, leaving the exetainer empty of $CO_2$.

*Bottom water and pore water sampling:*

Bottom water was extracted from the glass serum bottles collected from the CTD. The stopper was removed and a 20ml syringe was connected to a needle. 1ml of bottom water was extracted from the glass bottle and added to the 60ml prepared exetainer containing acid and synthetic air. For the pore water and bottom water sampling from the cores, the tape was punctured and rhizons, number 19.21.23F (Rhizosphere Research products B.V., Wageningen, Netherlands) with the pore size of 0.15µm, were quickly inserted through the holes and into the sediments. 20 ml syringes (type, brand) were connected to the rhizons and extracted 5ml of water (if possible) from the core, 1ml for $\delta^{13}C_{DIC}$ analyses and 4 ml for oxygen and pH analyses. If not possible then the 1ml for the $\delta^{13}C_{DIC}$ analyses was prioritized. The first sampling of water was done with the core standing vertically *(see Figure 16),* on subsequent stations the core was sampled when lying horizontal on the bench. The procedure was changed due to concern that as pore water was withdrawn from the lower section's gravity might facilitate the downward migration of pore water from the upper sections where

pore water concentrations tend to be higher due to lower sediment compaction. Bottom water was additionally collected from the multicore at the bottom water-sediment interface. Subsequently, bottom water was siphoned off prior to pore water sampling to avoid drawing bottom water down into the sediments as pore waters were drained out. After pore water recovery, the syringes were removed from the rhizons, a needle was attached, and 1ml of pore water was injected through a butyl rubber septa of previously prepared 60 ml exetainers (see section 4.2.2) and 3ml were added to small containers for $O_2$ and pH measurements. The pre-flushed exetainers contained 4 drops of 100% phosphoric acid ($H_3PO_4$) and exetainers with pore water samples were stored in a fridge until analysis; usually begun within hours of finishing the sampling. The aim was to minimize the time between sampling and analysis to reduce the chance for sample alteration due to biological activity/degradation within the water sample.


*Figure 16: The box core was sampled vertically with the spacing of 1-3cm (Photo taken by Malin Lunde).*

*Analyzing pore water:*

1ml of pore water were added to the prepared exetainers and left in a fridge until analysis. The $H_3PO_4$ in the exetainer drops the pH in the water and reacts with the pore water converting the dissolved inorganic carbon (DIC) in the water to aqueous $CO_2$ (see Bjerrum diagram in section 2.1). After a couple of hours, $CO_{2\,(aq)}$ equilibrate with $CO_{2(g)}$ due to the exetainer headspace containing no $CO_2$ before the pore water was injected to the exetainer. The $CO_2$ in the headspace is then sampled by a flushing needle on the Delta Ray and the carbon isotope ratio of the released $CO_{2(g)}$ is measured. The $\delta^{13}C_{DIC}$ in the $CO_2$ is determined via a calibration procedure in the Delta Ray using gas standards run in sequence with the sample (Assayag, et al., 2006)


*Figure 17: The setup of the Delta ray in the dry lab at RV Celtic Explorer (Photo taken by Malin Lunde).*

### 4.2.3 $O_2$, pH and nutrients analyses

In addition to the measurements and analyzes above, $O_2$, pH, phosphate and nitrate measurements were done on the pore water samples. 4ml of pore water were added to a container and $O_2$ was measured using professional plus multiparameter instrument *(see Figure 18)* from YSI (YSI, n.d.). This was not the instrument that was intended to be used on the cruise. The original one (microprobes for in-situ analyses) had better precision but was not delivered to the University of Galway before the cruise. The hand held $O_2$ and pH measurements are done in an open system under the influence of the atmosphere and therefor some interaction between the pore water and the atmosphere happens. In addition, temperature is an important parameter for the instrument so a second vial was used so that the temperature could be analyzed in parallel with the sample *(see figure 18).* For oxygen, the instrumental accuracy given is ± 0.2 mg/L but due to the way it was measured this accuracy does not apply for the data collected in this thesis. The precision of the measurements will be further discussed in section 6.1. After the $O_2$ values were recovered, the pH was measured using WTW pH/ION 735 meter *(see figure 19).* This ion meter was calibrated for each station and the accuracy for this parameter is ± 0.004 under ideal conditions but due to the method used to measure the pH on the cruise and the time it took to calibrate the parameter, this accuracy probably do not apply for the data collected in this thesis. Multiple measurements to test the uncertainty of the $O_2$ and the pH data were done but were not sufficient due to the exetainer being contaminated by air. The contaminated measurements are included in the appendix and are denoted in red color. Pore water for the phosphate and the nitrate were collected after the pore water for the DIC isotopes, oxygen and pH and a different method was used. The sampling was done by coworkers on the ship and further analyze of these samples were done later at the National University of Ireland, Galway by Audrey Morley (unpublished, pers.comm). The initial nutrient results for some stations were received 3 weeks before the deadline for this thesis (some of it just days before the deadline), limiting the use and incorporation of the data.

*Figure 18: The professional plus multiparameter instrument and the setup of the instrument in the wet lab (Photo taken by Malin Lunde).*


*Figure 19: pH were measured using WTW pH/ION meter (Photo taken by Malin Lunde).*

# 5. Results

In this study, I investigated the carbon cycle in sediments around the circumference of the Norwegian sea along the Norwegian, Svalbard, Greenland and Icelandic margins. The cycling of carbon is reconstructed using carbon isotopes from pore waters. In the following subchapters, the results from the carbon isotope analyses, the oxygen, pH, phosphate and nitrate analyses are presented separately and plotted versus depth. The carbon isotopes values are given in per mille (‰) relative to the VPDB standard with a precision of ± 0.145‰. Oxygen concentration are given in mg/L. All results are tabulated in the Appendix. As a reminder of the geographical position of the different stations a map is presented in Figure 20.

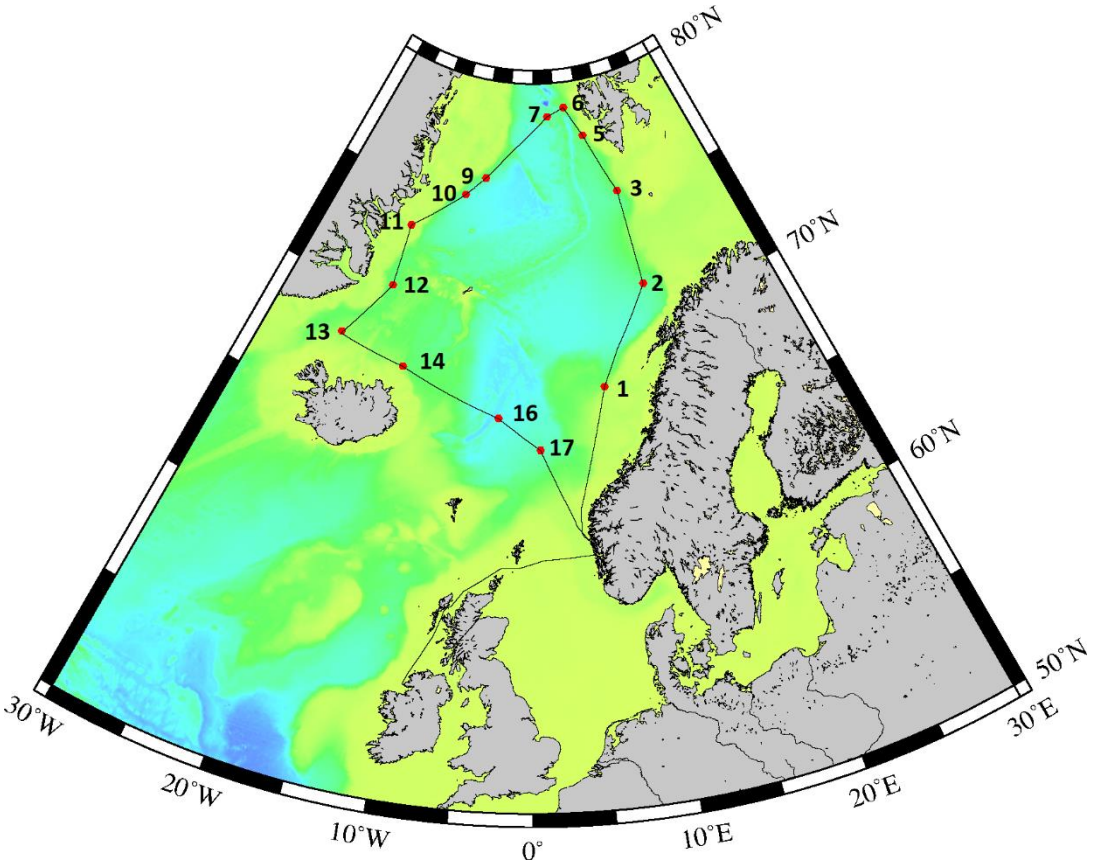


*Figure 20: Map with the different stations collected on the CIAAN cruise.*

## 5.1 Station 1 (66°58.10'N 07°38.2'E, 1042m water depth)

Two box cores, with a length of 25cm, and one gravity core, with a length of 435cm, was collected at Station *(see Figure 21).* No bottom water samples were extracted at station 1 because of the CTD and the multicore failing.

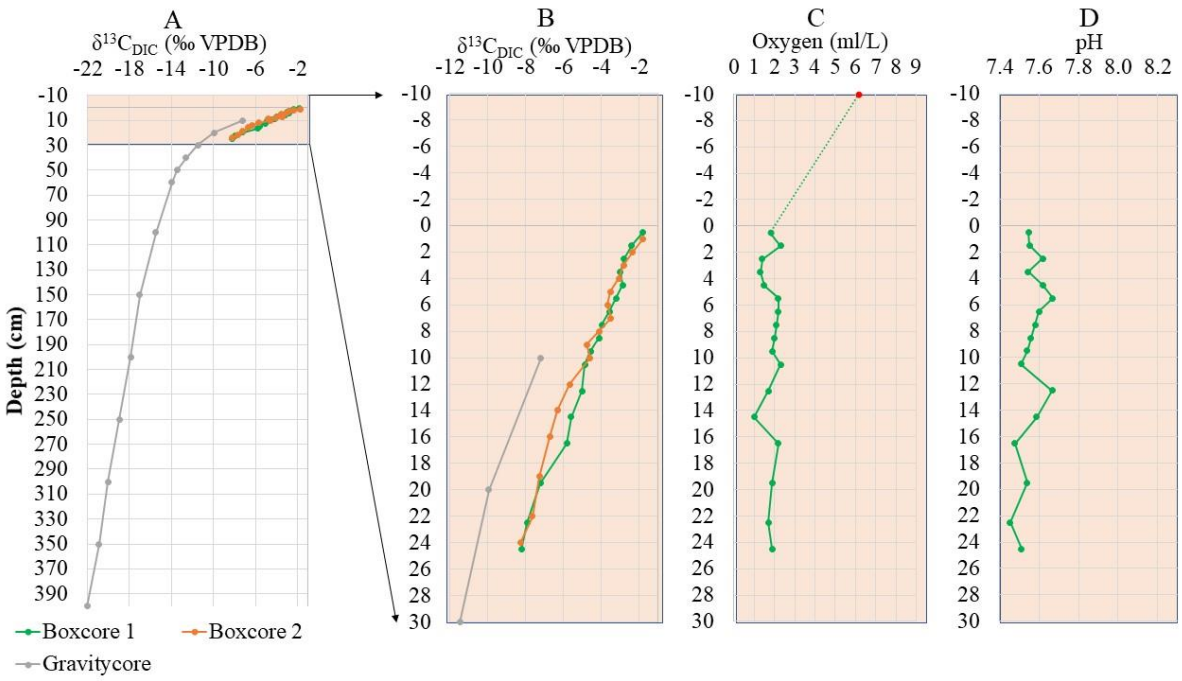


*Figure 21: Bottom and pore water parameters plotted versus depth in sediment from station 1. A) $\delta^{13}C$ of DIC downcore from 2 box cores and 1 gravity core. B) Blow up of $\delta^{13}C$ of DIC changes in the upper 30cm of the sediments. C) The oxygen concentration in pore water from upper 30cm of the box core—red data point represents bottom water $O_2$ from the CTD. D) pH values of pore waters extracted from the upper 30cm of the box core*

Two adjacent sub cores (push cores; referred to hereafter as box core's 1 and 2) were taken from the box core at station 1 and pore waters were extracted and analyzed from each as a check on pore water signal reproducibility. Box core 1was sampled for pore water beginning at 0.5cm below the sediment water interface, box core 2 beginning at 1cm. The $\delta^{13}C_{DIC}$ values in both box cores are similar and show a trend toward decreasing values with increasing depth in the sediment. Pore water carbon isotope values in the uppermost sample of both box core 1 and 2 (0.5 cm and 1.0 cm depths, respectively) were -1.8‰. This value is significantly lower than regional bottom water values (e.g., those from other stations and climatology) which tend to have positive delta values, typically around 1.0‰ (see other stations). At approximately 6 cm both cores have a $\delta^{13}C_{DIC}$ of -3.6‰. At 8cm both cores have a value of -8‰ and at the deepest measurement both have a $\delta^{13}C_{DIC}$ of -8.2‰. The isotopic values diverge slightly between the two cores in the interval between 12cm-17cm with the largest offset between the samples at 16 and 16.5cm. At this interval box core 1 has a $\delta^{13}C_{DIC}$ of -5.8‰ and box core 2 a value of -6.7‰, a difference of 0.9‰.

Pore waters were extracted and analyzed in one gravity core as well. Measurements were done in the upper part of the core to test and compare the results with the measurements from the box cores. The gravity core had $\delta^{13}C_{DIC}$ of -7.2‰ at 10cm and -9.9‰ at 20cm while the

box core had a $\delta^{13}C_{DIC}$ of -4.9‰ at 10cm and -7.2‰ at 20cm. The depth offset in the $\delta^{13}C_{DIC}$ values in the gravity core curve (similar values observed ˜10cm shallower than in box cores *(Figure 21, panel B*) could potentially indicate missing sediment at the top of the gravity core. Loss of core top sediment can frequently occur with this device during coring and core retrieval/handling due to poor sediment consolidation at the sediment water interface. The downcore isotope results show that the $\delta^{13}C_{DIC}$ decrease with depth is higher in the uppermost part of the core. $\delta^{13}C_{DIC}$ values decline by 6.4‰ over the top 25 cm of the sediments while in the rest of the 375cm long core the $\delta^{13}C_{DIC}$ decrease by an additional 13.7‰.

Pore water oxygen concentrations *(Figure 21, panel c)* are low in comparison to bottom water values and show little variability downcore. The oxygen concentration in the bottom water (from the $O_2$ sensor on the CTD) is 6.1 mg/L. The oxygen concentration is already as low as 1.8 mg/L at 0.5cm depth in the sediment, close to the value found in the bottommost sample of 1.9 mg/L at 24cm. Thus, both $\delta^{13}C_{DIC}$ and $O_2$ in the shallowest sediment samples are lower than the values found in the overlying bottom water. However, unlike the downcore trend toward lower values with depth for the carbon isotopes, pore water $O_2$ shows little to no trend with increasing depth—values are low and stay low around 1.9 mg/L. Similar to $O_2$, pore water pH varies from point to point and show little to no trend with increasing depth. At 0.5 cm the pH is 7.55, close to the value found in the bottommost sample of 7.51 at 24cm.

## 5.2 Station 2 (70°55.27'N 14°21.5'E, 2205m water depth)

One gravity core, with a length of 370cm, was collected at station 2. In addition, a water sample from the deepest CTD bottle was collected and used to measure the $\delta^{13}C_{DIC}$ of bottom waters overlying the sediments at the station *(see Figure 22).*

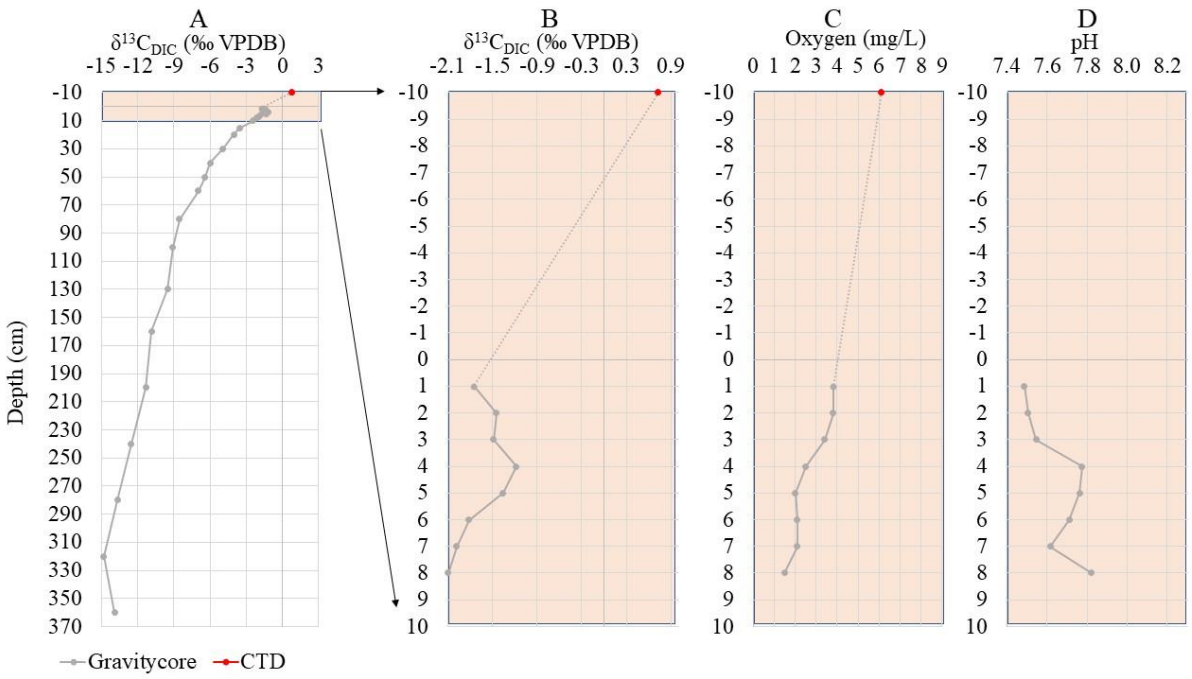


*Figure 22: Bottom and pore water parameters plotted versus depth in sediment from station 2. A) $\delta^{13}C$ of DIC pore waters (grey) versus depth in sediment from the gravity core—red data point represents bottom water values from the CTD plotted at a depth of -10cm to denote its position above the sediments. Color coding similar for all panels. B) Blow up of $\delta^{13}C$ of DIC changes in the upper 10cm of the sediments. C) Oxygen concentration in pore water from the upper 10cm of the gravity core. D) pH values of pore waters extracted from the upper 10cm of the gravity core.*

Pore waters were extracted and analyzed from the gravity core and the CTD (Niskin bottle 1 taken 43 meters above the bottom). The gravity core was sampled for pore water beginning at 1cm below the sediment water interface. The $\delta^{13}C_{DIC}$ values in the gravity core show a trend toward decreasing values with increasing depth in the sediment. $\delta^{13}C_{DIC}$ in station 2 is 0.7‰ in the bottom water. Pore water carbon isotope values in the uppermost sample of the gravity core (1cm) were -1.8‰. This value is significantly lower than the bottom water value. The downcore isotope results show that the $\delta^{13}C_{DIC}$ decrease with depth is higher in the uppermost part of the core. $\delta^{13}C_{DIC}$ values decline by 6.7‰ over the top 40 cm of the sediments while in the rest of the 320cm long core the $\delta^{13}C_{DIC}$ decreases by an additional 7.9‰.

Pore water oxygen concentrations *(Figure 22, panel c)* are low in comparison to bottom water values. The oxygen concentration in the bottom water (from the Niskin flask) is 6.1 mg/L and the shallowest pore water oxygen measurement (at 1 cm) is 3.8 mg/L. Thus, both $\delta^{13}C_{DIC}$ and $O_2$ in the shallowest sediment samples are lower than the values found in the overlying bottom water. Similar to the $\delta^{13}C_{DIC,}$ pore water $O_2$ show a decreasing trend with increasing depth. The $O_2$ decreases to 1.5 mg/L at 7cm. The pH varies from point to but shows an overall incline downcore. At 1cm the pH is 7.49 increasing to 7.82 at 7cm. In addition, from 1 to 4cm

both the $\delta^{13}C_{DIC}$ and the pH deviate toward higher values. This could be a change in the pore water microenvironment, or it can be due to water moving along the liner and influencing measurements further down in the sediments, a source of error due to the sampling.

## 5.3 Station 3 (74°59.76'N 13°56.9'E, 1765m water depth)

One gravity core, with a length of 430cm, and a CTD bottom water samples was collected at station 3 *(see Figure 23).*

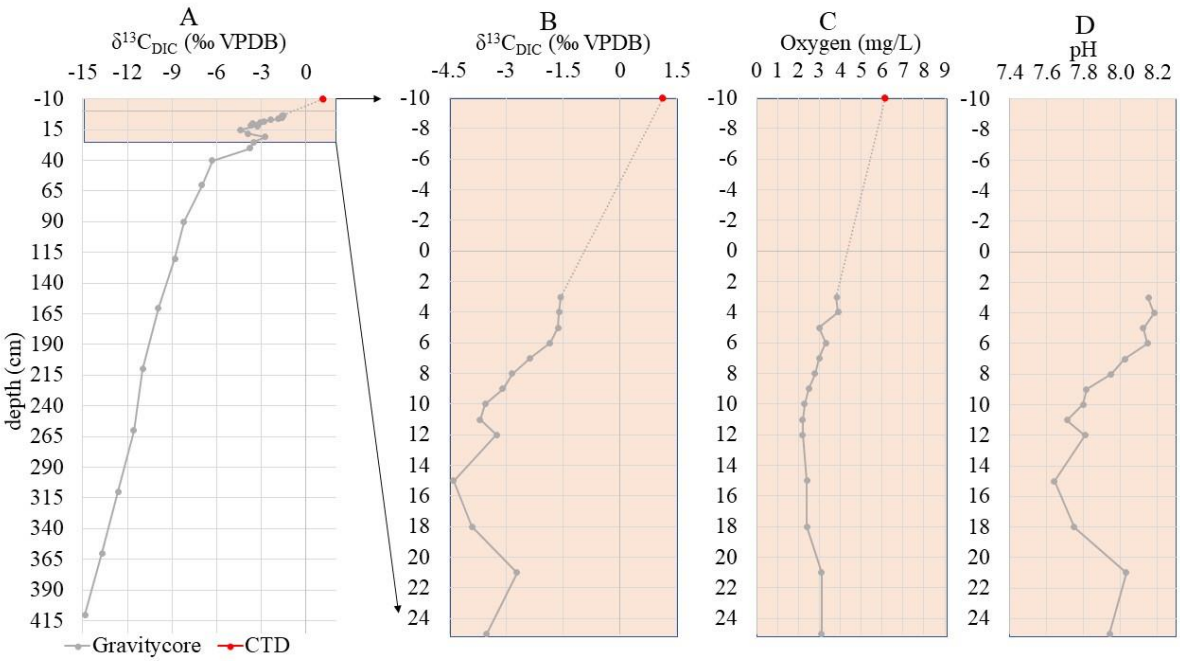


*Figure 23: Bottom and pore water parameters plotted versus depth in sediment from station 3. A) $\delta^{13}C$ of DIC pore waters (grey) versus depth in sediment from the gravity core—red data point represents bottom water values from the CTD plotted at a depth of -10cm to denote its position above the sediments. Color coding similar for all panels. B) Blow up of $\delta^{13}C$ of DIC changes in the upper 25cm of the sediments. C) Oxygen concentration in pore water from the upper 25cm of the gravity core. D) pH values of pore waters extracted from the upper 24cm of the gravity core.*

Pore waters were extracted and analyzed from the gravity core and the CTD (Niskin bottle 1 taken 35 meters above the bottom). The gravity core was sampled for pore water beginning at 3cm below the sediment water interface. The $\delta^{13}C_{DIC}$ values in the gravity core show a trend toward decreasing values with increasing depth in the sediment. The $\delta^{13}C_{DIC}$ in the bottom water is 1.1 ‰. Pore water carbon isotope values in the uppermost sample of the gravity core is -1.6 ‰. This value is again significantly lower than the bottom water value. The downcore isotope results show that the $\delta^{13}C_{DIC}$ decrease with depth is higher in the uppermost part of the

core. $\delta^{13}C_{DIC}$ values decline by 7.4‰ over the top 40 cm of the sediments while in the rest of the 410cm long core the $\delta^{13}C_{DIC}$ decreases by an additional 8.7‰.

Oxygen concentrations *(Figure 23, panel c)* show an overall trend of decreasing values with increasing depth from bottom water into the sediment. The concentration in the bottom water (from the $O_2$ sensor on the CTD) is 6.1 mg/L. The shallowest pore water oxygen measurement is 3.8 mg/L at 3cm depth in the sediment, close to the value found in the bottommost sample of 3.1 mg/L at 25cm. Thus, both $\delta^{13}C_{DIC}$ and $O_2$ in the shallowest sediment samples are lower than the values found in the overlying bottom water. However, unlike the downcore trend toward lower values with depth for the carbon isotopes, pore water $O_2$ shows little to no trend with increasing depth—values are low and stay low around 2-3 mg/L. Pore water pH varies from point to point. From 3cm to 15cm the overall trend is decreasing values with increasing depth. It decreases from 8.15 to 7.64. From 15 to 21 cm the results show a similar trend as in the interval 1 cm to 4 cm in station 2, where $\delta^{13}C_{DIC}$ and the pH increases abruptly from -4.4‰ to -2.7‰ and 7.64 to 8.03.

Nitrate and phosphate were also measured in the pore water from this station. The results are presented in Figure 24 (See station 5 and 9 for more nutrients). The uppermost measurement of nitrate is 6.42 µmol/L 3cm below the bottom water sediment interface decreasing to -0.04 µmol/L at 25cm. Pore water phosphate concentrations varies downcore but shows a opposite trend with increasing values with increasing depth. The uppermost measurement of phosphate is 6.03 µmol/L 3cm below the bottom water sediment interface increasing to 22.39 µmol/L at 25cm.

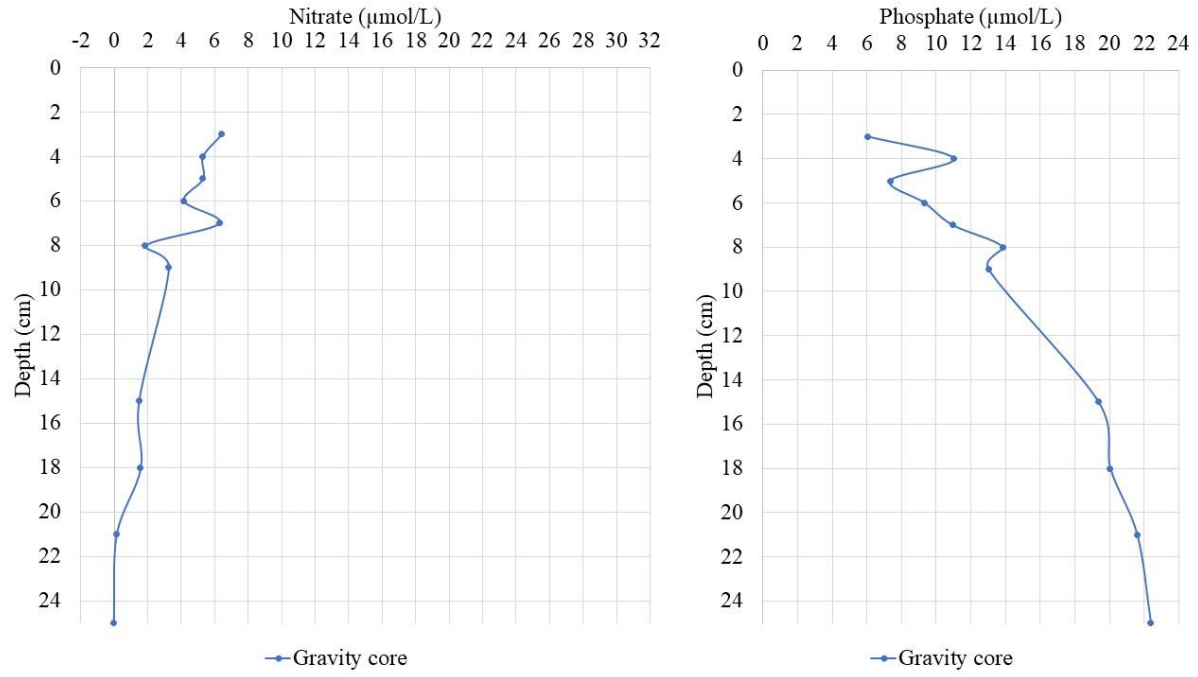


*Figure 24: Pore water nitrate and phosphate concentrations in µmol/L from the gravity core. The y axis represents the depth downcore given in cm.*

## 5.4 Station 5 (77°37.19'N 09°56.8'E, 1340m water depth)

One gravity core, with a length of 400cm, and a multicore, with a length of 40cm and a CTD bottom water samples was collected in station 5 *(see Figure 25).*

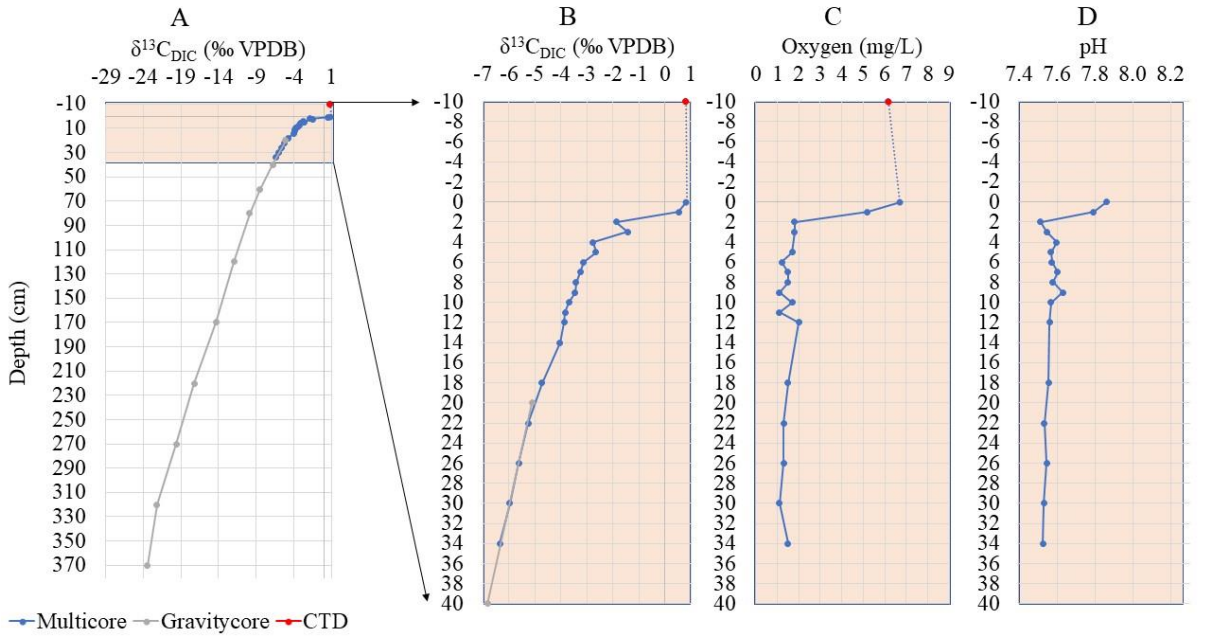


*Figure 25: Bottom and pore water parameters plotted versus depth in sediment from station 5. A) $\delta^{13}C$ of DIC pore waters versus depth in sediment from the multicore and the gravity core—red data point represents bottom water values from the CTD plotted at a depth of -10cm to denote its position above the sediments. Color coding similar for all panels. B) Blow up*

*of $\delta^{13}C$ of DIC changes in the upper 40cm of the sediments. C) Oxygen concentration in pore water from the upper 40cm of the multicore. D) pH values of pore waters extracted from the upper 40cm of the multicore.*

Pore waters were extracted and analyzed from the multicore, the gravity core and the CTD (Niskin bottle 1 taken 17 meters above the bottom). The multicore was sampled for pore water beginning at 0cm, at the bottom water-sediment interface. The $\delta^{13}C_{DIC}$ value from the multicore show a trend toward decreasing values with increasing depth in the sediment. Pore water carbon isotope values in the uppermost sample of the multicore were 0.8 ± 0.1‰ which is approximately the same $\delta^{13}C_{DIC}$ as in the bottom water.

The gravity core had a $\delta^{13}C_{DIC}$ of -5.1‰ at 20cm while the $\delta^{13}C_{DIC}$ from the multicore at 20cm was -5.0‰. In addition, the $\delta^{13}C_{DIC}$ from the multicore at 34cm is 6.4‰ while the $\delta^{13}C_{DIC}$ from the gravity core at 40cm is -6.8‰. The $\delta^{13}C_{DIC}$ from the multicore and the gravity core are similar at the same depth with little difference. This contrasts with the situation in station 1 where loss of core top sediment during coring is a problem. In this station overlapping pore water porfiles confirm that most of the upper sediments are recovered by the gravity corer. The downcore isotope results show that $\delta^{13}C_{DIC}$ decrease with depth is faster in the uppermost part of the core. $\delta^{13}C_{DIC}$ values decline by 7.6‰ over the top 40 cm of the sediments while in the rest of the 370cm long core the $\delta^{13}C_{DIC}$ decreases by an additional 16.6‰.

The pore water $O_2$ concentration *(Figure 25, panel c).* at 0cm is 6.7 mg/L. The bottom water $O_2$ concentration is 6.2 mg/L (from the $O_2$ sensor on the CTD). Thus, both $\delta^{13}C_{DIC}$ and $O_2$ in the shallowest sediment samples are approximately the same as the values found in the overlying bottom water. From 0 to 2cm the oxygen decreases to 1.8 mg/L. Similar to the $O_2$, the pH decreases in the top 0-2cm from 7.86 to 7-51. However, unlike the downcore trend toward lower values with depth for the carbon isotopes, pore water $O_2$ and the pH shows little to no trend with increasing depth past 2cm—values are low and stay low around 1-2 mg/L for the oxygen and 7.50 for the pH.

The full gradient from the bottom water to the sediment appears to be captured in station 5. The $\delta^{13}C_{DIC}$ and the $O_2$ in the bottom water is approximately the same in the shallowest pore water sample. Then further downcore the oxygen is being consumed, the $\delta^{13}C_{DIC}$ decreases and the pH decrease as $CO_2$ is added to the DIC pool.

In addition to the above analysis, nitrate and phosphate were measured in the pore water. The results are presented in Figure 26. The uppermost measurement of nitrate is 9.76 µmol/L at

the bottom water sediment interface. It then increases the first 1cm to 15.74 µmol/L. Further downcore it decreases to 0.18 µmol/L at 120cm and then from 120cm to 170cm it increases to 5.07 µmol/L. Similar to the nitrate, phosphate varies downcore. The overall trend for the phosphate is one of increasing values with increasing depth. The uppermost measurement of phosphate is 1.64 µmol/L 1cm below the bottom water sediment interface increasing to 21.85 µmol/L at 170cm.

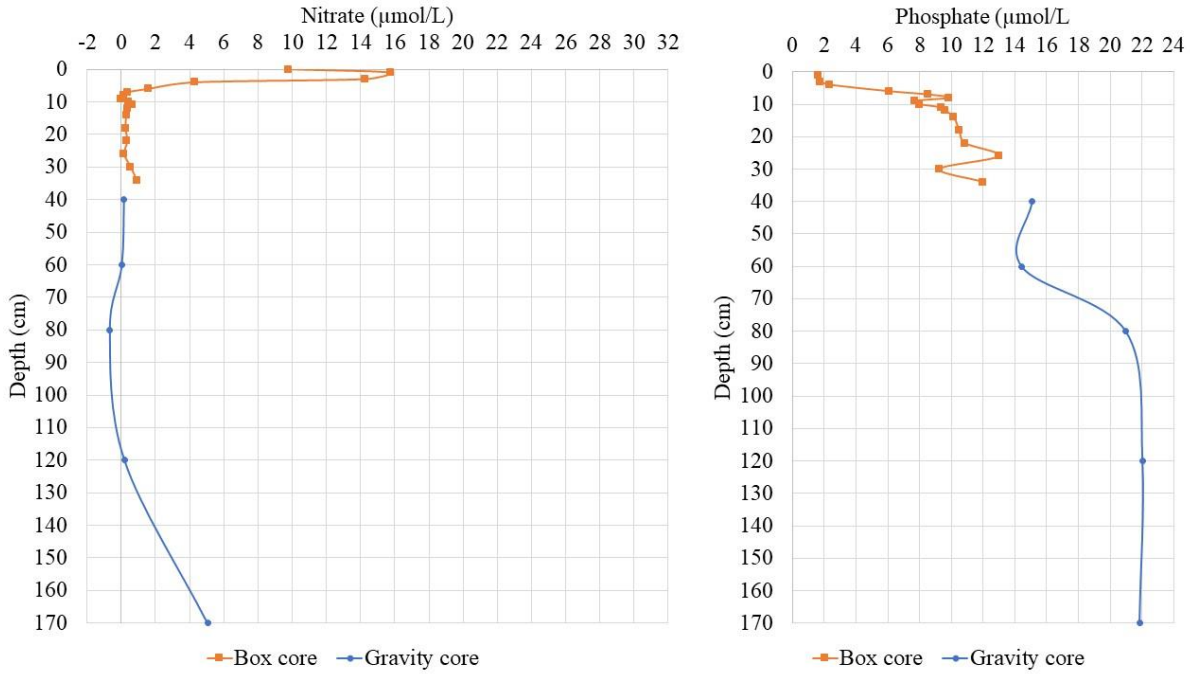


*Figure 26: Nitrate and phosphate is measured in the gravity core and is presented in µmol/L. The y axis represents the depth downcore given in cm.*

## 5.5 Station 7 (78°35.06'N 03°04.36'E, 2521m water depth)

One gravity core, with a length of 321cm and a CTD bottom water samples was collected in our northernmost station *(see Figure 27)*

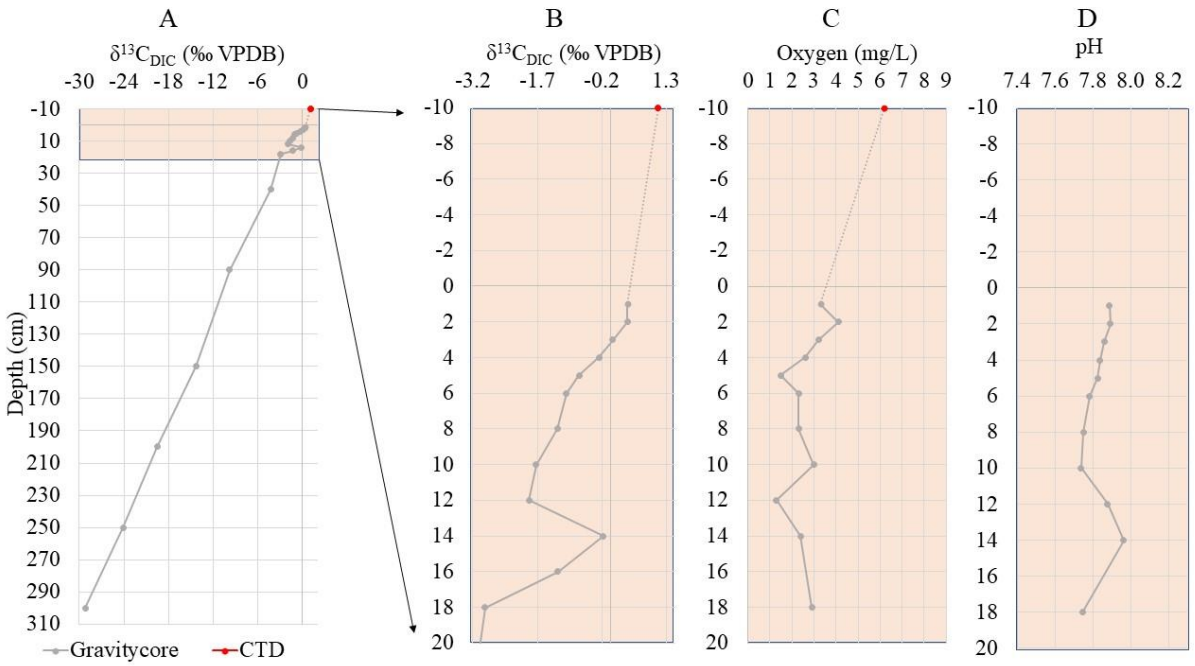


*Figure 27: Bottom and pore water parameters plotted versus depth in sediment from station 7. A) $\delta^{13}C$ of DIC pore waters (grey) versus depth in sediment from the gravity core—red data point represents bottom water values from the CTD plotted at a depth of -10cm to denote its position above the sediments. Color coding similar for all panels. B) Blow up of $\delta^{13}C$ of DIC changes in the upper 20cm of the sediments. C) Oxygen concentration in pore water from the upper 20cm of the gravity core. D) pH values of pore waters extracted from the upper 20cm of the gravity core*

Pore waters were extracted and analyzed from the gravity core and the CTD (Niskin bottle 1 taken 15 meters above the bottom). The gravity core was sampled for pore water beginning at 1cm below the sediment water interface. The $\delta^{13}C_{DIC}$ values in the gravity core show a trend toward decreasing values with increasing depth in the sediment. The $\delta^{13}C_{DIC}$ is 1.1‰ in the bottom water. Pore water carbon isotope values in the uppermost sample (1cm) of the gravity core is 0.5‰. This value is slightly lower than the bottom water value of 1.1‰. The downcore isotope results show that the $\delta^{13}C_{DIC}$ decreases stadily throughout the core reaching values approaching -30‰ near three meters depth in the sediments.

Oxygen concentrations vary from point to point *(Figure 27, panel c).* The concentration in the bottom water (from the $O_2$ sensor on the CTD) is 6.2 mg/L. The shallowest pore water oxygen measurement is 3.3 mg/L at 1cm below the bottom water sediment interface. This value is close to the value found in the bottommost sample of 2.9 mg/L at 18cm. Thus, both $\delta^{13}C_{DIC}$ and $O_2$ in the shallowest sediment samples are lower than the values found in the overlying bottom water. However, unlike the downcore trend toward lower values with depth for the carbon isotopes, pore water $O_2$ varies but show little to no trend with increasing depth. The pH in the shallowest measurement is 7.89 and it decreases down to 7.74 at 12 cm. From 12 to

14 cm the results show a similar situation as in station 2 and 3. The $\delta^{13}C_{DIC}$ and the pH deviate toward higher values.

## 5.6 Station 9 (75°49.93'N 08°11.12'W, 1983m water depth)

One gravity core, with a length of 510cm, one box core a the length of 30cm and a CTD bottom water samples was collected at Station 9 *(see Figure 28).*

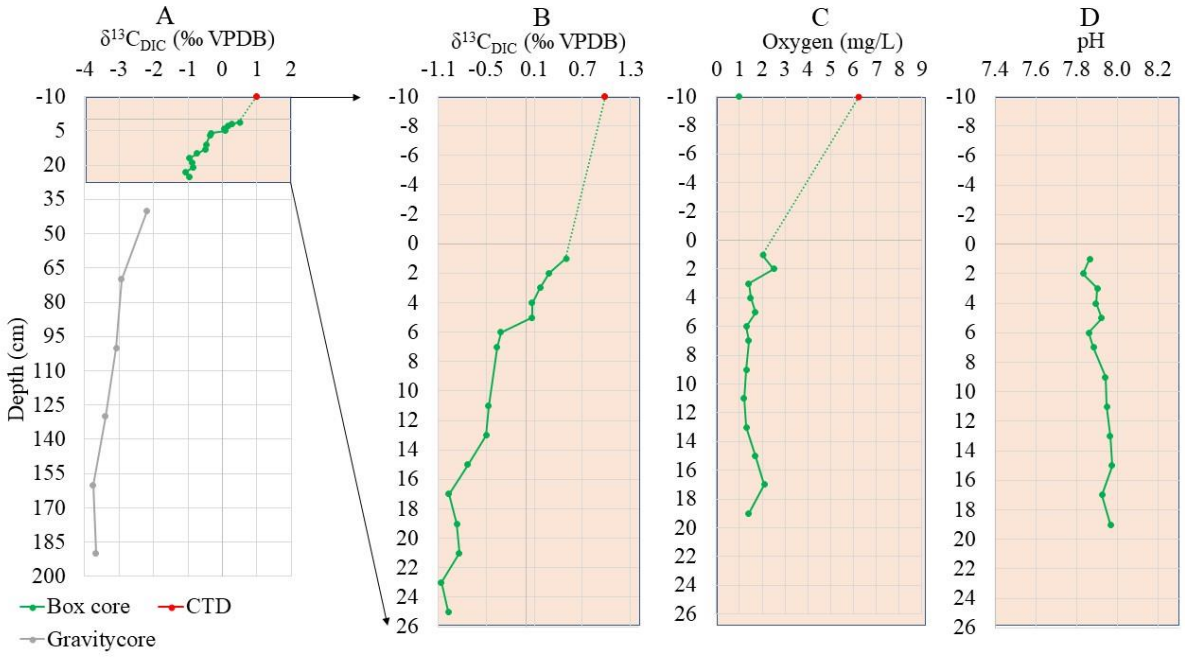


*Figure 28: Bottom and pore water parameters plotted versus depth in sediment from station 9. A) $\delta^{13}C$ of DIC pore waters versus depth in sediment from the box core and the gravity core—red data point represents bottom water values from the CTD plotted at a depth of -10cm to denote its position above the sediments. Color coding similar for all panels. B) Blow up of $\delta^{13}C$ of DIC changes in the upper 26cm of the sediments. C) Oxygen concentration in pore water from the upper 26cm of the box core. D) pH values of pore waters extracted from the upper 26cm of the box core*

Pore waters were extracted and analyzed from the box core, the gravity core and the CTD (Niskin bottle 1 taken 17 meters above the bottom). One push core was taken from the box core at station 9 and pore waters were extracted and analyzed from the push core. The push core was sampled for pore water beginning at 1cm below the sediment water interface. The $\delta^{13}C_{DIC}$ in the bottom water is 1.0‰ in station 9. Pore water carbon isotope values in the uppermost sample (1cm) of the box core were 0.5‰. This value is slightly lower than regional bottom water value. The $\delta^{13}C_{DIC}$ values in the box core and gravity core show a trend toward decreasing values with increasing depth in the sediments. The downcore isotope results show that the $\delta^{13}C_{DIC}$ decrease is moderately higher in the uppermost part of the core. $\delta^{13}C_{DIC}$

values decline by 2.0‰ over the top 25 cm of the sediments while in the rest of the 190cm long core the $\delta^{13}C_{DIC}$ decreases by an additional 2.7‰.

Pore water $O_2$ concentrations *(Figure 28, panel c)* are low in comparison to bottom water values and show little variability downcore. The oxygen concentration in the bottom water (from the $O_2$ sensor on the CTD) is 6.1 mg/L but is already as low as 2 mg/L at 1cm depth in the sediment close to the value found in the bottommost sample of 1.4 mg/L at 19cm. Thus, both $\delta^{13}C_{DIC}$ and $O_2$ in the shallowest sediment samples are lower than the values found in the overlying bottom water. However, unlike the downcore trend toward lower values with depth for the carbon isotopes, pore water $O_2$ shows little to no trend with increasing depth—values are low and stay low around 1.9 mg/L. Pore water and pH varies from point to point, but with only a minor overall increase in values downcore. At 1cm the pH is 7.87 increasing to 7.97 at 19cm.

Nitrate and phosphate were also measured in the pore water from this station. The results are presented in Figure 29. The uppermost measurement of nitrate is 29.89 µmol/L 1cm below the bottom water sediment interface and its stable around this value all the way down to 19cm then it decreases to 0,08 µmol/L at 100cm and is low through the rest of the core. Pore water phosphate concentrations show a markedly different downcore pattern from nitrate. Showing little to no trend with increasing depth - values are low and stay low around 2-3 µmol/L.

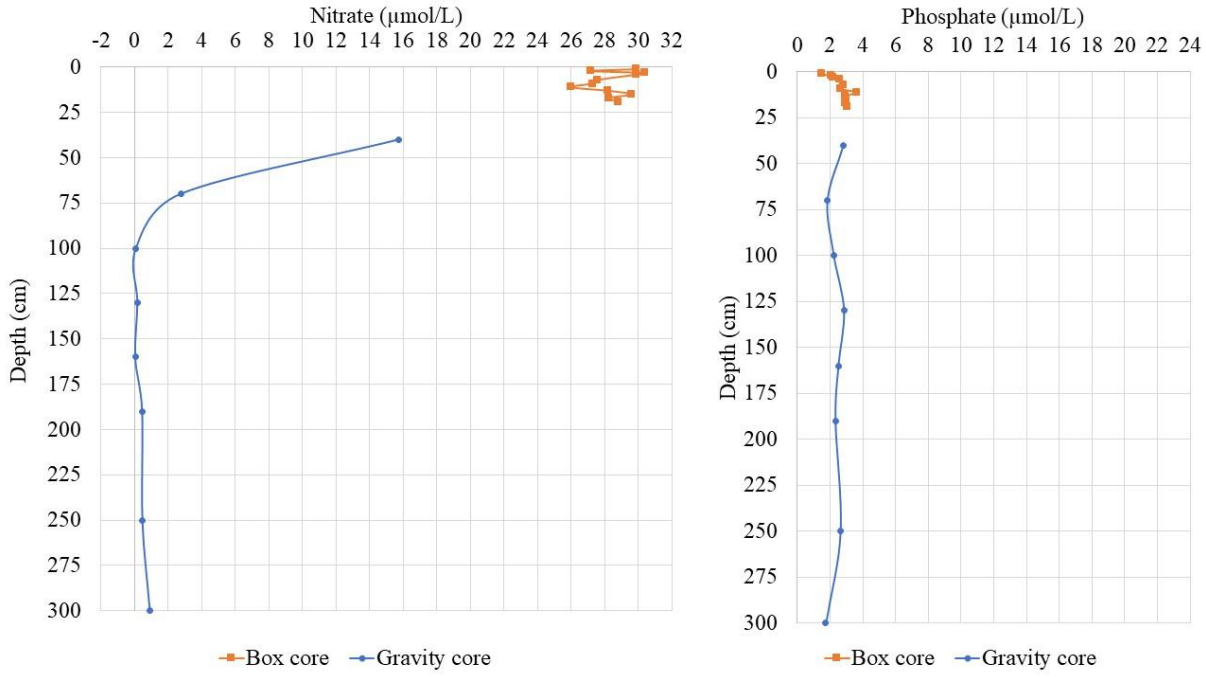


*Figure 29: Nitrate and phosphate concentrations in pore water from the gravity core is presented in µmol/L. The y axis represents the depth downcore given in cm.*

## 5.7 Station 10 (75°00.00'N 11°85.28'W, 2637m water depth)

One gravity core, with a length of 481cm, one multicore with a length of 40cm and a CTD bottom water samples was collected at Station 10 *(see Figure 30).*

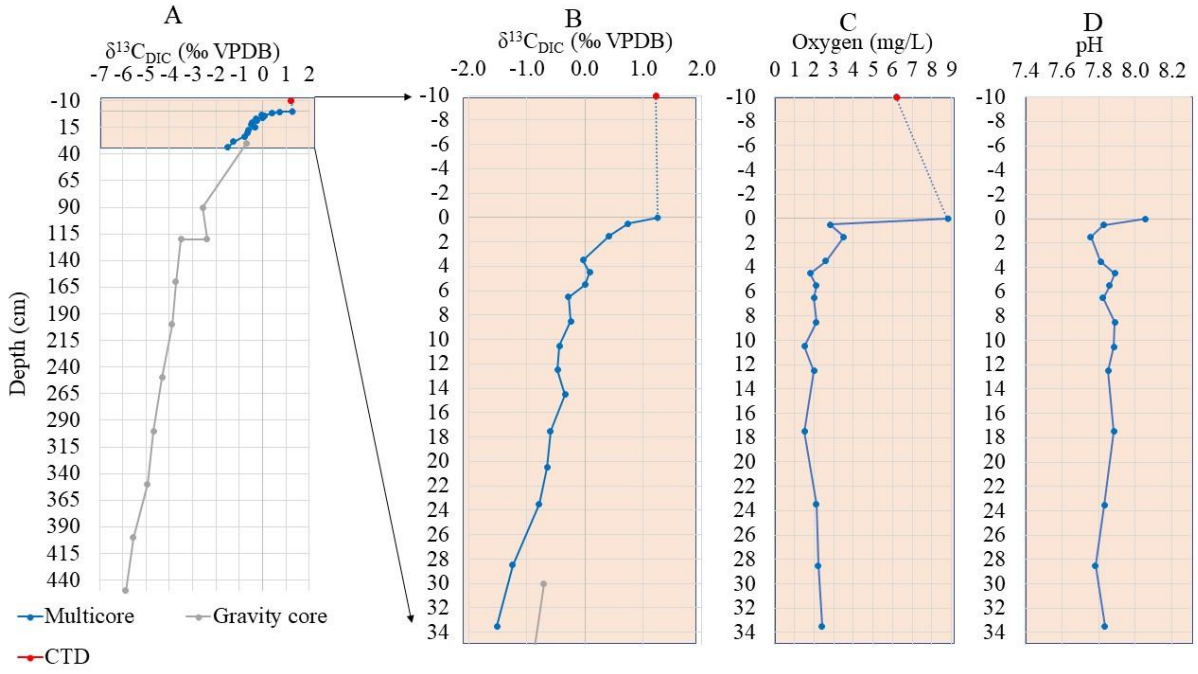


*Figure 30: Bottom and pore water parameters plotted versus depth in sediment from station 10. A) δ $\delta^{13}$C of DIC pore waters versus depth in sediment from the multicore and the gravity core—red data point represents bottom water values from the CTD plotted at a depth of -10cm to denote its position above the sediments. Color coding similar for all panels. B) Blow up of $\delta^{13}$C of DIC changes in the upper 34cm of the sediments. C) Presents the oxygen concentration in pore water from the upper 34cm of the multicore. D) pH values of pore waters extracted from the upper 34cm of the multicore.*

Pore waters were extracted and analyzed from the multicore, the gravity core and the CTD (Niskin bottle 1 taken 11 meters above the bottom). The multicore was sampled for pore water beginning at the sediment water interface at 0cm. $\delta^{13}C_{DIC}$ in station 10 is 1.2‰ in the bottom water. Pore water carbon isotope values in the uppermost sample of the multicore is 1.2‰, approximately the same as the bottom water. The downcore isotope results show that the $\delta^{13}C_{DIC}$ decrease is higher in the uppermost part of the core. $\delta^{13}C_{DIC}$ values decline by 2.7 over the top 33 cm of the sediments while in the rest of the 450cm long core the $\delta^{13}C_{DIC}$ decreases by an additional 4.4‰.

The gravity core had a $\delta^{13}C_{DIC}$ of -0.7‰ at 30 cm while the $\delta^{13}C_{DIC}$ from the multicore at 30cm was -1.4‰. The $\delta^{13}C_{DIC}$ at 20cm in the multicore is -0.7‰. The depth offset in the $\delta^{13}C_{DIC}$ values in the gravity core curve (similar values observed 10cm shallower in the multicore *(Figure 30, panel b*) could potentially indicate that pore water from closer to the bottom water sediment interface (with higher $\delta^{13}C_{DIC}$ values) move along the liner of the

gravity core and influences the samples collected at deeper depths and therefor the $\delta^{13}C_{DIC}$ values from 30cm in the gravity core show values closer to the bottom water value. Alternatively, the gravity core captured a more complete sediment sequence than the multicore which seems unlikely, or there are very differences in the downcore changes occurring on small spatial scales (coring spot to coring spot).

Oxygen concentrations *(Figure 30, panel c)* decline sharply in the uppermost sediments and then show only small point to point changes. The concentration in the bottom water (from the $O_2$ sensor on the CTD) is 6.2 mg/L. The pore water $O_2$ concentration at the shallowest measurement (0cm) is 8.8 mg/L, slightly higher than the bottom water concentration and probably an error connected to the method used to measure $O_2$ in the pore water. Thus, both $\delta^{13}C_{DIC}$ and $O_2$ in the shallowest sediment samples are similar to the values found in the overlying bottom water suggesting the full gradient from the bottom water to the sediment is represented in station 10. From 0 to 0.5cm the oxygen decreases to 2.8 mg/L. Similar to the $O_2$, the pH decreases in the top 0.5cm from 8.06 to 7.82. Unlike the downcore trend toward lower values with depth for the carbon isotopes, pore water $O_2$ and pH shows little to no trend with increasing depth past 0.5cm—values are low and stay low around 2 mg/L for the oxygen and 7.8 for the pH and even show a slight increasing trend in the deeper parts of the core.

## 5.8 Station 11 (73°09.41'N 18°04.48'W, 287m water depth)

One multicore with a length of 19.5cm and a CTD bottom water samples was collected at Station 11 *(see Figure 31).*

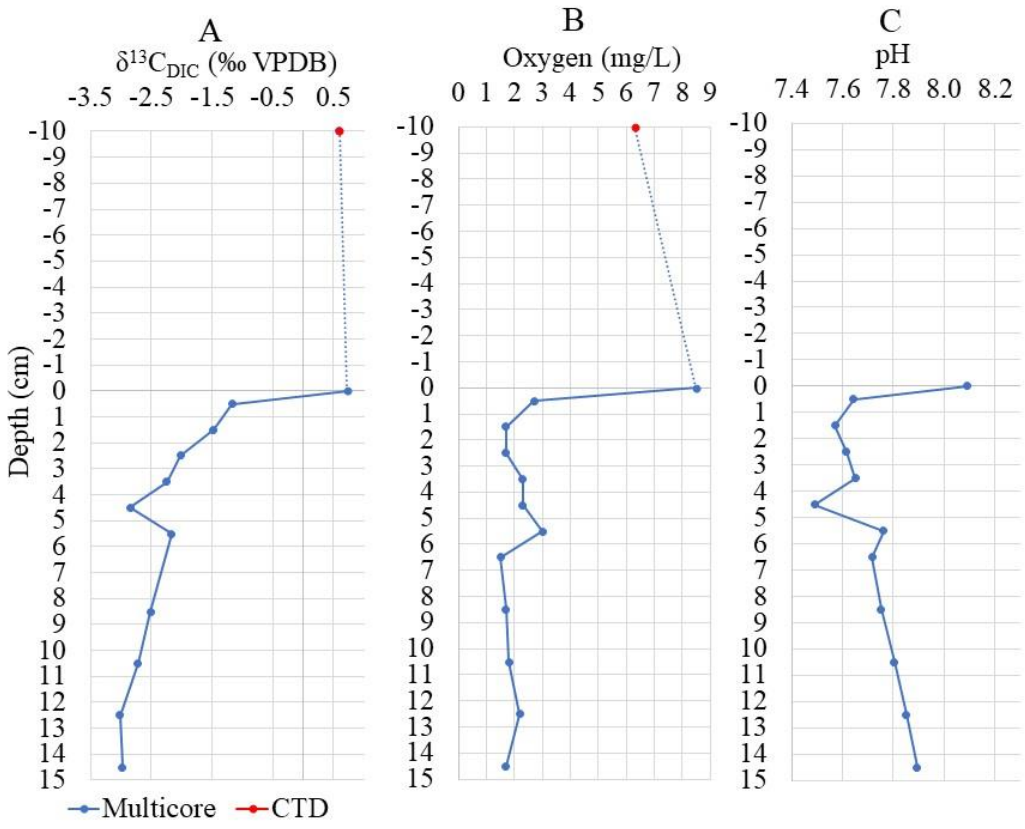


*Figure 31: Bottom and pore water parameters plotted versus depth in sediment from station 11. A) $\delta^{13}C$ of DIC pore waters versus depth in sediment from the multicore—red data point represents bottom water values from the CTD plotted at a depth of -10cm to denote its position above the sediments. Color coding similar for all panels. B) Oxygen concentration in pore water from the box core. C) pH values of pore waters extracted from the upper 15cm of the multicore.*

Pore waters were extracted and analyzed from the multicore and the CTD (Niskin bottle 1 taken 10 meters above the bottom). The multicore was sampled for pore water beginning at the bottom water – sediment interface (0cm). The $\delta^{13}C_{DIC}$ values in the multicore show a trend toward decreasing values with increasing depth in the sediment. $\delta^{13}C_{DIC}$ in the bottom water at station 11 is 0.6‰. The pore water carbon isotope value in the in shallowest measurement (0cm) is 0.7‰. The downcore isotope results show that the $\delta^{13}C_{DIC}$ decrease is higher in the uppermost part of the core. $\delta^{13}C_{DIC}$ values decline by 2.6‰ over the top 2.5cm of the sediments while in the rest of the 14cm long core the $\delta^{13}C_{DIC}$ decreases by an additional 1.0‰.

Oxygen concentrations *(Figure 31, panel c)* decrease rapidl in the top 5cm and then plateau in value. The concentration in the bottom water (from the $O_2$ sensor on the CTD) is 6.3 mg/L. The shallowest pore water oxygen measurement is 8.5 mg/L, slightly higher than the bottom water value. Thus, both $\delta^{13}C_{DIC}$ and $O_2$ in the shallowest sediment samples are similar to the

values found in the overlying bottom water indicating that full transition from the bottom water to the sediment is captured in the sampling. Similar to the $O_2$, the pH decreases in the top 1,5cm from 8.09 to 7.57. However, unlike the downcore trend toward lower values with depth for the carbon isotopes, pore water $O_2$ shows little to no trend with increasing depth past 1.5cm—values are low and stay low around 2 mg/L for the oxygen while the pH increases to 7.893 at 14.5cm. At approximately 3.5 to 4.5cm the $\delta^{13}C_{DIC}$ and the pH suddenly decreases, the opposite situation as in station 2,3 and 7 but in this station the decrease could also be a change in the pore water microenvironment.

## 5.9 Station 12 (70°29.57'N 17°55.49'W, 1674m water depth)

One multicore with a length of 40cm and a CTD bottom water samples was collected at Station 12 *(see Figure 32).*

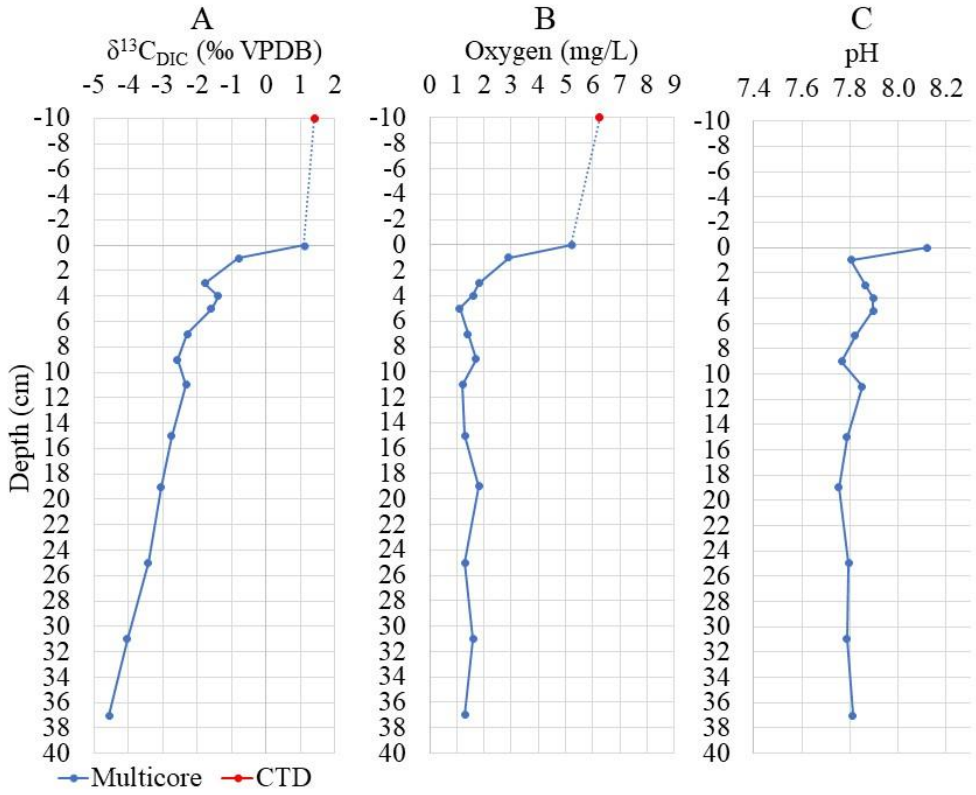


*Figure 32: Bottom and pore water parameters plotted versus depth in sediment from station 12. A) $\delta^{13}C$ of DIC pore waters versus depth in sediment from the multicore—red data point represents bottom water values from the CTD plotted at a depth of -10cm to denote its position above the sediments. Color coding similar for all panels. B) Oxygen concentration in pore water from the box core. C) pH values of pore waters extracted from the upper 40cm of the multicore.*

Pore waters were extracted and analyzed from the multicore and the CTD (Niskin bottle 1 taken 12 meters above the bottom). The multicore was sampled for pore water beginning at the bottom water – sediment interface (0cm). The $\delta^{13}C_{DIC}$ values in the multicore show a trend toward decreasing values with increasing depth in the sediment. $\delta^{13}C_{DIC}$ in the bottom water at station 12 is 1.4‰. The pore water carbon isotope value in the in shallowest measurement (0cm) is 1.1‰. The downcore isotope results show that the $\delta^{13}C_{DIC}$ decrease is higher in the uppermost part of the core. $\delta^{13}C_{DIC}$ values decline by 2.9‰ over the top 3cm of the sediments while in the rest of the 37cm long core the $\delta^{13}C_{DIC}$ decreases by an additional 2.8‰.

Power water oxygen concentrations *(Figure 32, panel c)* decline rapidly in the upper few centimeters and plateau after 3cm depth. The concentration in the bottom water (from the $O_2$ sensor on the CTD) is 6.3 mg/L. The shallowest pore water oxygen measurement is 5.2 mg/L, slightly higher than the bottom water value. Thus, both $\delta^{13}C_{DIC}$ and $O_2$ in the shallowest sediment samples are similar to the values found in the overlying bottom water suggesting the full gradient from the bottom water to the sediment is represented in station 12. Similar to the $O_2$, the pH decreases in the top 1cm from 8.12 to 7.80. However, unlike the downcore trend toward lower values with depth for the carbon isotopes, pore water $O_2$ shows little to no trend with increasing depth past 3cm—values are low and stay low around 1-2 mg/L while the pH shows little to no trend with increasing depth past 1cm with values around 7.8.

## 5.10 Station 16 (65°48.07'N 03°29.35'W, 2890m water depth)

One multicore with a length of 40cm was collected at Station 16 *(see Figure 33).*

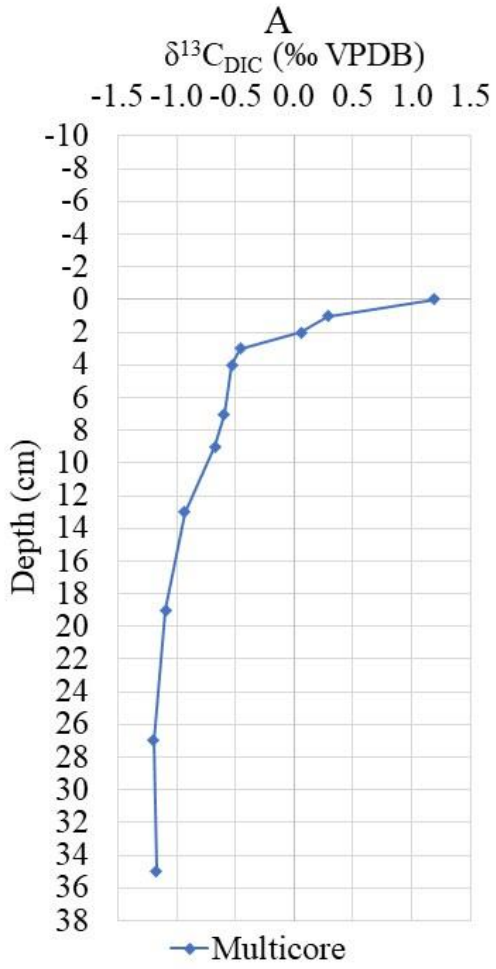


*Figure 33: This figure presents the $\delta^{13}C_{DIC}$ results from station 16.*

The multicore was sampled for pore water beginning at the bottom water – sediment interface (0cm). $\delta^{13}C_{DIC}$ in station 16 is 1.2‰ at 0cm and it decreases down to -1.2‰ at 35cm depth. The downcore isotope results show that the $\delta^{13}C_{DIC}$ decrease is higher in the uppermost part of the core. $\delta^{13}C_{DIC}$ values decline by 1.7‰ over the top 3cm of the sediments while in the rest of the 35cm long core the $\delta^{13}C_{DIC}$ decreases by an additional 0.7‰.

## 5.11 All stations

The collected pore water $\delta^{13}C_{DIC}$ results from the different core sites are presented in Figure 34 and 35. The general trend in $\delta^{13}C_{DIC}$ is decreasing values downcore with steeper gradients in the upper part of the cores.

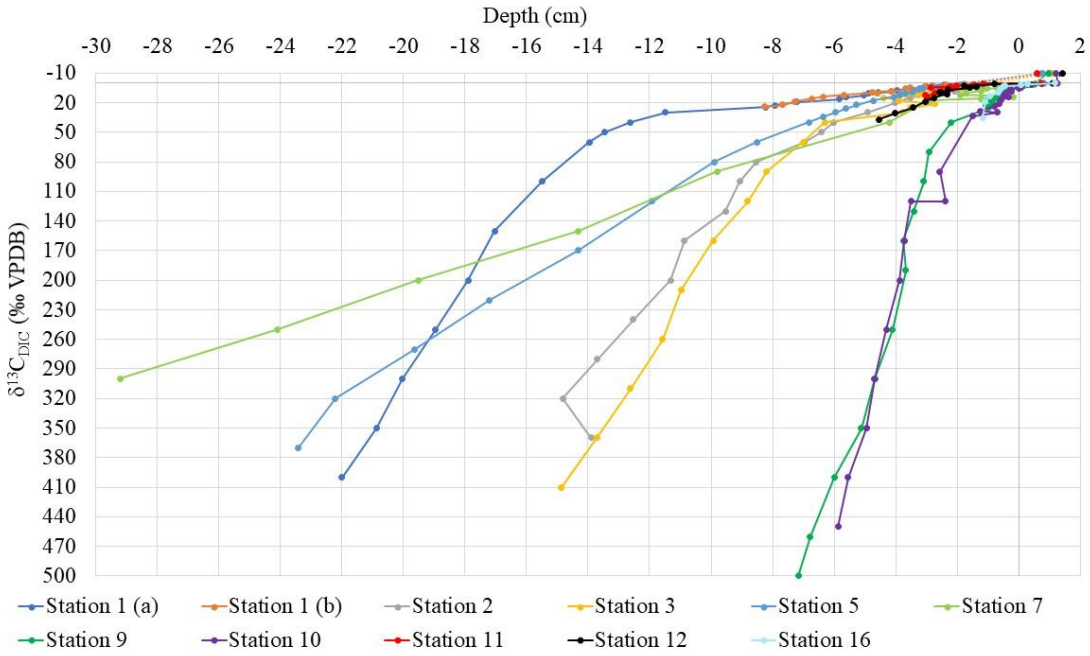


*Figure 34: $\delta^{13}C_{DIC}$ versus depth for station 1-16.*

In the deeper parts of the cores the changes in isotope values with depth tend to taper off (lower rate of change with depth) with station 7 marking a clear exception where the overall trend does not change, and much lower values are reached than at the other sites. The slope from 40cm to the deepest part is -0,096/cm respectively. While the other stations have a high range of change in the upper part and then little range of change at the deepest parts of the core. The slope between 40cm and the deepest measured value in these cases is fluctuating from -0,01/cm to -0,05/cm.

The $\delta^{13}C_{DIC}$ in the upper 40cm of the core is decreasing more in station 1,2,3 and 5 than in station 9,10 and 16 *(see Figure35)*. Station 1 has the biggest decline in $\delta^{13}C_{DIC}$ in the upper 40cm, declining from 1.0‰ to -12.6‰ at 40cm *(see Figure 21, panel B)*, while Station 9 and 10 has the lowest decline starting at 0.9‰ and 1.2‰ decreasing to about -2.2 and -1.8 at 40cm *(see Table 2)*. At 10 and 25cm the shallowest stations have lower $\delta^{13}C_{DIC}$ than the deeper ones with the exception of station 9, 11 and 12 *(see Table 2)*. These stations have a higher $\delta^{13}C_{DIC}$ in the pore water than other station with the same water depth. Station 9-16 are located on the western side of the study area while station 1-7 are located on the eastern side. There appear to be a geographical variability in the downcore results with differencese between the west side and the east side of the Nordic seas and this observation will be further discussed in subchapter 6.2.

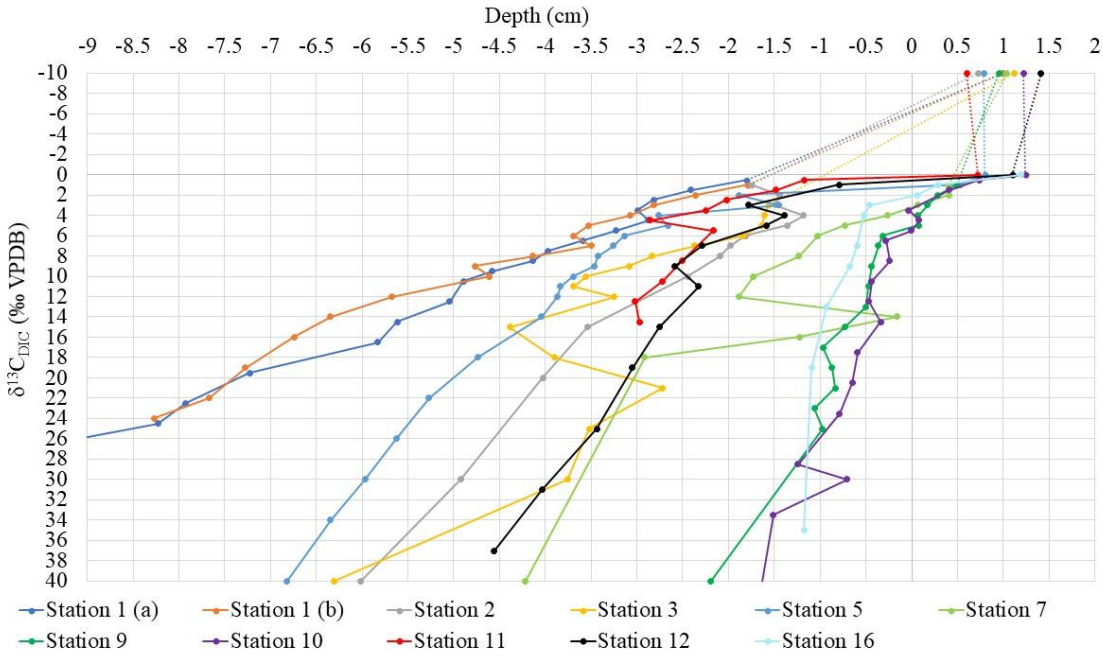


*Figure 35: $\delta^{13}C_{DIC}$ versus depth in the upper 40cm for each station. Dashed lines connect to bottom water values (denoted with depth of -10cm to indicate they overly the sediments).*

| Station | Depth (m) | $\delta^{13}C_{DIC}$ at 10cm (‰ VPDB) | $\delta^{13}C_{DIC}$ at 25cm (‰ VPDB) | $\delta^{13}C_{DIC}$ at 300 cm (‰ VPDB) |
|---|---|---|---|---|
| 1 | 1042 | -4.6 | -8.2 | -20.0 |
| 5 | 1340 | -3.7 | -5.6 | -21.2 |
| 3 | 1765 | -3.5 | -3.5 | -12.4 |
| 11 | 287 | -2.7 | No data | No data |
| 2 | 2205 | -2.4 | -4.5 | -14.3 |
| 12 | 1674 | -2.4 | -3.4 | No data |
| 7 | 2521 | -1.7 | -3.3 | -29.2 |
| 16 | 2890 | -0.7 | -1.1 | No data |
| 9 | 1983 | -0.4 | -1 | -4.7 |
| 10 | 2637 | -0.4 | -0.9 | -4.7 |

*Table 2: Pore water $\delta^{13}C_{DIC}$ values at the different stations at depths of 10, 25 and 300cm in addition to the water depth of the stations. The stations are arranged from the lightest $\delta^{13}C_{DIC}$ at 10cm. Stations situated on the west side of the study area are denoted by red text and the stations on the eastern side are in blue.*

Only 15cm and 40cm of cores were extracted at station 11, 12 and 16 and the $\delta^{13}C_{DIC}$ from the Delta Ray shows that stations 11 and 12 follow the same trend as for station 2, 3 and 7 *(see Figure 34 and 35)*. Station 16 follow the same trend as for station 9 and 10.

Bottom water $0_2$ concentrations from niskin bottles from the CTD are 6-8 mg/L in all stations *(see Figure 36)*. Oxygen is consumed in the top 10cm of all stations *(see Figure 37)*. $O_2$ at stations 1,5,9,11 and 12 decreases most rapidly with depth. The concentration of oxygen is below 2 mg/L by approximately 0.5-3cm. $O_2$ declines more gradually at station 2,3,7 and 10 is below 2 mg/L by approximately 5-10cm.

The gradient from bottom water to sediment interface is captured well in some stations. In station 5 the gradient is captured with the same $\delta^{13}C_{DIC}$ in the uppermost pore water sample as the bottom water $\delta^{13}C_{DIC}$. Oxygen is consumed in the top part, $\delta^{13}C_{DIC}$ decreases, $CO_2$ is produced, and the pH lowered. In station 1 on the other hand, the box core does not capture the same gradient. The $\delta^{13}C_{DIC}$, the oxygen and the pH have a sharp drop from bottom water to the topmost sediment and are then fairly stable through the sediments. These results could reflect the ability of two different methods, multicore vs box core, to recover the surface most sediments and the sharp gradients they contain. Another explanation is that the sampling procedure got better in later stations and therefor there is a different in the quality of the data in Station 1 compared to station 5. These results will be further discussed in section 6.1.

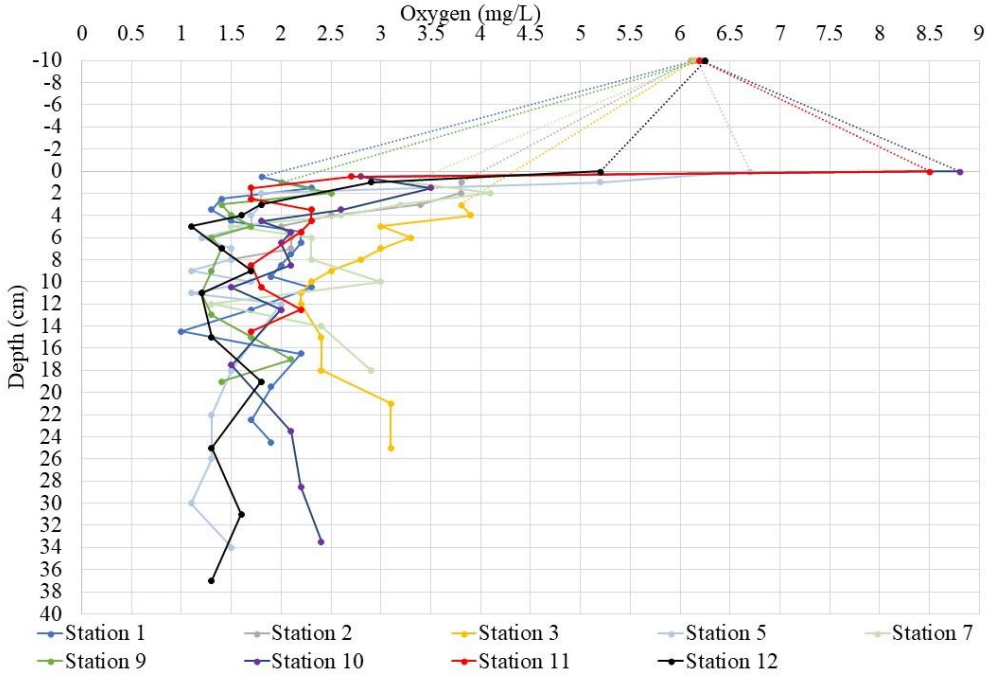


*Figure 36: Oxygen concentrations measured in the bottom water and pore water from the bottom water interface to 40cm in the sediments. Dashed lines connect to bottom water values denoted with negative depths (-10cm).*

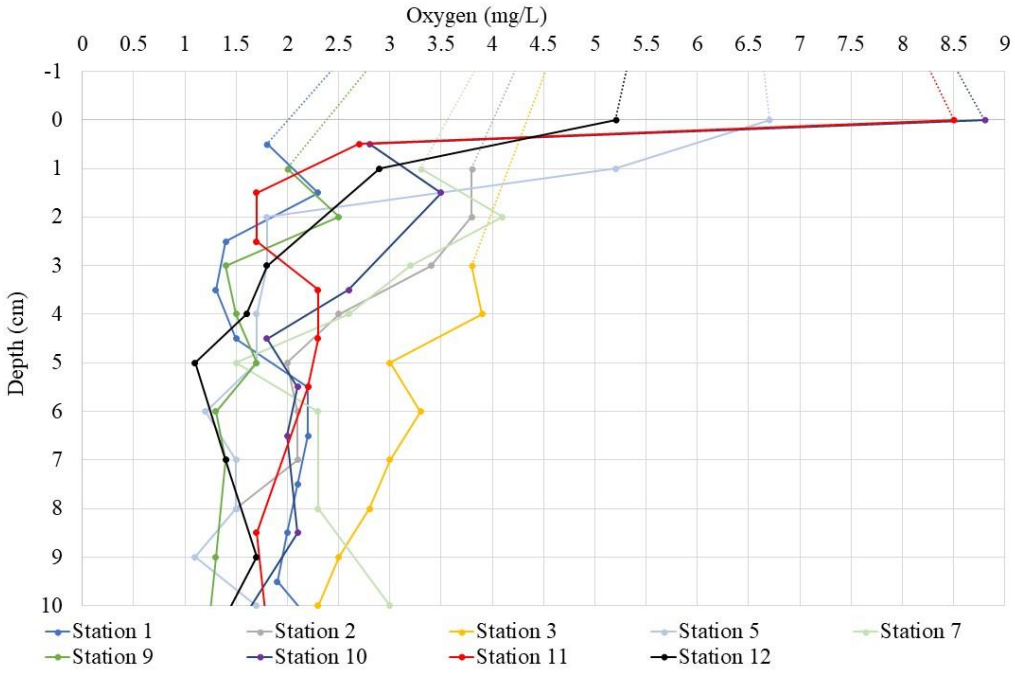


*Figure 37: The oxygen concentration in the upper 10cm of the sediments from the different sites.*

# 6. Discussion

Oxygen is often assumed to be the primary factor for organic matter respiration in the ocean and in shallow sediments in oceanic settings. This dominance has led some researchers to use the change in $\delta^{13}C_{DIC}$ ($D\delta^{13}C_{DIC}$) between bottom water values and pore water values at the $O_2$ penetration depth as a proxy for bottom water $O_2$ concentration. The assumption being that the entire $\delta^{13}C_{DIC}$ change is driven by aerobic respiration of isotopically light organic matter—with bottom water oxygen concentration determining the amount of organic matter remineralization. Yet near coastal zone studies suggest that in some settings shallow organic matter respiration can far exceed what is explained by bottom water $O_2$ alone (Canfield, et al., 1993). Here I use the $\delta^{13}C_{DIC}$ pore water results from around the Nordic Seas to examine the extent to which, and the underlying factors determining whether, bottom water $O_2$ controls the amount of organic matter sourced carbon added to the DIC pool in shallow marine sediments. In order to assess this, I analyze the pattern and rates of $\delta^{13}C_{DIC}$ change in order to identify patterns and possible mechanisms. I use the $\delta^{13}C_{DIC}$ and DIC changes to confirm that the DIC changes are dominated by organic matter respiration. Then, in order to test previous assumptions that bottom water $O_2$ modulates the amount of organic matter turnover in shallow sediments, I develop a simple stoichiometric model for predicting $O_2$ changes using $\delta^{13}C_{DIC}$ and oceanic Redfield-isotope relationships.

## 6.1 Evaluation of data quality.

Prior to analyzing features of the data and discussing it versus other results it is important to first evaluate the quality, and level of (un)certainty, in my data. In this section the errors/issues connected to this thesis is presented and the effect on the data discussed.

The temperature in the lab was not stable due to variation in the outside temperature which caused drift in the data for a subset of the data. This drift was corrected for with the drift correction described in section 4.2.2. After the drift correction the precision of the Delta Ray was 0.145‰ or better. However, it is important to note that this uncertainty is more than an order of magnitude smaller than the signal being interpreted in this thesis.

The orientation of the cores, vertical or horizontal, while extracting the pore water samples may also influence the results. The first samples were extracted with the core standing vertically which could lead to water migrating from shallower depth to deeper depths in the core or for water to move along the liner of the cores. This concern was resolved by extracting

pore water from the cores while laying horizontally instead and by taking bottom water samples with both the CTD and the core top of the multicore. Because of the large downcore trends in $\delta^{13}C$, areas influenced by liner water were often easy to identify and occurred most commonly on the gravity cores where the non-transparent liners made it more difficult to confirm a firm contact between liner and sediments during sampling.

As mentioned in the last part of the results chapter, the fragile sediments at the gradient from bottom water to sediment interface are captured in only some stations and its crucial to collect the upper 1cm of the sediments in order to capture this gradient. The gradient is captured in station 5, 10, 11 and 12. A multicore was used at all of these stations while in the other stations a box core or gravity core was used to collect the upper part of the sediments. The core method therefore influenced the recovery of this critical near-surface property gradient, and the data quality is better when a multicore is used as a sampling device. In addition, pore water samples are collected at 0cm (at the interface) with the use of a multicore while in the box core or gravity core the uppermost pore water sample is at 0.5-3cm. Pore water samples could not be sampled in the interface in these two core methods due to poor quality or non-preservation of the core tops.

In addition, in station 2,3,7 and 11 an increase/decrease in both $\delta^{13}C_{DIC}$ and pH is observed at certain depths. These phenomena tend to happen in gravity cores and not in the multicore and is assumed to be an error due to water moving along the liner of the core and poor contact between sediment and liner during sampling. It could also represent a natural variability such as a borrow in the cores, either way the coherent increase/decrease in both parameter indicates that the instrument used for the pH is able to detect areas of increased/decreasing pH and it gives credibility to the pH data.

The oxygen measured by hand at 0cm is typically slightly higher than the $O_2$ measured in the bottom water with the $O_2$ sensor on the CTD. In station 10 the oxygen in the pore water at the bottom water sediment interface is 8.8 mg/L while the CTD sensor measure the bottom water to be 6.2 mg/L. In station 11 the oxygen in the pore water at the shallowest measurement is 8.5 mg/L while the CTD sensor measure the bottom water $O_2$ to be 6.3 mg/L. A higher $O_2$ concentration in the sediments compare to the bottom water is not plausible, or at least exceedingly unlikely, so this indicates an error connected to handheld analyzer used for the pore water measurements. In addition, the lowest oxygen measurement done by hand is 1-2.2 mg/L for the different stations, even at 300cm in the core where other electron acceptors should be dominant and oxygen absent. The handheld measurements were carried out in an

open system with the influence of the atmosphere in the shipboard wet lab and some interaction between the atmosphere and the pore water occurred. This may explain why handheld measurements appear to have a lower limit around 2 mg/L (commonly) and never reach 0, even in the deepest portions of the core and after nitrate declines which is a clear indication of anoxia. The offset between the CTD oxygen concentration measurement and the pore water measurements suggest a systematic error of approximately + 2 mg/L for the oxygen measurements in the pore water (and bottom water overlying the cores when compared to the CTD). Consequently, in the following sections the oxygen penetration depth is defined as the depth at which oxygen goes below 2 mg/L.

Nitrate concentrations can be used to determine the oxygen penetration depth as well. When sub-oxic or anoxic conditions are reached denitrification starts and pore water nitrate decreases. Thus, declining pore water nitrate values provide a complementary indicator for identifying the oxygen penetration depth. The oxygen penetration depth set in each station after the correction of the 2 mg/L offset, is presented in Table 3. In station 3 the oxygen penetration is relatively deep and the oxygen concentration decreases slowly. At 10-11cm the oxygen is gone. At 3cm in the pore water nitrate is around 6µmol/L, lower than the regional bottom water value of approximately 14.5µmol/L and is stable around this value all the way down to 7cm. From 7 cm to 21cm nitrate slowly decreases down to 0µmol/kg. This is consistent with sub-oxic to anoxic conditions present after 7cm in the core, although perhaps with some local denitrification above this point. In station 5 the oxygen concentration decreases rapidly in the upper part of the sediments, and the penetration depth is at approximately 2cm. The nitrate concentration varies between 10 and 16µmol/L from 0-3cm, similar to the bottom water value *(see figure 10).* At 3cm it starts to decrease and by approximately 7cm the nitrate is gone. The observation that nitrate starts decreasing once the oxygen concentration is below 2 mg/L supports the conclusion of a +2 mg/L offset in the $O_2$ measurements. The same pattern is not observed for station 9. In station 9 the oxygen decrease rapidly in the upper part and the oxygen penetration depth is 3cm while the nitrate concentration is high and stable around 30µmol/L in the upper 20cm, a concentration considerably higher than the bottom water values of approximately 14.5µmol/L. The higher nitrate values are consistent with oxidation of organic matter in the upper sediments releasing nutrients and carbon—although with oxygen so low (at or below the 2 mg/L threshold within a few cm of the sediment interface) one should have expected nitrate to decline from this point onward. In addition, the carbon isotope drop at this site is not very rapid suggesting

limited rates of oxidation and carbon turnover relative to other sites. Lower rates of oxidation in the upper sediments would also explain why nitrate does not decrease rapidly—i.e. if there was still some oxygen present. This highlights the difficulty in using the hand-held oxygen measurements in precisely identifying the oxygen penetration depth at some locations. However, overall the nitrate and oxygen data provide a reasonably good and consistent estimate of the oxygen penetration depth for most sites (where both are available). Unfortunately nitrate data was only available for some sites and oxygen measurements alone are used to estimate penetration depth for the other locations.

As mentioned in section 2.2.2 surface sediments represents an active biogeochemical reactor where microbial, oxidation, reduction, precipitation, and dissolution processes occur (Luff & Moll, 2004). In the upper part oxic respiration is dominant, then once oxygen is gone, nitrate is being reduced. During the microbial degradation of organic matter, phosphate is released to the pore water, but the main release of phosphate occurs in suboxic zone (Schulz & Zabel, 2006, p. 220). Ergo, the pore water profiles should show a decrease in oxygen in the upper part, then once oxygen is gone the nitrate should decrease. In addition, phosphate should increase with depth in the sediments, especially when nitrate is being reduced. In Figure 38 the oxygen, nitrate and phosphate for station 5 is presented. The profiles follow the expected patterns. Oxygen decreases down to approximately 2 cm after which it is low to absent (sub-oxic to anoxic). Nitrate is constant until 3cm then it starts to decrease and is gone by approximately 7cm consistent with sub-oxic to anoxic conditions below 2-3cm. Phosphate concentration is 1.64µmol/L at 1cm, close to but slightly elevated from the bottom water value of approximately 1µmol/L suggesting some initial OM respiration already in the top centimeter consistent with the decrease in oxygen in the top cm's (vs. bottom water). Phosphate concentrations are relatively stable around 2µmol/L until 4cm, then it increases drastically down to 8 cm. From 8cm and through the rest of the core the pore water phosphate concentration increases gradually. These pore water profiles from station 5 match the theoretically expected profiles and indicates that the different zonation's (e.g., aerobic, sub-oxic, anoxic etc.) are reliably captured in our cores and by our analyses.

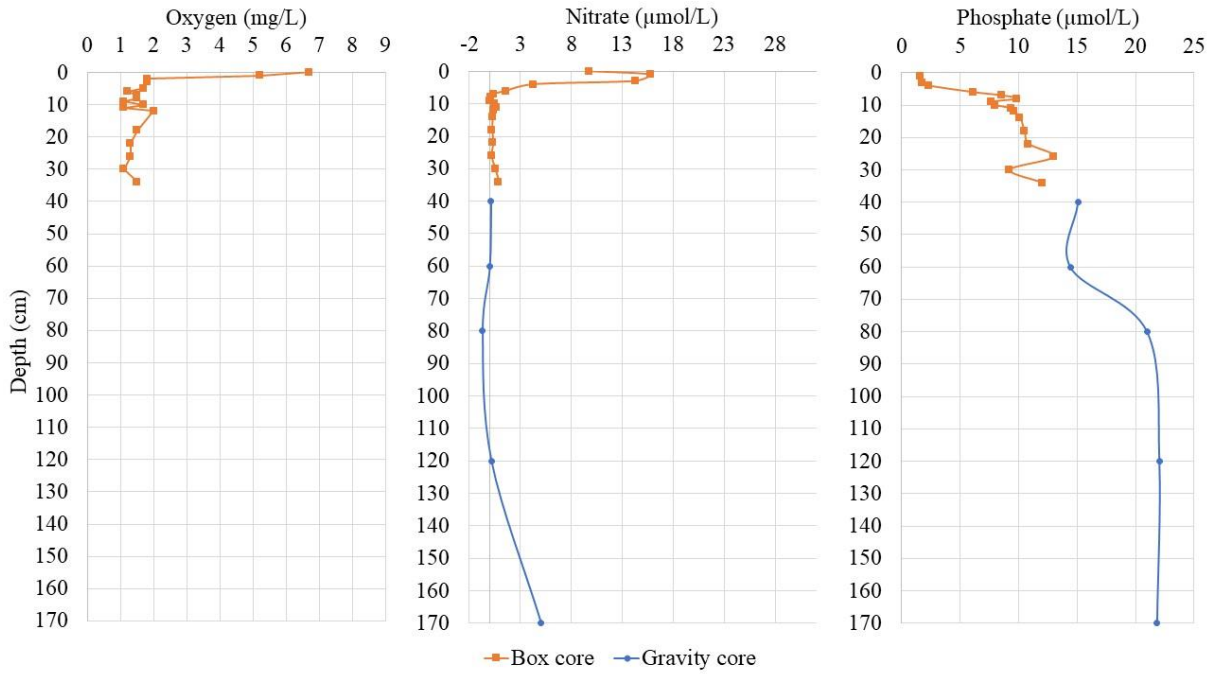


*Figure 38: Oxygen is given in mg/L, nitrate and phosphate is given in µmol/L downcore in station 5.*

This uncertainty for the different analysis is small compared to the data collected. Overall, the data quality allows me to identify key features in the cores related to organic carbon turnover and the role of oxygen in this process—although with some uncertainty in the precise level at which $O_2$ penetrates into the cores. I address this uncertainty and its significance further when discussing the stoichiometric estimates of $O_2$ penetration and the use of carbon isotope pore water gradients as a bottom water proxy.

## 6.2: The relationship between $\delta^{13}C$, oxygen, and water depth

The results from chapter 5 show the $\delta^{13}C_{DIC}$, the oxygen concentration, the water depth, the geographical position for each station. In this section I further investigate the relationship between these parameters in order to characterize the pattern and change in $\delta^{13}C_{DIC}$ and oxygen.

The first step is to investigate if there is a correlation between how much $\delta^{13}C_{DIC}$ decreases and how deep oxygen penetrates the sediments *(see Figure 39).* The oxic zone is assumed to increases with increasing water depth and decrease with increased organic flux to the sediment. (Schulz & Zabel, 2006, p. 193). As mentioned in section 6.1 there is an offset of +2 mg/L for the oxygen concentration in the shipboard measurements. The oxygen penetration

depth is defined as the depth at which oxygen concentrations drops to below 2 mg/L and a list with all stations and their oxygen penetration depths is presented in Table 3.

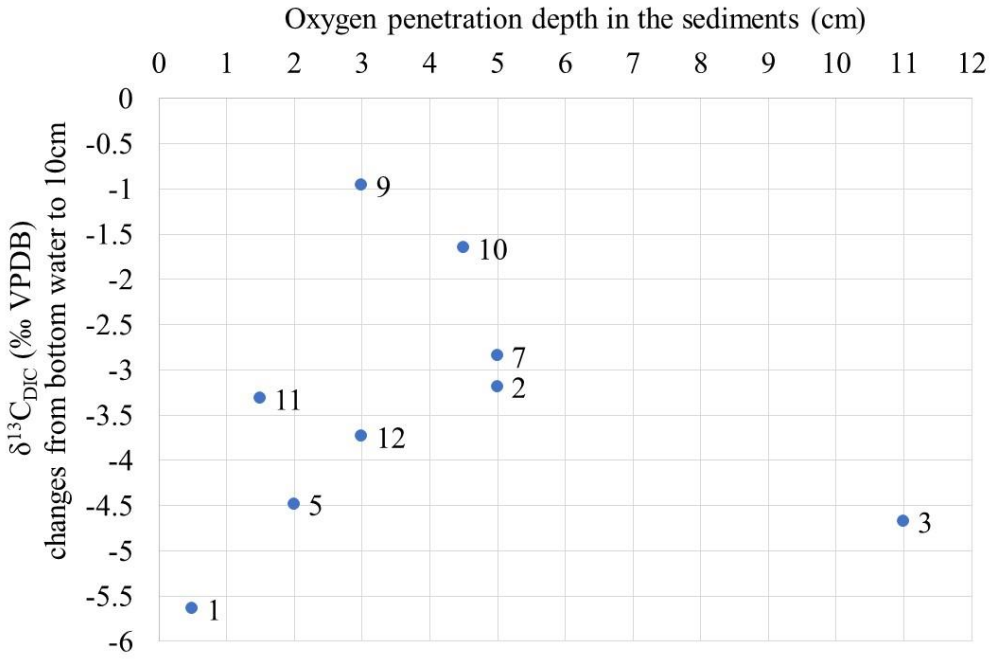


*Figure 39: $\delta^{13}C$ changes from bottom water to 10cm in the sediments plotted against the oxygen penetration depth for each station.*

| **Station number** | **Water depth (m)** | **Oxygen penetration depth (cm)** | **$\delta^{13}C$ at 10 cm depth (‰ VPDB)** | **$\delta^{13}C$ at $O_2$ penetration depth (‰ VPDB)** |
|---|---|---|---|---|
| 1 | 1042 | 0.5 | -4.8 | 1.8 |
| 11 | 287 | 1.5 | -2.7 | -1.5 |
| 5 | 1340 | 2 | -3.7 | -1.9 |
| 12 | 1674 | 3 | -2.5 | -1.9 |
| 9 | 1983 | 3 | -0.5 | 0.2 |
| 10 | 2637 | 4.5 | -0.5 | 0 |
| 7 | 2521 | 5 | -1.7 | -0.7 |
| 2 | 2205 | 5 | -2.4 | -1.4 |
| 3 | 1765 | 11 | -3.6 | -3.7 |

*Table 3: Table with the oxygen penetration depth and the water depth of each station.*

Figure 39 shows some correlation. The stations with shallow oxygen penetrations depth have the largest $\delta^{13}C$ change from bottom water to 10cm (station 1,5,11,12). Likewise, the oxygen penetration depth appears to be connected to the water depth of the different stations *(see Table 3).* Shallow stations have a shallower oxygen penetration depth, except station 3 with a deep oxygen penetration depth yet the water depth is intermediary (1700m). This pattern is not particularly surprising. It simply indicates that where there is more organic matter respiration (larger $\delta^{13}C$ change) there is less penetration of oxygen into the sediment (shallower oxygen penetration depth) as the oxygen is rapidly utilized. The same pattern is seen in other studies. McClorke and Emerson (1988) investigated three North Atlantic cores, core A (3000m water depth), core B (1500m water depth) and core C (1000m water depth). Core A had a $O_2$ penetration depth of 12cm. In core B the oxygen penetrated down to 4cm and core C the $O_2$ penetration depth is 3cm. McClorke and Emerson (1988) also concluded that oxygen is consumed more slowly further offshore, in deeper waters and therefor penetrates the sediments further down. Jørgensen and Kasten (2006) also conclude that the supply of oxygen to the sediments is transport limited. In coastal marine sediments with high productivity the oxygen content is reduced and the thickness of the oxic surface layer of the sediment is only a few mm or cm (Jørgensen & Kasten, 2006). The $\delta^{13}C$ change is also connected to the water depth as shown in section 5.11. This correlation is further discussed in in the section below and the $\delta^{13}C$ change vs water depth of the different stations is presented in Figure 40.

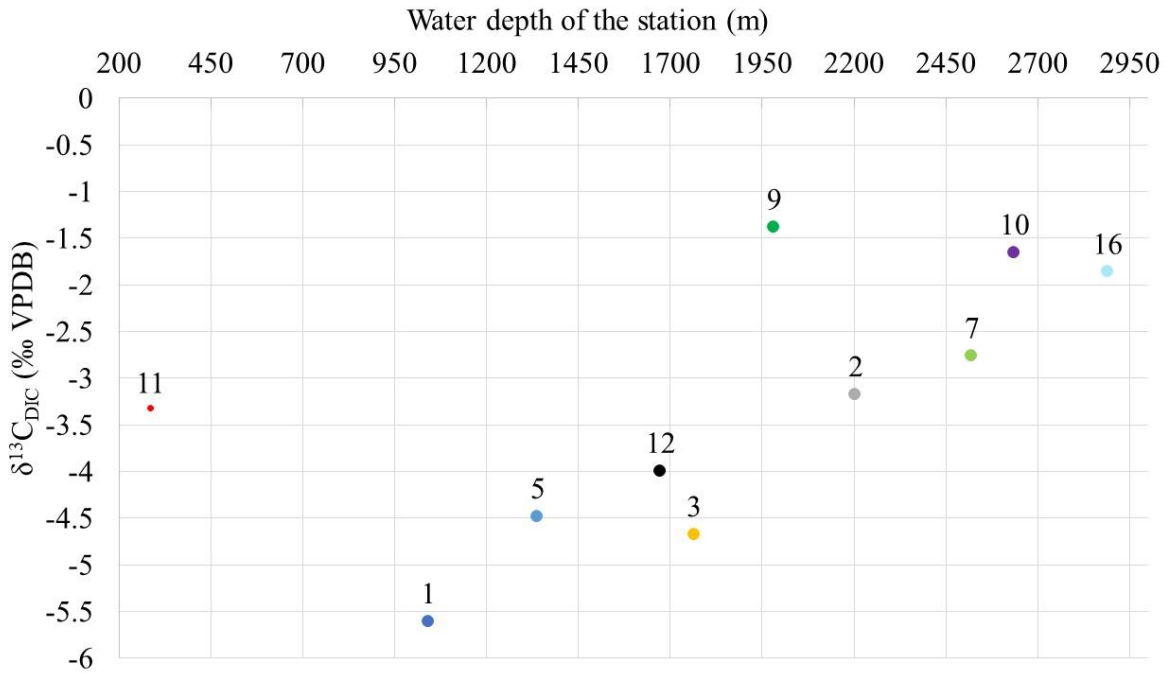


*Figure 40: Show the difference in $\delta^{13}C$ from bottom water to 10cm on the y axis and the depth of the station on the x-axis.*

Some correlation between the water depth and the $\delta^{13}C$ difference between bottom water and 10cm is apparent *(see Figure 40).* The shallower the station the larger the difference in $\delta^{13}C$. The exception being station 11 which stands out as the shallowest station with a water depth of only 275m but the $\delta^{13}C$ change is less than at other shallow stations like station 1,3,5 and 12. Station 9 stands out as well. The water depth at this station is similar to the water depths of station 2 and 3 but the $\delta^{13}C$ change is significantly lower than for the other stations. The same can be said about station 12 which is approximately 1700m deep, the same as station 3 but the $\delta^{13}C$ is -2.4‰ at 10cm in station 12 and -3.5‰ in station 3. These results shows that there is a geographically dependent difference in the rates of downcore $\delta^{13}C$ change *(see Figure 41).* The stations with same water depth on the west side of the study area are higher in $\delta^{13}C$ (at 10 cm) compared to stations at the east side. This can be related to the signal of the carbon source (different sources of carbon to the DIC pool with different isotopic values) or it can be related to the amount of carbon being added to the sediment (simply more isotopically light carbon added to the DIC pool). In order to differentiate between these two possibilities, I next investigate the carbon source and the carbon flux to the sediment.

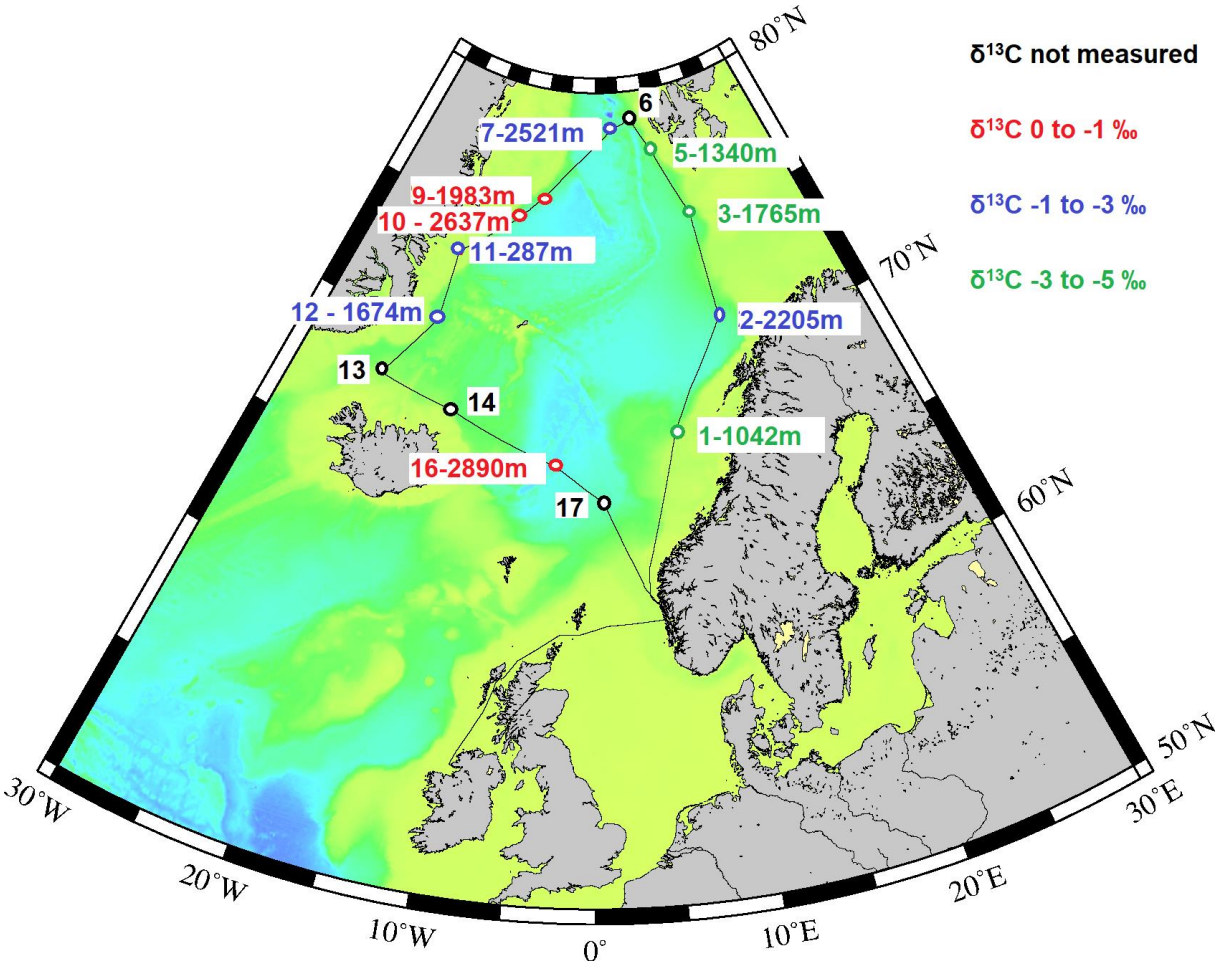


*Figure 41: This map gives an overview of the different station and the pore water $\delta^{13}C_{DIC}$ measured at 10cm into the sediments. The red colored stations have a $\delta^{13}C_{DIC}$ of 0 to -1‰, the blue stations have a $\delta^{13}C_{DIC}$ of -1 to -3‰ and the green stations have a $\delta^{13}C_{DIC}$ of -3 to -5‰. Eastern (shallow) stations show lower values than western (deeper) stations.*

## 6.3 Organic matter (OM) signature

The initial DIC of pore water reflects the DIC of seawater during sedimentation. Modification of this original DIC concentration primarily occurs through organic and inorganic cycling of carbon with respiration of organic carbon being a primary post depositional influence on pore water DIC. The $\delta^{13}C$ signature of these processes is quite different. The $\delta^{13}C$ in organic matter is approximately -25‰, or -20 to -22‰ (Meyers, 1995) in typical marine organic matter—although it can be as low as -30‰ in high latitude settings (Goericke & Fry, 1994). By contrast, the $\delta^{13}C$ in marine carbonate is around 0‰ (Hoefs, 2015, p. 69). Accordingly, organic matter respiration is indicated by low $\delta^{13}C$ values (Hebbeln & Berner, 1993). Low pore water $\delta^{13}C_{DIC}$ values, relative to bottom water DIC, are found in all stations. Station 1, 3, 5 and 11 have the most significant drop in $\delta^{13}C$ in the upper part of the sediments. These are also the shallowest stations which can indicate higher organic

matter input at these locations due to less water column respiration (since the vast majority of organic matter produced in the photic zone is respired in the water column). The $\delta^{13}C$ signature of the $CO_2$ change downcore can be calculated using isotopic mass balance equations *(see equation 6).*

$$a)\ d_{bw} * Q_{bw} + d_1 * Q_1 = d_T * Q_T$$

$$b)\ d_1 = \frac{(d_T * Q_T) - (d_{bw} * Q_{bw})}{Q_1}$$

*Equation 6: Isotopic mass balance equation used to calculate the signature of the $CO_2$ change downcore. D being the isotopic values of a substance ($\delta^{13}C$). Q being the quantity of the substance (amount of $CO_2$). Bw representing the values in bottom water, 1 representing the values at depth 1 and T representing the total change in isotopic value and quantity for one interval.*

Applying this mass balance equation allows the isotopic value of the substance being remineralized to $CO_2$ to be quantified *(see Table 4 and Figure 42).* To estimate the DIC changes, which were not measured directly due to low sample yields from the pore waters, we use the total $CO_2$ yield for each sample as estimated by the Delta Ray during analyses ($SCO_2$). These values were corrected for differences in sample volume (ie. not all samples were exactly 1 ml). Volumes were determined by weighing the full sample glasses after returning to shore. When applying equation 6 for the total change occurring downcore at each site the isotopic value of carbon being added to the DIC pool is typically between -20 and -30‰— close to the values expected for marine organic matter *(see Table 4).* Examining the mean isotopic value of carbon added to the DIC pool in the pore waters there appears to be a tentative relationship with station depth, although the number of stations and the uncertainty in the calculations preclude firm conclusions. Nevertheless, station 5 with a water depth of 1296m has a signature of -30‰ for the carbon isotopic value of $CO_2$ being added to the DIC pool. The isotopic value of carbon added to pore water DIC at stations 1 and 11, which are 1050m and 287m deep respectively, is -25‰. The remaining stations (2,3,9,10,12,16) with a depth of 1740-2850m have a signal of -16 to -21‰. In short, the deeper stations are not as negative as the shallow-intermediate ones (apart from station 7). Although this could indicate a different source of organic matter at these locations, due to preferential respiration within the water column or perhaps small influences of methane derived carbon at the high productive and intermediate sites, such correlations may just be circumstantial, with all stations having a signature of approximately -25‰ ±8‰. More data and better estimates of

DIC change, the primary source of error in these calculations, would be needed to confirm these depth related patterns.

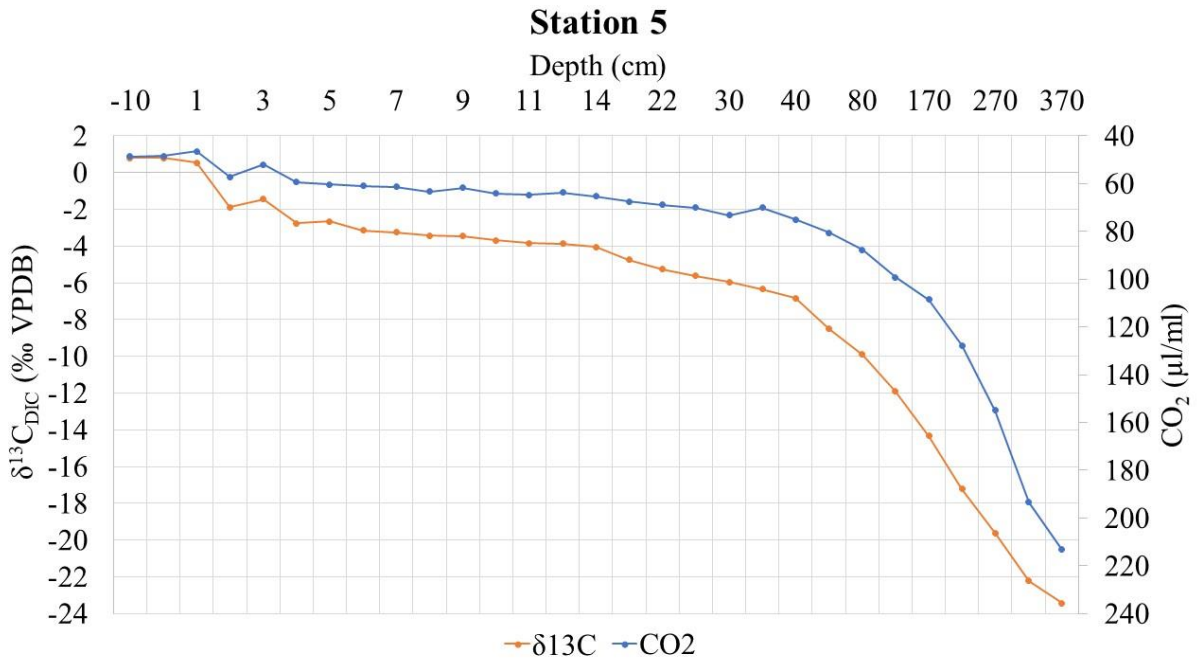


*Figure 42: The orange curve represents the pore water $\delta^{13}C_{DIC}$ in ‰ VPDB downcore for station 5. The blue curve represents µl $CO_2$ per ml pore water downcore. The increase in $CO_2$ and decrease in $\delta^{13}C$ is due to organic matter being respired.*

| **Station** | **Water depth (m)** | **Depth in sediments (cm)** | **Delta ray $CO_2$ in sample (µl/ml)** | **$\delta^{13}C$ (‰ VPDB)** | **$CO_2$ changes downcore (µl/ml)** | **Mean $\delta^{13}C$ (‰ VPDB) of the $CO_2$ added downcore** |
|---|---|---|---|---|---|---|
| 1 | 1042 | Bottom water | 53.2 | -1.80 | | |
| | | 400 | 354.7 | -22.00 | 301.5 | -25.6 |
| 2 | 2205 | Bottom water | 43.6 | 0.74 | | |
| | | 360 | 155.9 | -13.90 | 112.3 | -19.6 |

| | | | | | | |
|---|---|---|---|---|---|---|
| 3 | 1765 | Bottom water | 45.8 | 1.12 | | |
| | | 410 | 177.9 | -14.87 | 132.1 | -20.4 |
| 5 | 1340 | Bottom water | 48.6 | 0.79 | | |
| | | 370 | 213.2 | -23.42 | 164.6 | -29.8 |
| 7 | 2521 | Bottom water | 48.1 | 1.12 | | |
| | | 8 | 51.6 | -1.23 | 3.5 | -33.8* |
| 9 | 1983 | Bottom water | 46.0 | 0.95 | | |
| | | 100 | 56.6 | 3.08 | 10.6 | -20.5 |
| 10 | 2637 | Bottom water | 46.9 | 1.22 | | |
| | | 120 | 59.5 | -3.51 | 12.6 | -21.1 |
| 11 | 287 | Bottom water | 46.7 | 0.60 | | |
| | | 4.5 | 53.9 | -2.85 | 7.2 | -25.2* |
| 12 | 1674 | Bottom water | 44.2 | 1.10 | | |
| | | 37 | 60.6 | -4.55 | 16.4 | -19.8 |
| 16 | 2890 | Bottom water | 45.7 | 1.19 | | |

| | | | | | | |
|---|---|---|---|---|---|---|
| | | 27 | 52.7 | -1.19 | 7.0 | -16.7* |

*Table 4: The $\delta^{13}C$ and $CO_2$ change between bottom water and the depth with the highest $CO_2$ concentration are used to calculate the mean $\delta^{13}C$ value of $CO_2$ added downcore at each station. The stations denoted with ''*'' in the right column have high(er) uncertainty because of the relatively small changes in $\delta^{13}C$ and/or $CO_2$ resulting in a lower signal/noise ratio.*

Regardless of the small differences between sites, the mass balance calculation clearly reveals that it is organic matter being respired in the sediment and producing the declining $\delta^{13}C$ of DIC values in pore water downcore. This raises an important question and one of the main objectives of this thesis, why is the $\delta^{13}C$ downcore so different on the east side compared to the west side when the $\delta^{13}C$ signature indicates that its organic matter being respired in all stations and the bottom water oxygen concentration is the same for all stations. Put another way, if bottom water oxygen is the primary control on organic matter respiration why are there such dramatic differences between sites with such similar bottom water oxygen concentrations? Differences in organic matter flux to the sediment between the sites may provide one answer. Even if oxygen is present, organic matter must also be present in sufficient amounts in order to be remineralized. Figure 11 in section 3.4.4 shows the long-term productivity of carbon in the surface water of the Nordic Seas. The net productivity is generally higher along the Norwegian margin compared to the Greenland margin and consequently a higher flux of organic matter to the sediment is likely along the Norwegian margin (Gregg, 2003). More organic matter available in the sediments means more organic matter to respire resulting in lower $\delta^{13}C_{DIC}$. Critically, not all organic matter respires at the same rates and regions with high organic matter fluxes to the sediment (and shallow sites with less water column respiration) likely receives a higher fraction of easily respired organic matter than deeper and lower productivity regions. This might further help explain the high rates of carbon turnover, shallow oxygen penetration and rapid decline in $\delta^{13}C_{DIC}$, in the eastern sites. In short, we find that bottom water oxygen is not a particularly good indicator for oxygen penetration depth or the magnitude of $\delta^{13}C_{DIC}$ change in shallow sediments. Instead, the flux in carbon to the sediments appears to be a more important factor in organic matter respiration than the concentration of $O_2$ available from the bottom water. This inference could be further tested by measuring organic carbon content in the sediments as well as the annual flux of organic matter to the sediments at these different locations. Unfortunately, the organic carbon measurements planned to be carried out by international collaborators could not be completed in time for this thesis (due to pandemic shutdowns).

## 6.4 Stoichiometric model

In section 6.3 the preliminary conclusion is that the flux of carbon to the seafloor is more important in setting the rate and intensity of carbon respiration than the concentration of oxygen in bottom water. If correct, this raises questions as to how much of the respiration is aerobic and ultimately whether the amount of carbon remineralization between bottom water and the depth of oxygen penetration a function of bottom water oxygen as is assumed when using this gradient as a bottom water oxygen proxy. In essence, is $\delta^{13}C$ acceptable to use as an $O_2$ proxy?

Since DIC in pore water originates from DIC in seawater it's possible to estimate the partitioning between seawater DIC and organically derived $CO_2$ based on the $\delta^{13}C$ using the ocean wide empirical relationships (Eide, et al., 2017). The related $O_2$ consumption can be further calculated using the method presented in section 2.3. Adding the Redfield ratio to equation 4 gives a decrease of 1.1‰ in $\delta^{13}C$ per 138µmol/kg oxygen consumed. The possibility of a lower $\delta^{13}C$ for the phytoplankton due to being in high latitudes need to be considered (Eide, et al., 2017). This alternative estimate gives a slope of 1.7‰ per 138µmol/kg of oxygen consumed. Since the exact carbon isotopic value of sedimentary organic matter at each site is not known I apply equation with both a 1.1 and a 1.7 slope in order to estimate the full range in the uncertainty. To give an estimate of how changes in $\delta^{13}C_{DIC}$ in pore water is related to oxygen and nutrients using different slopes, using a slope of 1.1 every 1‰ drop in $\delta^{13}C$ corresponds with a $PO_4$ increase of 0.909 and decrease of $O_2$ by 125.5µmol/kg. Using a slope of 1.7, a 1‰ decline in $\delta^{13}C$ corresponds to a change in $O_2$ of -81.2µmol/kg. In this thesis the $O_2$ concentration is given in µmol/L and therefor the changes of 125.5umol/kg and 81.2umol/kg is multiplied with 1.025 (density of seawater) to convert to the correct unit. The decrease in $O_2$ every 1‰ drop in $\delta^{13}C$ is -128.8µmol/L with the 1.1 slope and -83.2µmol/L with the 1.7 slope. The oxygen concentration measured with the CTD is used in addition to the change in $\delta^{13}C$ downcore, to calculate the oxygen concentration at each depth. The $O_2$ concentrations calculated downcore with the 1.1 and 1.7 slope for station 12 is presented in Figure 43 together with the $\delta^{13}C$ values downcore. The depth where the hand-held $O_2$ measurements where below 2 mg/L are denoted with a yellow line. A black, dashed horizontal line in the graph marks the $O_2$ concentration=0.

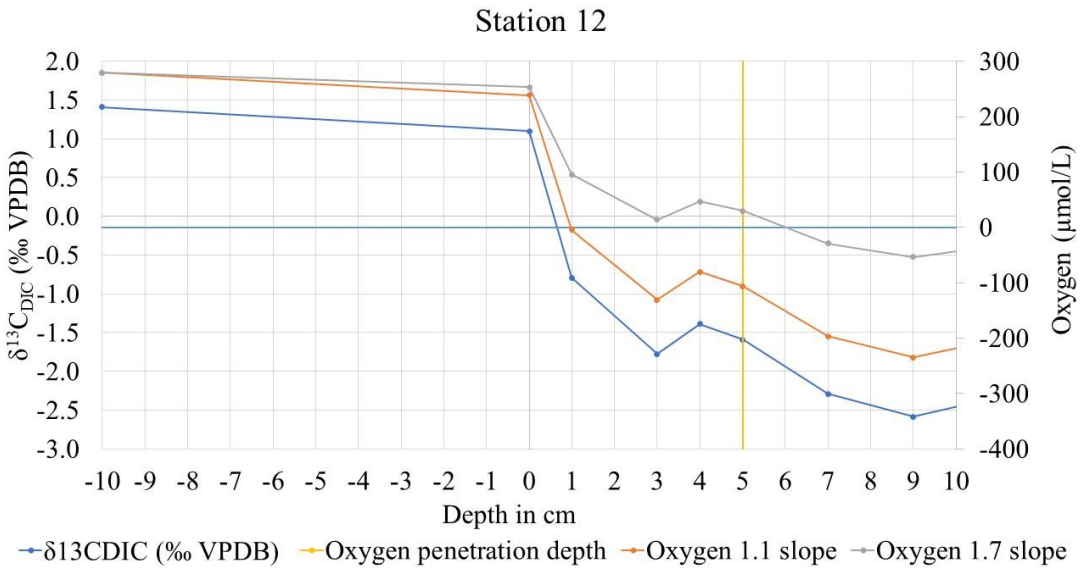


*Figure 43: The stoichiometrically estimated $O_2$ concentrations downcore for station 12 with the 1.1 slope is marked as an orange curve. The 1.7 slope estimate is marked with a grey curve and the original $\delta^{13}C$ values on which the calculations are based are indicated with a blue curve. The $O_2$ penetration depth found using direct $O_2$ measurements is indicated with a vertical yellow line and falls at 5cm, within the range (1cm -6cm) of the $\delta^{13}C$ based estimates.*

The depth at which the slope for the 1.1 and 1.7 calculations goes below this dashed horizontal line marks the depth in the sediment were the $O_2$ is calculated to be gone. For station 12 the 1.1 slope calculations resulted in a $O_2$ penetration depth of 1 cm and the 1.7 slope a $O_2$ penetration depth of 6cm. Meaning that the $O_2$ penetration depth must lie somewhere between 1 and 6cm if the $\delta^{13}C$ can be used as an $O_2$ proxy. In this case the hand-held measurements indicated a $O_2$ penetration down to 5cm in the sediments which falls within the range from the calculated penetration depths. This plot was made for every station to test the $\delta^{13}C$ as an $O_2$ proxy. In station 2,5, 7 and 12 the $O_2$ penetration depth measured falls in between the $O_2$ penetration depth calculated with 1.1 and 1.7 meaning that the $\delta^{13}C$ change downcore gives a plausible estimate of the $O_2$ concentration downcore and can be used to get an approximate of how deep oxygen is penetrating the sediments. Or conversely, the $\delta^{13}C$ gradient between bottom water and oxygen penetration depth may reflect the amount of bottom water oxygen (albeit with a large range/error due to potential differences in the $\delta^{13}C$ of locally respired organic matter).

In Figure 44, the $O_2$ penetration depths calculated with the 1.1 and 1.7 slope is plotted as two points for each station against the $O_2$ penetrations depth assumed from the hand-held measurements. The $\delta^{13}C_{DIC}$ measurements had a precision of ±0.14‰ which influences the calculated $O_2$ concentrations. Consequently, the precision of the calculated $O_2$ concentrations

is ±30µmol/L for the 1.1 slope and ±19µmol/L for the 1.7 slope, resulting in a ±1cm for the $O_2$ penetration depths. This precision is denoted as black lines in each point in Figure 44.

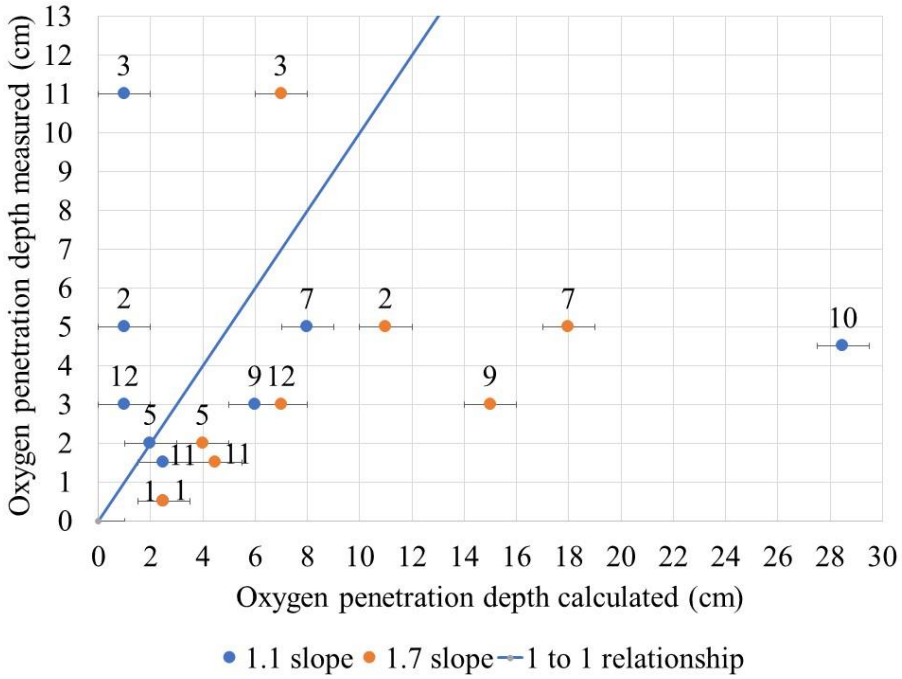


*Figure 44: Oxygen penetration depth calculated using equation 4 vs oxygen penetration depth measured. The blue dots are the results with the 1.1 slope and the orange dots are the results with the 1.7 slopes. Numbers represents the different stations. Station 1 has the same oxygen penetration depth with both slopes. In station 10 the oxygen penetration depth calculated with the 1.7 slope is 61cm and is not included in this graph. The blue line represents if the relationship between the calculated oxygen penetration depth and the measured oxygen penetration depth were 1:1. The grey line in each point indicates the ± 1cm for the calculated $O_2$ penetration depths.*

The graph includes a blue line representing the 1:1 relationship between the calculated $O_2$ penetration depth and the $O_2$ penetration depth from the hand-held measurements. Thus, if the calculated $O_2$ penetration depth is 5cm and the hand-held measurements also indicated a $O_2$ penetration depth of 5cm then this point would be plotted on the blue line. This is the case in station 5 when a slope of 1.1 is used for the calculation—which represents the global average value and is based on typical/common values for organic matter $\delta^{13}C$. However, since there is a chance that the $\delta^{13}C$ of some types of organic matter can be more depleted in high latitudes the 1.7 slope point represents the extreme case that all OM in each site has the more extreme/unusual OM values. Thus, the range between the oxygen penetration depth calculated with slopes of 1.1 and 1.7, blue and orange points in Figure 44 respectively, illustrates the full range of uncertainty in the calculated oxygen penetration depth based on carbon isotopes. Measuring the isotopic value of OM at each site would help to significantly narrow this uncertainty for each location. Unfortunately, sediment was not yet available after

the cruise to carry out these measurements. Thus, when the blue line is situated between the two points (1.1 and 1.7 slope calculations) it indicates that the measured $O_2$ penetration depth could fall within the possible range of calculated possible $O_2$ depths. Thus, downcore $\delta^{13}C$ changes provide (potentially) reasonable estimates of $O_2$ penetration depth at stations 2, 12, and 5 implying that aerobic respiration may dominate the isotopic changes in a simple way at these sites. In station 3, the calculated $O_2$ penetration depth is somewhere between 0 and 8cm in the sediments while the hand-held measurements indicated an $O_2$ penetration down to 11cm in the sediments. In this case the calculated ones are underestimated suggesting more carbon isotope changes (remineralization of organic matter) than is explained by the measured oxygen changes. In station 1,7,9, 10 and 11 the calculated $O_2$ penetration depths are deeper than the measurements done by hand suggest. In these cases, the $O_2$ penetration depth is overestimated using $\delta^{13}C$ as an $O_2$ proxy. Thus, we observe multiple deviations from simple stoichiometric changes indicating that aerobic respiration is not consistently/simply explaining pore water carbon and carbon isotope changes in shallow sediments. This clearly complicates the use of bottom water to pore water $\delta^{13}C$ gradients as a proxy for bottom water oxygen.

These simple stoichiometry calculations confirm that the oxygen can only partially explain the $\delta^{13}C$ changes in the upper 10cm. In addition, the $\delta^{13}C$ keeps decreasing once oxygen is consumed and the preliminary conclusion is that the flux of carbon to the seafloor is more important in setting the rate and intensity of carbon respiration than the concentration of oxygen in bottom water. However, without better *in situ* pore water oxygen data, complementary nitrate data for every site to confirm the oxygen measurements, and local organic matter isotope data to constrain the slope of the stoichiometric relationship between oxygen and $\delta^{13}C_{DIC}$ changes there is still considerable uncertainty in our oxygen penetration comparisons. Thus, it is worth considering a slightly simpler approach for constraining just how much oxygen respiration could change $\delta^{13}C_{DIC}$ in shallow sediments—i.e. between bottom water and the oxygen penetration depth.

Oxygen in bottom water at most station lies close to 7 ml/L with the maximum value of approximately 7.2 ml/L near station 10 *(see Figure 10 panel D).* This provides an upper limit of the amount of oxygen available in bottom water for aerobic respiration. Using the stoichiometric relationships derived above—for aerobic respiration a 1‰ change in $\delta^{13}C_{DIC}$ requires a consumption of between 83.2 to 128.8 mmol/L of $O_2$ depending on the isotope value of organic matter suggest that consuming all of the available oxygen in bottom water

could explain at most a drop in $\delta^{13}C_{DIC}$ of 2.6 to 3.9 ‰ between bottom water and the sediment anoxic zone. Bottom water $\delta^{13}C_{DIC}$ values are around 1‰±0.5 for the region today. Thus, consuming all oxygen would drop these values to -1.6 to -2.9‰ (±0.5‰) by the oxygen penetration depth assuming simple stoichiometric changes. However, this value likely represents an absolute lower limit for $\delta^{13}C_{DIC}$ values that can be explained by oxygen consumption since bottom water values today have been decreased by up to 1‰ or more by fossil fuel burning and the isotopic Suess effect (see Eide et al., 2017). To the extent that pore waters represent a history of bottom water since deposition, pore water $\delta^{13}C_{DIC}$ values were likely significantly higher than modern bottom water values. Thus, pore water $\delta^{13}C_{DIC}$ values lower than -1 to -2‰ are difficult to explain through aerobic respiration alone. $\delta^{13}C_{DIC}$ values at stations 1, 2, 5, 11 and 12 all fall within this upper limit *(see Table 3)* suggesting they are seeing near the maximum amount of isotopic change explainable by aerobic processes alone. However, at station 3 the isotopic changes significantly exceed changes that are easily explained by oxygen alone, reaching values as low as -4.7‰ by the oxygen penetration depth. This suggests that other electron acceptors are playing a role in organic matter respiration even in shallow sediments at this location.

An even larger change in pore water $\delta^{13}C_{DIC}$ is observed in the upper part of the sediments in the Nansen Legacy data from 2018—the results that motivated this thesis. The 2018 data is presented in Figure 45. The $\delta^{13}C_{DIC}$ decreases by 5.9‰ from bottom water to 0.5cm into the sediment in 04MC and by 2.4‰ in the 08MC. In the CIAAN results (this study) the largest $\delta^{13}C_{DIC}$ decrease (in the upper 1cm) is 2.5‰ at station 2 and the largest change seen down to the oxygen penetration depth is approximately -4.7‰ at station 3. The Nansen Legacy data with larger change in $\delta^{13}C_{DIC}$ indicate even stronger and more efficient organic matter respiration and even less of the changes can be explained by the oxygen. Thus, not only is bottom water oxygen a poor predictor of the rate and intensity of carbon respiration in sediments, but in some settings, it appears as if other electron acceptors are doing a large amount of carbon turnover, even in very shallow sediments. In particular, Arctic shelf regions (i.e. Barents Sea results from Nansen Legacy cruise in 2018) show particularly strong changes in pore $\delta^{13}C_{DIC}$ –exceeding the values observed in other settings around the Nordic Seas (this study). I speculate that, similar to the processes used to explain regional differences in this study, these changes may be explained by the shallow water depths and high organic matter input to the sediments in the Barents Sea. Water depths are shallower than most of our sites and there are rich benthic communities in these regions due to the high flux of organic matter

(food) to the sediments (The Nansen Legacy, 2018). The analysis of other parameters such as sedimentary composition and pore water concentrations of nitrate, Mn, Fe, $SO_4$, $H_2S$ (i.e. other electron acceptors) would be a natural next step in order to further identify and quantify the role of alternative electron acceptors in these settings marked by high (excess) carbon turnover.

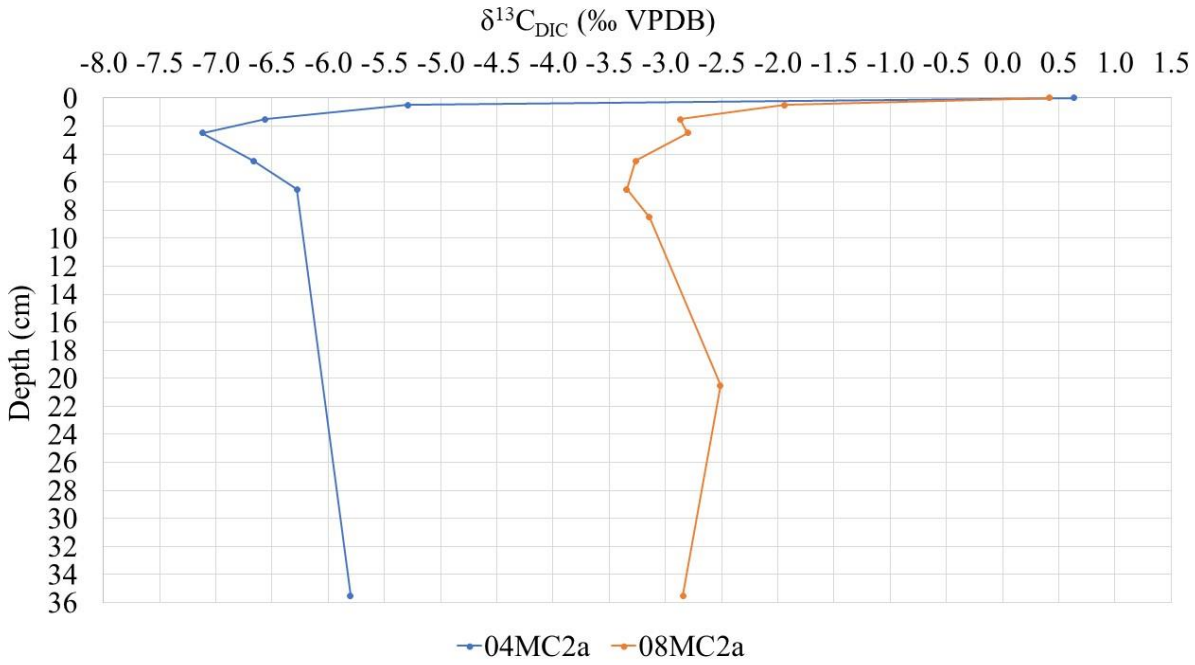


*Figure 45: $\delta^{13}C_{DIC}$ values downcore in two multicores from the Nansen Legacy cruise in 2018.*

## 6.5 Future predictions for the carbon turnover in marine sediments.

Over just 50 years (1960-2010) the oceanic oxygen reserves have decreased by 2% due to the warming of the ocean (Laffoley & Baxter, 2019). In addition, the oxygen minimum zones in the ocean are expanding (Baroni, et al., 2020). It is conventionally held that one consequence of future deoxygenation and warming on the ocean is enhanced organic carbon burial in marine sediments because of less carbon turnover due to less $O_2$ in the bottom water. In this way, ocean deoxygenation may provide a negative feedback on the carbon cycle changes (rising $CO_2$) by increasing organic matter burial drawing more carbon out of the ocean and atmosphere (Baroni, et al., 2020). Ultimately, this could provide an important negative feedback on the global warming (Baroni, et al., 2020). In this thesis the bottom water oxygen is nearly the same at all sites but with very different patterns and amounts of carbon turnover. The amount of organic matter flux to the sediment appears much more important than the excess of $O_2$ regarding the carbon turnover. Meaning $O_2$ is not the limiting factor in these

environments or at least at these stations. In the future there might be more stored carbon but the data for this thesis suggest that the carbon recycling can continue even though bottom water $O_2$ decreases at least in some settings. An important next step is to further characterize what conditions, and electron acceptors, allow such high (excess) organic matter respiration in the shallowest sediments at some sites.

## Summary of conclusion

On the basis of stable isotope, $O_2$, pH and nutrients measurements, I identify a pattern of higher rates of carbon turnover in the Nordic Sea than observed in many oceanic settings. It is established under what geographic conditions such high sedimentary carbon turnover rates occur and identify a correlation with productivity patterns and water depth. The main conclusions of the study are summarized as followed:

- The carbon isotope results show strong depletions in the shallow sediments relating to the addition of respired organic carbon to the dissolved inorganic carbon (DIC) pool. The strongest gradients ($\delta^{13}C$ difference of 5-6‰ between bottom water values and values 10cm in the sediments) occur in the eastern Nordic Seas, sites west of Svalbard and in shallower sites most likely due to higher productivity and organic matter input at these locations.
- None of the sites studied from around the Nordic Seas show pore water isotope gradients as strong as observed in the Arctic shelf (Barents Sea), although the proximal station 3 shows the most similar pattern.
- Stoichiometric estimates suggest that aerobic respiration dominates in the upper portion of the cores at most sites, but cannot explain all of the changes downcore, including in the upper centimeters at some sites, e.g. for station 3.
- Our results suggest that carbon isotope-based approaches to reconstructing past ocean $O_2$ levels may be strongly impacted in some environments by other factors sustaining higher rates of carbon respiration than is explained simply by bottom water $O_2$.
- Nitrate data is used to confirm oxygen penetration depths and contribute to some of the carbon turnover in the upper part of the sediments.
- I posit that other electron acceptors must be playing an important role in sub-Arctic and Arctic settings supporting carbon turnover in excess to that explained by $O_2$.
- Predictions of increased sedimentary carbon uptake in future climate conditions may not apply, or need to be reconsidered, in these settings.

# References


Anon., 2020. *Project Description.* [Internett]
Available at: https://arvenetternansen.com/project-description/

Assayag, N. et al., 2006. Improved method for isotopic and quantitative analysisof dissolved inorganic carbon in natural water samples. *RAPID COMMUNICATIONS IN MASS SPECTROMETRY*, 21 May, Issue 20, p. 2243–2251.

Baroni, I. R., Palastanga, V. & P, S. C., 2020. Enhanced Organic Carbon Burial in Sediments of Oxygen Minimum Zones Upon Ocean Deoxygenation. *Marine Science*, 22 January, Issue 6.

Belanger, P. & Streeter, S. S., 1979. Distribution and ecology of benthic foraminifera int he norwegian-greenland sea. *marine microplaeontology*, 6 December , Volum 5, pp. 401-428.

Berner, R. A., 1982. Burial of organic carbon and pyrite sulfur in the modern ocean: Its geochemical and environmental signifacance. *American Journal of Science*, Issue 282, pp. 451-473.

Canfield, D. E. et al., 1993. Pathways of organic carbon oxidation in three continental margin sediments. *Marine Geology*, July, 1-2(113), pp. 27-40.

Carmack, E. C., Swift, J. H., Reid, J. L. & Kolterman, P. K., 1990. The formation of Greenland Sea Deep Water: double diffusion or deep convection?. *Deep Sea Research*, 19 March, 37(9), pp. 1385-1424.

Cole, J. J., 2013. The carbon cycle - a brief introduction to global biogeochemistry. I: *Fundamentals of Ecosystem Science.* New York: Academic Press, pp. 109-135.

Debajyoti, P. & Grzegorz, S., 2006. Assessment of carbonate-phosphoric acid analytical technique performed. *International Journal of Mass Spectrometry*, 8 December, Issue 262, pp. 180-186.

Dylmer, C. V., Giraudeau, J., Hanquiez, V. & Husum, K., 2014. The coccolithophores Emiliania huxleyi and Coccolithus pelagicus: Extant populations from the Norwegian-Iceland Sea and Fram Strait. *Biogeosciences discussions*, 9 September, pp. 15077-15106.

Eide, M., Olsen, A., Ninnemann, U. S. & Johannessen, T., 2017. A global ocean climatology of preindrustrial and modern ocean δ13C. *Global biochemical cycles*, 3(31), pp. 515-534.

FARLAB - University of Bergen, 2019. *FARLAB: website for the University of Bergen.* [Internett]
Available at: https://www.uib.no/en/FARLAB/119785/%CE%B413c-dissolved-inorganic-carbon
[Funnet 25 March 2021].

Flanders Marine Institute, n.d. *VLIZ.* [Online]
Available at: http://www.vliz.be/en/reineckboxcorer-en
[Accessed 29 January 2021].

Goericke, R. & Fry, B., 1994. Variations of marine plankton D13C with latitude, temperature, and dissolved CO2 in the world ocean. *Global biogeochemical cycles*, Issue 8, pp. 85-90.

Gouretski, V. & Koltermann, K., 2004. *WOCE Global Hydrographic Climatology*, Hamburg: Bundesamt für Seeschifffahrt und Hydrographie.

Greenland climate research centre, n.d. *Research program - greenland benthic habitats: website for Greenland Climate Research Centre.* [Online]
Available at: https://gcrc.gl/research-programs/greenland-benthic-habitats/
[Accessed 19 march 2021].

Gregg, W., 2003. *NASA GSFC Earth Observatory*. [Internett]
Available at: https://www.nasa.gov/centers/goddard/news/topstory/2003/0815oceancarbon.html
[Funnet 13 May 2021].

Hebbeln, D. & Berner, H., 1993. Surface sediment distribution in the Fram strait. *Deep-sea Research*, 27 February, 9(40), pp. 1731-1745.

Hedges, J. I. & Keil, R. G., 1995. Sedimentary organic matter preservation: an assessment and speculative synthesis. *Marine chemistry*, April, 2-3(49), pp. 81-115.

Heinze, C. et al., 2015. The ocean carbon sink – impacts, vulnerabilities and challenges. *Earth System Dynamics*, June, pp. 327-358.

Hoefs, J., 2015. *Stable isotope geochemistry.* Göttingen: Springer.

Hoogakker, B. A. A. et al., 2015. Glacial–interglacial changes in bottom-water. *Nature geoscience*, January, Issue 8, pp. 40-43.

Hoogakker, B. A. A. et al., 2018. Glacial expansion of oxygen-depleted seawater in. *Nature*, 18 October, Issue 562, pp. 410-413.

Hopkins, T. S., 1990. The GIN Sea A synthesis of its physical oceanography and. *Earth Science Reviews*, 27 June, Issue 30, pp. 175-318.

Hunter, S. et al., 2007. Deep western boundary current dynamics and associated. *Deep sea Reasearch*, 11 September, 1(54), pp. 2036-2066.

IAEA, n.d. *Reference Product for Enviroment and Trade: Website for IAEA.* [Online]
Available at: https://nucleus.iaea.org/sites/ReferenceMaterials/Pages/Stable-Isotopes.aspx
[Accessed 26 May 2021].

Ibrahim, A. S. A., Olsen, A., Lauvet, S. K. & Rey, F., 2014. Seasonal Variations of the Surface Nutrients and Hydrography in the Norwegian Sea. *International Joundal of Environemtna Science and Development*, October, 5(5), pp. 496-505.

Jørgensen, B. B. & Boetius, A., 2007. Feast and famine - mirobial life in the deep-sea bed. *Nature*, 10 September, Volum 5, pp. 770-781.

Jørgensen, B. B. & Kasten, S., 2006. Sulfur cycling and methane oxidation. In: *Marine Geochemistry.* Aarhus: s.n., pp. 271-309.

KC Denmark AS, n.d. *KC Denmark.* [Online]
Available at: https://www.kc-denmark.dk/products/sediment-samplers/multi-corer/multi-corer-4-x-oe100-mm.aspx
[Accessed 29 January 2021].

Laffoley, D. & Baxter, J., 2019. *Ocean deoxygenation: Causes, impacts, consequences and solutions,* Gland: s.n.

LaMourie, M. J., 2020. *Atlantic Ocean; website for Britannica.* [Internett]
Available at: https://www.britannica.com/place/Atlantic-Ocean
[Funnet 20 May 2021].

Lenton, T. M. & Watson, A. J., 2000. Regulation of nitrate, phosphate, and oxygen in the ocean. *Global biogeochemical cycles*, 1 March, 1(14), pp. 225-248.

Luff, R. & Moll, A., 2004. Seasonal dynamics of the North Sea sediments using a three-dimensional coupled sediment-water model system. *Contitental shelf Research*, 12 March, Issue 24, pp. 1099-1127.

McCorkle, D. C. & Emerson, S. R., 1988. The relationship between pore water carbon isotopic composition. *Geochimica et Cosmochimica Acta*, Issue 52, pp. 1169-1178.

McCorkle, D. C. E. S. R. & Quay, P. D., 1985. Stable carbon isotopes in marine porewaters. *Earth and Planetary Science Letters*, 20 November, Issue 75, pp. 13-26.

Meyers, P. A., 1995. Preservation of elemental and isotopic source identification of sedimentary organic matter. *Chemical Geology*, pp. 289-302.

Middelburg, J. J., 2018. Reviews and syntheses: to the bottom of carbon processing at the seafloor. *Biogeosciences*, 19 January, Issue 15, pp. 413-327.

Mørkved, P. T., n.d. *FARLAB.* [Online]
Available at: https://www.uib.no/en/FARLAB/119777/delta-ray-co2%C2%A0isotope%C2%A0ratio-isotope-spectrometer%C2%A0
[Accessed 29 January 2021].

National snow and ice data center, 2021. *National snow and ice data center.* [Internett]
Available at: http://nsidc.org/arcticseaicenews/
[Funnet 10 March 2021].

Ocean exploration and research, n.d. *Ocean exploration and research.* [Online]
Available at: https://oceanexplorer.noaa.gov/facts/ctd.html
[Accessed 29 January 2021].

Sauter, E. J., Schluter, M. & Suess, E., 2000. Organic carbon flux and remineralization in surface sediments from the northern North Atalntic derived from pore-water oxygen microporfiles. *Deep-sea research*, 27 April, 1(48), pp. 529-553.

Schulz, H. D. & Zabel, M., 2006. *Marine Geochemistry.* 2 red. Bremen: Springer.

Simpkins, K., 2019. *Long-term data on atmospheric carbon dioxide reveals an intensification of carbon uptake by Northern Hemisphere vegetation; website for Future Earth.* [Internett]
Available at: https://futureearth.org/2019/04/03/long-term-data-on-atmospheric-carbon-dioxide-reveals-an-intensification-of-carbon-uptake-by-northern-hemisphere-vegetation/
[Funnet 26 March 2021].

Skogen, M. D., Budgell, P. W. & Rey, F., 2007. Interannual variability in Nordic seas primary production. *ICES journal of Marine Science*, 22 May, Issue 64, pp. 889-898.

Smith, R. W. et al., 2015. High rates of organic carbon burial in fjord sediments globally. *Nature geoscience*, Issue 8, pp. 450-453.

The Nansen Legacy, 2018. *Cruise Report Nansen Legacy paleo cruise RV "Kronpris Haakon" September 26. October 19, 2018,* s.l.: The Nansen Legacy.

YSI, n.d. *YSI.* [Online]
Available at: https://www.ysi.com/proplus
[Accessed 29 January 2021].

Aarnes, H., 2020. *Bjerrumdiagram.* [Internett]
Available at: https://snl.no/bjerrumdiagram
[Funnet 5 May 2021].

# Appendix

**Appendix A:** Oxygen- and carbon isotope measurements from the different cores.

- Table A.1 Mean values of isotope measurements from the Delta Ray and the oxygen measurements from CTD and using professional plus multiparameter instrument from YSI.
- Table A.2 Mean values of nutrients measurements from The University of Galway.

## Appendix A

### Table A.1

| Name: | Dyp (cm) | $CO_2$ (µl/ml) | $\delta^{13}C$ (‰) | Oxygen | pH | Salinity |
|---|---|---|---|---|---|---|
| | -10 | | | 6.16 | | 34.90 |
| BC01-06-01 | 0.5 | 53.2 | -1.80 | 1.8 | 7.55 | |
| | 1.5 | 53.8 | -2.41 | 2.3 | 7.55 | |
| | 2.5 | 58.8 | -2.82 | 1.4 | 7.62 | |
| | 3.5 | 54.6 | -2.99 | 1.3 | 7.55 | |
| | 4.5 | 54.7 | -2.87 | 1.5 | 7.62 | |
| | 5.5 | 55.9 | -3.23 | 2.2 | 7.67 | |
| | 6.5 | 57.9 | -3.58 | 2.2 | 7.60 | |
| | 7.5 | 57.5 | -3.97 | 2.1 | 7.58 | |
| | 8.5 | 59.7 | -4.14 | 2 | 7.56 | |
| | 9.5 | 58.3 | -4.58 | 1.9 | 7.54 | |
| | 10.5 | 61.5 | -4.89 | 2.3 | 7.51 | |
| | 12.5 | 62.8 | -5.04 | 1.7 | 7.67 | |
| | 14.5 | 64.9 | -5.62 | 1 | 7.59 | |
| | 16.5 | 22.1 | -5.83 | 2.2 | 7.48 | |
| | 19.5 | 76.7 | -7.23 | 1.9 | 7.54 | |
| | 22.5 | 79.4 | -7.93 | 1.7 | 7.45 | |
| | 24.5 | 83.4 | -8.23 | 1.9 | 7.51 | |

| Name: | Dyp (cm) | $CO_2$ (µl/ml) | $\delta^{13}C$ (‰) | Oxygen | PH | Salinity |
|---|---|---|---|---|---|---|
| BC01-06-02 | 1 | 56.9 | -1.8 | | | |
| | 2 | 61.0 | -2.4 | | | |
| | 3 | 58.2 | -2.8 | | | |
| | 4 | 57.7 | -3.1 | | | |
| | 5 | 55.6 | -3.5 | | | |
| | 6 | 58.7 | -3.7 | | | |
| | 7 | 62.5 | -3.5 | | | |
| | 8 | 59.3 | -4.1 | | | |
| | 9 | 60.2 | -4.8 | | | |
| | 10 | 57.0 | -4.6 | | | |
| | 12 | 67.0 | -5.7 | | | |
| | 14 | 71.9 | -6.3 | | | |
| | 16 | 70.6 | -6.7 | | | |
| | 19 | 76.7 | -7.3 | | | |
| | 22 | 78.7 | -7.7 | | | |
| | 24 | 81.8 | -8.3 | | | |

| Name: | Dyp (cm) | $CO_2$ (µl/ml) | $\delta^{13}C$ (‰) | Oxygen | pH | Salinity |
|---|---|---|---|---|---|---|
| GC01-03-01 | 10 | 72.3 | -7.21 | | | |
| | 20 | 92.5 | -9.96 | | | |
| | 30 | 112.7 | -11.48 | | | |
| | 40 | 125.0 | -12.62 | | | |
| | 50 | 132.5 | -13.47 | | | |
| | 60 | 138.1 | -13.96 | | | |
| | 100 | 175.1 | -15.50 | | | |
| | 150 | 208.7 | -17.04 | | | |
| | 200 | 240.9 | -17.90 | | | |
| | 250 | 270.2 | -18.96 | | | |
| | 300 | 309.2 | -20.04 | | | |
| | 350 | 349.5 | -20.88 | | | |
| | 400 | 354.7 | -22.00 | | | |

| Name: | Dyp (cm) | $CO_2$ (µl/ml) | $\delta^{13}C$ (‰) | Oxygen | pH | Salinity |
|---|---|---|---|---|---|---|
| | -10 | | 0.73 | 6.11089156 | | 34.91 |
| GC02-03-01 | 1 | 51.6 | -1.75 | 3.8 | 7.49 | 35 |
| | 2 | 57.5 | -1.45 | 3.8 | 7.51 | 35 |
| | 3 | 54.8 | -1.49 | 3.4 | 7.55 | 35.5 |
| | 4 | 52.4 | -1.18 | 2.5 | 7.78 | 36 |
| | 5 | 55.3 | -1.36 | 2.0 | 7.76 | 36 |
| | 6 | 57.1 | -1.82 | 2.1 | 7.71 | 37 |
| | 7 | 58.1 | -1.98 | 2.1 | 7.62 | 36.5 |
| | 8 | 58.0 | -2.10 | 1.5 | 7.82 | 36.5 |
| | 10 | 60.2 | -2.45 | | | |
| | 15 | 65.5 | -3.54 | | | |
| | 20 | 66.6 | -4.03 | | | |
| | 30 | 67.7 | -4.93 | | | |
| | 40 | 71.4 | -6.01 | | | |
| | 50 | 72.4 | -6.42 | | | |
| | 60 | 76.8 | -6.96 | | | |
| | 80 | 83.2 | -8.53 | 2.9 | 7.37 | 36.5 |
| | 100 | 78.3 | -9.08 | | | |
| | 130 | 91.1 | -9.53 | | | |
| | 160 | 106.8 | -10.87 | 2.9 | 7.38 | 36 |
| | 200 | 109.7 | -11.31 | | | |
| | 240 | 127.3 | -12.53 | | | |
| | 280 | 141.8 | -13.69 | 3 | 7.33 | 36.5 |
| | 320 | 139.1 | -14.82 | | | |
| | 360 | 155.9 | -13.90 | | | |

| Name: | Dyp (cm) | $CO_2$ (µl/ml) | $\delta^{13}C$ (‰) | Oxygen | pH | Salinity |
|---|---|---|---|---|---|---|
| | | | | 6.13708973 | | |
| GC03-03-01 | 3 | 47.4 | -1.57 | 3.8 | 8.15 | |
| | 4 | 45.8 | -1.61 | 3.9 | 8.18 | |
| | 5 | 48.4 | -1.63 | 3 | 8.12 | |
| | 6 | 47.7 | -1.84 | 3.3 | 8.15 | |
| | 7 | 50.4 | -2.37 | 3.0 | 8.02 | |
| | 8 | 53.1 | -2.83 | 2.8 | 7.95 | |
| | 9 | 56.4 | -3.08 | 2.5 | 7.82 | |
| | 10 | 59.7 | -3.56 | 2.3 | 7.80 | |
| | 11 | 61.4 | -3.69 | 2.2 | 7.71 | |
| | 12 | 57.4 | -3.25 | 2.2 | 7.81 | |
| | 15 | 63.7 | -4.38 | 2.4 | 7.64 | |
| | 18 | 62.8 | -3.90 | 2.4 | 7.75 | |
| | 21 | 53.4 | -2.72 | 3.1 | 8.03 | |
| | 25 | 57.5 | -3.52 | 3.1 | 7.94 | |
| | 30 | 59.9 | -3.76 | | | |
| | 40 | 80.2 | -6.30 | | | |
| | 60 | 87.8 | -7.01 | | | |
| | 90 | 98.5 | -8.19 | 2.8 | 7.49 | |
| | 120 | 100.2 | -8.81 | | | |
| | 160 | 116.4 | -9.94 | | | |
| | 210 | 132.3 | -10.98 | | | |
| | 260 | 135.3 | -11.57 | | | |
| | 310 | 146.7 | -12.62 | | | |
| | 360 | 163.1 | -13.71 | | | |
| | 410 | 177.9 | -14.87 | | | |

| Name: | Dyp (cm) | $CO_2$ (µl/ml) | $\delta^{13}C$ (‰) | Oxygen | pH | Salinity |
|---|---|---|---|---|---|---|
| MC05-04-01 | 0 | 48.4 | 0.80 | 6.7 | 7.86 | 37 |
| | 1 | 46.5 | 0.53 | 5.2 | 7.79 | 36 |
| | 2 | 57.2 | -1.89 | 1.8 | 7.51 | 37 |
| | 3 | 52.0 | -1.45 | 1.8 | 7.55 | 37 |
| | 4 | 59.4 | -2.77 | x | 7.60 | 36 |
| | 5 | 60.4 | -2.66 | 1.7 | 7.57 | 36 |
| | 6 | 60.9 | -3.14 | 1.2 | 7.57 | 36 |
| | 7 | 61.3 | -3.26 | 1.5 | 7.60 | 36 |
| | 8 | 63.4 | -3.43 | 1.5 | 7.58 | 36 |
| | 9 | 61.7 | -3.46 | 1.1 | 7.63 | 35 |
| | 10 | 64.2 | -3.70 | 1.7 | 7.57 | 36 |
| | 11 | 64.6 | -3.83 | 1.1 | | 37 |
| | 12 | 63.7 | -3.87 | 2 | 7.56 | N/A |
| | 14 | 65.2 | -4.04 | | | |
| | 18 | 67.5 | -4.74 | 1.5 | 7.56 | 37 |
| | 22 | 68.8 | -5.27 | 1.3 | 7.53 | 36.5 |
| | 26 | 70.0 | -5.63 | 1.3 | 7.55 | 36 |
| | 30 | 73.2 | -5.97 | 1.1 | 7.53 | 36.5 |
| | 34 | 70.1 | -6.35 | 1.5 | 7.53 | 36 |

| Name: | Dyp (cm) | $CO_2$ (µl/ml) | $\delta^{13}C$ (‰) | Oxygen | pH | Salinity |
|---|---|---|---|---|---|---|
| GC05-03-01 | 20 | 64.7 | -5.11 | | | |
| | 40 | 75.0 | -6.82 | | | |
| | 60 | 80.6 | -8.52 | | | |
| | 80 | 87.7 | -9.90 | | | |
| | 120 | 99.2 | -11.92 | | | |
| | 170 | 108.6 | -14.32 | | | |
| | 220 | 127.7 | -17.21 | | | |
| | 270 | 154.9 | -19.63 | | | |
| | 320 | 193.3 | -22.22 | | | |
| | 370 | 213.2 | -23.42 | | | |

| Name: | Dyp (cm) | $CO_2$ (µl/ml) | $\delta^{13}C$ (‰) | Oxygen | pH | Salinity |
|---|---|---|---|---|---|---|
| | -10 | | | 6.18164901 | | 34.9167 |
| GC07-03-01 | 1 | 45.1 | 0.40 | 3.3 | 7.89 | 35 |
| | 2 | 46.3 | 0.40 | 4.1 | 7.89 | 35.5 |
| | 3 | 46.9 | 0.06 | 3.2 | 7.86 | 35 |
| | 4 | 47.9 | -0.27 | 2.6 | 7.84 | 36 |
| | 5 | 49.6 | -0.73 | 1.5 | 7.83 | 36.5 |
| | 6 | 50.5 | -1.03 | 2.3 | 7.78 | 35.5 |
| | 8 | 51.6 | -1.23 | 2.3 | 7.75 | 37 |
| | 10 | 51.6 | -1.73 | 3 | 7.74 | 37 |
| | 12 | 51.6 | -1.89 | 1.3 | 7.88 | 37 |
| | 14 | 44.9 | -0.16 | 2.4 | 7.96 | 36.5 |
| | 16 | 45.0 | -1.22 | | | |
| | 18 | 52.9 | -2.92 | 2.9 | 7.75 | 37 |
| | 40 | 44.1 | -4.21 | | | |
| | 60 | | | | | |
| | 90 | 19.4 | -9.80 | | | |
| | 150 | 31.5 | -14.31 | | | |
| | 200 | 38.7 | -19.53 | | | |
| | 250 | 40.0 | -24.10 | | | |
| | 300 | 44.8 | -29.22 | | | |

| Name: | Dyp (cm) | $CO_2$ (µl/ml) | $\delta^{13}C$ (‰) | Oxygen | pH | Salinity |
|---|---|---|---|---|---|---|
| | -10 | | | 6.22956704 | | 34.9176 |
| BC09-06-01A | 1 | 47.4 | 0.49 | 2 | 7.87 | 36 |
| | 2 | 46.6 | 0.29 | 2.5 | 7.83 | 35.5 |
| | 3 | 47.0 | 0.18 | 1.4 | 7.90 | 34 |
| | 4 | 49.4 | 0.07 | 1.5 | 7.89 | 36 |
| | 5 | 47.5 | 0.07 | 1.7 | 7.92 | 35 |
| | 6 | 48.3 | -0.32 | 1.3 | 7.86 | 34 |
| | 7 | 48.2 | -0.36 | 1.4 | 7.88 | 35.5 |
| | 9 | 47.9 | -0.44 | 1.3 | 7.94 | 36.5 |
| | 11 | 48.1 | -0.47 | 1.2 | 7.95 | 36 |
| | 13 | 48.7 | -0.50 | 1.3 | 7.97 | 36.5 |
| | 15 | 49.7 | -0.73 | 1.7 | 7.97 | 37 |
| | 17 | 49.6 | -0.97 | 2.1 | 7.93 | 35 |
| | 19 | 51.5 | -0.87 | 1.4 | 7.97 | 36 |
| | 21 | 49.1 | -0.84 | | | |
| | 23 | 49.1 | -1.06 | | | |
| | 25 | 48.8 | -0.97 | | | |

| Name: | Dyp (cm) | $CO_2$ (µl/ml) | $\delta^{13}C$ (‰) | Oxygen | pH | Salinity |
|---|---|---|---|---|---|---|
| | -10 | | | | | |
| GC09-03-01 | 40 | 57.7 | -2.19 | | | |
| | 70 | 58.1 | -2.93 | | | |
| | 100 | 56.6 | -3.08 | | | |
| | 130 | 55.0 | -3.40 | | | |
| | 160 | 54.0 | -3.75 | | | |
| | 190 | 52.3 | -3.67 | | | |
| | 250 | 51.0 | -4.11 | | | |
| | 300 | 48.9 | -4.68 | | | |
| | 350 | 42.4 | -5.11 | | | |
| | 400 | 41.5 | -5.99 | | | |
| | 460 | 37.7 | -6.79 | | | |
| | 500 | 38.8 | -7.16 | | | |

| Name: | Dyp (cm) | $CO_2$ (µl/ml) | $\delta^{13}C$ (‰) | Oxygen | pH | Salinity |
|---|---|---|---|---|---|---|
| | -10 | | | 6.2 | | 34.9 |
| MC10-04-01 | 0 | 47.7 | 1.24 | 8.8 | 8.06 | 36.0 |
| | 0.5 | 45.8 | 0.74 | 2.8 | 7.83 | 36.0 |
| | 1.5 | 45.2 | 0.41 | 3.5 | 7.76 | 36.0 |
| | 3.5 | 46.5 | -0.03 | 2.6 | 7.81 | 36.0 |
| | 4.5 | 48.2 | 0.08 | 1.8 | 7.89 | 36.0 |
| | 5.5 | 44.2 | 0.00 | 2.1 | 7.86 | 36.0 |
| | 6.5 | 52.8 | -0.28 | 2.0 | 7.82 | 36.5 |
| | 8.5 | 47.5 | -0.24 | 2.1 | 7.89 | 36.0 |
| | 10.5 | 48.9 | -0.44 | 1.5 | 7.88 | 36.0 |
| | 12.5 | 44.4 | -0.47 | 2.0 | 7.85 | 35.0 |
| | 14.5 | 56.8 | -0.34 | | | |
| | 17.5 | 39.0 | -0.59 | 1.5 | 7.88 | 35.5 |
| | 20.5 | 52.6 | -0.65 | | | |
| | 23.5 | 54.9 | -0.79 | 2.1 | 7.83 | 36.5 |
| | 28.5 | 47.9 | -1.24 | 2.2 | 7.78 | 37.0 |
| | 33.5 | 49.7 | -1.51 | 2.4 | 7.83 | 35.0 |

| Name: | Dyp (cm) | $CO_2$ (µl/ml) | $\delta^{13}C$ (‰) | Oxygen | pH | Salinity |
|---|---|---|---|---|---|---|
| GC10-03-01 | 30 | 49.2 | -0.71 | | | |
| | 90 | 51.6 | -2.57 | | | |
| | 120 | 53.5 | -2.39 | | | |
| | 120 | 59.5 | -3.51 | | | |
| | 160 | 54.3 | -3.71 | | | |
| | 200 | 54.0 | -3.88 | | | |
| | 250 | 54.8 | -4.30 | | | |
| | 300 | 52.3 | -4.68 | | | |
| | 350 | 52.5 | -4.95 | | | |
| | 400 | 54.5 | -5.55 | | | |
| | 450 | 57.9 | -5.88 | | | |

| Name: | Dyp (cm) | $CO_2$ (µl/ml) | $\delta^{13}C$ (‰) | Oxygen | pH | Salinity |
|---|---|---|---|---|---|---|
| | -10 | | | 6.30860938 | | 34.8633 |
| MC11-04-01 | 0 | 46.2 | 0.72 | 8.5 | 8.09 | 37 |
| | 0 | | | 7.5 | 8.10 | 37 |
| | 0.5 | 47.1 | -1.17 | 2.7 | | 36 |
| | 0.5 | | | 4.5 | 7.64 | |
| | 1.5 | 48.8 | -1.48 | 1.7 | 7.57 | 36 |
| | 2.5 | 51.1 | -2.02 | 1.7 | 7.62 | 36 |
| | 3.5 | 51.3 | -2.24 | 2.3 | 7.65 | 36 |
| | 4.5 | 54.0 | -2.85 | 2.3 | 7.49 | 36 |
| | 5.5 | 49.4 | -2.16 | 3 | 7.76 | 36 |
| | 5.5 | | | 2.2 | 8.11 | |
| | 6.5 | 9.9 | 2.84 | 1.5 | 7.72 | 36 |
| | 8.5 | 50.3 | -2.51 | 1.7 | 7.75 | 36 |
| | 10.5 | 51.2 | -2.72 | 1.8 | 7.80 | 35 |
| | 12.5 | 50.3 | -3.02 | 2.2 | 7.85 | 36 |
| | 14.5 | 50.4 | -2.97 | 1.7 | 7.89 | 35 |

| Name: | Dyp (cm) | $CO_2$ (µl/ml) | $\delta^{13}C$ (‰) | Oxygen | pH | Salinity |
|---|---|---|---|---|---|---|
| | -10 | | | 6.25486954 | | 34.9154 |
| MC12-04-01 | 0 | 44.2 | 1.10 | 5.2 | 8.12 | 37 |
| | 1 | 47.0 | -0.79 | 2.9 | 7.80 | 34.5 |
| | 3 | 52.7 | -1.78 | 1.8 | 7.87 | 35 |
| | 4 | 52.6 | -1.39 | 1.6 | 7.90 | 34 |
| | 5 | 50.4 | -1.59 | 1.1 | 7.90 | 35.5 |
| | 7 | 56.6 | -2.29 | 1.4 | 7.82 | 35 |
| | 9 | 57.0 | -2.59 | 1.7 | 7.76 | 36.5 |
| | 11 | 55.9 | -2.33 | 1.2 | 7.85 | 35 |
| | 15 | 54.5 | -2.75 | 1.3 | 7.79 | 35 |
| | 19 | 50.2 | -3.05 | 1.8 | 7.75 | 35 |
| | 25 | 49.2 | -3.44 | 1.3 | 7.79 | 35.5 |
| | 31 | 58.5 | -4.03 | 1.6 | 7.79 | 36 |
| | 37 | 60.6 | -4.56 | 1.3 | 7.81 | 35.5 |

| Name: | Dyp (cm) | $CO_2$ (µl/ml) | $\delta^{13}C$ (‰) | Oxygen | pH | Salinity |
|---|---|---|---|---|---|---|
| | -10 | | | 9.19623012 | | 34.9101 |
| MC16-04-01 | 0 | 45.7 | 1.19 | | | |
| | 1 | 47.2 | 0.29 | | | |
| | 2 | 46.5 | 0.06 | | | |
| | 3 | 47.8 | -0.46 | | | |
| | 4 | 48.1 | -0.53 | | | |
| | 7 | 48.9 | -0.59 | | | |
| | 9 | 50.3 | -0.67 | | | |
| | 13 | 50.9 | -0.93 | | | |
| | 19 | 49.5 | -1.09 | | | |
| | 27 | 52.7 | -1.19 | | | |
| | 35 | 55.3 | -1.17 | | | |

Table A.2

| Core | Station | Depth | [PO4] µmol/L | [NO3] µmol/L |
|---|---|---|---|---|
| GC | 3 | 3 | 6.03 | 6.42 |
| | 3 | 4 | 11.02 | 5.29 |
| | 3 | 5 | 7.35 | 5.3 |
| | 3 | 6 | 9.33 | 4.16 |
| | 3 | 7 | 10.94 | 6.27 |
| | 3 | 8 | 13.84 | 1.86 |
| | 3 | 9 | 13.02 | 3.25 |
| | 3 | 15 | 19.37 | 1.47 |
| | 3 | 18 | 20.05 | 1.57 |
| | 3 | 21 | 21.6 | 0.13 |
| | 3 | 25 | 22.39 | -0.04 |

| Core | Station | Depth | [PO4] µmol/L | [NO3] µmol/L |
|---|---|---|---|---|
| MUC | 5 | 0 | | 9.76 |
| | 5 | 1 | 1.64 | 15.74 |
| | 5 | 3 | 1.76 | 14.27 |
| | 5 | 4 | 2.35 | 4.32 |
| | 5 | 6 | 6.09 | 1.57 |
| | 5 | 7 | 8.55 | 0.38 |
| | 5 | 8 | 9.86 | 0.15 |
| | 5 | 9 | 7.67 | 0 |
| | 5 | 10 | 8 | 0.45 |
| | 5 | 11 | 9.37 | 0.65 |
| | 5 | 12 | 9.62 | 0.38 |
| | 5 | 14 | 10.13 | 0.29 |
| | 5 | 18 | 10.48 | 0.24 |
| | 5 | 22 | 10.85 | 0.34 |
| | 5 | 26 | 12.98 | 0.17 |
| | 5 | 30 | 9.23 | 0.55 |
| | 5 | 34 | 12.01 | 0.9 |
| GC | 5 | 20 | 15.11 | 0.84 |
| | 5 | 40 | 15.08 | 0.15 |
| | 5 | 60 | 14.43 | 0.02 |
| | 5 | 80 | 21 | -0.68 |
| | 5 | 120 | 22.04 | 0.18 |
| | 5 | 170 | 21.85 | 5.07 |

| Core | Station | Depth | [PO4] µmol/L | [NO3] µmol/L |
|---|---|---|---|---|
| BC | 9 | 1 | 1.47 | 29.89 |
| | 9 | 2 | 2.06 | 27.15 |
| | 9 | 3 | 2.15 | 30.4 |
| | 9 | 4 | 2.57 | 29.89 |
| | 9 | 7 | 2.83 | 27.56 |
| | 9 | 9 | 2.65 | 27.28 |
| | 9 | 11 | 3.63 | 26 |
| | 9 | 13 | 2.92 | 28.2 |
| | 9 | 15 | 3 | 29.62 |
| | 9 | 17 | 2.94 | 28.25 |
| | 9 | 19 | 3.04 | 28.83 |
| GC | 9 | 40 | 2.83 | 15.75 |
| | 9 | 70 | 1.83 | 2.75 |
| | 9 | 100 | 2.22 | 0.08 |
| | 9 | 130 | 2.86 | 0.17 |
| | 9 | 160 | 2.51 | 0.04 |
| | 9 | 190 | 2.33 | 0.45 |
| | 9 | 250 | 2.65 | 0.47 |
| | 9 | 300 | 1.74 | 0.91 |